A Solid-State ^{35}Cl and ^{81}Br NMR and Computational Study of Chlorine and Bromine Electric Field Gradient and Chemical Shift Tensors in Haloanilinium Halides

Robert John Attrell

A thesis submitted to the Faculty of Graduate and Postdoctoral Studies in partial fulfillment of the requirements for the degree of

Master of Science

at the Ottawa-Carleton Chemistry Institute

Department of Chemistry, University of Ottawa

uOttawa

L'Université canadienne
Canada's university

Université d'Ottawa · University of Ottawa

Candidate	Supervisor
Robert John Attrell	Professor D. L. Bryce

Acknowledgements

The first sentence of an acknowledgments section is almost always the hardest to write. That being said, hopefully this won't take up too much of your time. I am, of course, referring only to this section; in the chapters following it you may find yourself lost and confused, but do not fret. After 5 years of magical, er, I mean scientific training; you too could find yourself on the precipice of completing a master's degree in Chemistry, looking over the edge into the gaping maw of 'real life'. Since I never got a chance to free-write about my undergraduate studies, and since the cast of that freak-show has many of the same characters as its post-baccalaureate reincarnation, I plan to combine all of my thanks below.

I can only hope that the next five years of my life will be anywhere near as fun as the past five. First and foremost, I would like to thank the University of Ottawa. Just over half a decade ago, you were just a fancy pamphlet which had found itself atop a pile of brochures compiled in a hasty trip to a high school out-of-province university fair. Less than a year after that fair, I was on the marble staircase outside Tabaret Hall, wondering to myself why it was called that. Also, I was looking for my dad, because I was alone for the first time in a new province a four hour flight from anyone I knew, and I was pretty scared. The university, as well as the city of Ottawa, much to my delight, turned out to be a beautiful, engaging, wonderful place to spend the span of two University degrees (and perhaps more, but I'll get to that later). While many friends I had in Calgary were cast asunder by my new life, this city held many surprises.

The first of these was my first non-familial roommate and definitely most exotic friend, Carl. You have motivated me to do so much better for myself than I ever thought I could. Between your late-night TV lullabies, your beautiful and powerful subwoofer and your ridiculous Weetabix addiction, I could fill a long-running TV series worth of plotlines with our

enterprises and adventures. Also, I'm fairly certain that I would've failed BCH 2333 if you hadn't made me memorize that entire textbook (and I certainly wasn't going to buy that massive, $200 tome; I hope it's keeping a large section of a bookshelf of yours somewhere free from dust), but that being said I'm certain there are some labs you wouldn't have done nearly as well on if it weren't for my mad scientist skillz. And of course I have you to thank for being at least 100x better at basketball than when I first picked up a ball as a pasty tall kid who could shoot as well from half court as from the foul line (not well) growing up.

In first and second year I lived in residence, and met so many awesome people who graced my life with theirs that I'm almost positive I'm going to forget someone crucial. Kathleen, without you I would just be a tub of goo now, thanks for making me enjoy running again. Also, you still haven't gotten back to me about that beer, rembember? Amaan knows what I'm talking about. Speaking of the world's least well known Aziz Ansari impersonator/suave brown guy (for those of you not getting that reference); you helped make those early chem. classes and labs bearable. I looked to you for inspiration when I was made Residence Advisor (haha RA, get it?), just kidding you are clearly the superior supervisory being. Also, I guess I should congratulate/thank you for taking care of Erin with me, though the government did pay us handsomely for that task. Oh Erin, House and NCIS wouldn't have been nearly as much fun without you, and though both those shows live on (I'm sure in no small part thanks to us) they are not quite the same when I watch them alone. If I see you even half as many times as you promise to come to Ottawa in the coming years, I will consider that a success. Also, I never did thank you for all that help in dealing with your crazy roommate, but it did mean that you got to see me more, so it's not a total loss. Josie, we have had some rough times, but they weren't all bad. Remember when you tried to murder my dad with a golf

ball? That was satisfying, wasn't it? And you bought me a basketball and some bus tickets for Valentine's Day, that's incredibly romantic. You clearly know what you're doing in that department. I hope teaching brings you what you're looking for, and that your essay writing skills will eventually improve beyond my sleepy, middle of the night levels.

Madison Wayland (nee Darnell), I never knew you. I really miss your lesbian haircut and early morning/late night visits, and I was very sad to see you leave Ottawa. Though you may never read this, I think I miss time with you more than anybody else I don't see any more. I still get the Prestige and the Illusionist confused because we watched those back-to-back, what a dumb idea that was. We had some good times making those rez boards, and I completely ignored what you taught me in completing the "Seems Newbee Runz" board as an RA. Thanks for mixing me my first drink ever (though as an aspiring mixologist you should know better than to give a rookie drinker 6 shots of spiced rum in less than an hour, my bathroom floor was never so comfortable as that night). I hope to one day see you again.

Jane, I think of all the people who have left my life for the time-being, but who I certainly expect to see again at some point, you would be my favorite. We have had so many good times, between classes and singing and cooking and middle of the day Skype chats, you are one of the coolest people I know. I never did say this, though I probably should have much earlier for the record. I did not make it with everybody else to see Thoroughly Modern Millie, though I think you already know that. I think you know that it wasn't at all because I didn't want to see it, although I don't actually remember what was going on that day instead. I hope that this platform is adequate for giving you my sincerest apologies, and for asking your forgiveness in this matter. Though I did see a play with you, I still haven't seen you perform on stage, which is highly troubling. I consider you my oldest friend in Ottawa, simply because you were one of the

first people I met here, but also because you are awesome and more than worthy of the title. Come back soon!

Krista, I know you will make something of yourself, look me up when you get back from Down Under. Marc, we had some good times (thanks again for a great Flames game), but honestly where are you now? We all want to know. Kalie, I knew you as Erin's roommate and not a whole lot more, but you rock. And women's rugby is clearly the best sport ever. Kate, you were a super awesome RA and I'm still very sad I don't get to walk down to the front desk and see your smiling face, though congratulations on your new family and I wish nothing but the best for you in the years to come. Damien, though we don't know each other as well as I might like, I still consider you my token black friend and could listen to you sing all day. Becca, similarly, we really haven't spent much time in each other's company, but the time we have spent has been wonderful, you are one of the nicest, sweetest people I know, and I'm certain you will spend many years saving lives and taking care of people with a huge smile and a helping hand. Eric, you continue to dazzle me with your amazing abilities with a tennis racket, or bass guitar. Even though that piece of paper says you're an engineer, I will never think of you in that way. Matt, calm down, I'll get to you later.

While everyone I've mentioned so far has been an influence on me and I feel has contributed at least in small part to my completing this degree, no group of people has meant as much to me in the achievement of this qualification as those who I consider to be the founding members of the undergraduate chemistry club. The idea that we couldn't start a sanctioned club based on drinking every once in a while was a bureaucratic lynchpin to the only chance I ever had to participate in a university club.

Carolyn, though we met in 1st year psychology and you thought I was a jerk (which I probably was a little bit), I'm eternally grateful to you for all the help you've given me the last few years. Whether it was helping study for our myriad classes together, or hanging out drinking, or being the only sane people in a big room full of Frisbee players, you have always been fun to be around. Your awkwardness will continue to fascinate me and make me laugh. You have been around to talk to when I've been down on life, work and school, and have been ready and eager to celebrate and mourn the good times and the bad. For all of this, and so much more, I thank you.

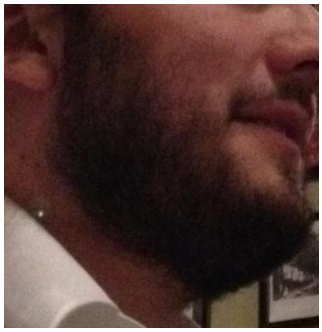

Schematic 1: The awesome beard of Nicholas Maddox. I will forever be envious of your manly mane.

Nick, you have an awesome beard. The number of pictures taken of us where it looks like we're making out, or about to make out, would astound even people who know us well. I very much appreciate having you around to bounce ideas off of, and our discussions about chemistry, women, algorithms, and scientific/technological advancements will always be some of my fondest memories of University. While your devotion to the Maple Leafs confuses me to no end, I still love you for it. When we get our condo with a beer fridge in every room and a Subway franchise in the kitchen, I will be a happy man. A manny, manny man.

Lizzie, you will always be the one that got away. I can tell you absolutely anything, and with that freedom comes no apparent responsibility. I'm very sorry that I sometimes choose to abuse your nature by creating fictitious scenarios to get you to pay attention to me, I can't help

it. Though we didn't meet as early as we could have in University, I'm very glad some classes here are only reasonably offered in English, so that we got to spend the better part of MSSM, and most of the time from then until now getting to know each other. You are awesome to spend time with, and though we find ourselves on opposite sides of an opinion more often than not, your level-headedness has helped me out in more ways than I'm sure I'm aware of.

Chantal, I'm really sorry I gave you the impression that I was a douche when we were almost neighbours all those years ago, I hope you can forgive me for that. I really enjoyed the time last year when we were both incredibly crippled and yet you still took care of me when I was what I'm going to call 'super-crippled' and hopped up on oxy, I hope I wasn't too much trouble. Someday I really do hope we can go for a run, medicine will catch up!

Julie, I really enjoyed softball this summer, thanks for convincing me to do that. I'm glad you were there through my return to sports, and I hope that in the months and years to come that we can continue to become better friends, and that we can stop having arguments where we're both trying to make the same point.

Switching tacks a little bit, I would like to talk for a little while about the importance of family in my life and as influences in completing this degree. Mom and Dad, it goes without saying that you have had the biggest impact on my life up to this point. Socially, emotionally, mentally, genetically, you have always shown me what is right and guided me towards who I am today. You deserve the most thanks of all in what I have accomplished so far. When I was contemplating abandoning my schooling for a green pasture in the distance, you convinced me to keep with it. While I haven't seen what effect this will have on my future yet, I am keen to be proven wrong in my potentially misguided desire to jump ship. You have been supportive of my every endeavour, and have never allowed me to cede to any limitations I might have encountered

in my life. You have always cultivated a home environment where I was able to achieve whatever my goals were, and so I have been able to grow in ways I perhaps never imagined were possible. From learning to speak and read practically simultaneously, to learning simple calculus in junior high, to playing soccer with people 4-5 years older than me and learning to hold my own, you have always allowed me to succeed. Between doing my own laundry, cooking meals, cleaning up after myself, you allowed me to learn the skills necessary to make it on my own. Even though I can't explain my research to you with any confidence that you've understood, I hope I have made you proud.

Michael, what can I say to you today? I know that we don't always agree on everything (airplane on a conveyor belt comes to mind), but I have always thoroughly enjoyed spending time with you, no matter where we end up. Our scientific discussions are always interesting (though not, I'm sure, to people around us) and learning to play hockey, tennis, and football (I'm sure I'm forgetting others) was a delight. I wish you all the best in life with Maria, and you remain the only people to have visited and stayed with me in Ontario (though others have certainly seen me on their way through town). I am honoured that you chose me as your best man. For that and many other things I am forever grateful, and I look forward to see you again soon!

Steph, you have grown up SO fast. It always stuns me that you've managed to always be 2 years younger than me, even though it's a temporal fact. Though we don't always get along, we will always be friends, and the fighting has really gone down quite a bit since we hit puberty. We also stopped looking as alike as we did, which is probably a good thing. Some days I really do wish you lived here, or that I was a little bit closer to home so that I could see

you more, but I know that you'll do great on your own! Isn't higher education awesome!? I love you.

Next, I would like to move on to the members of the indomitable Bryce Nation, beginning with the original graduate alumnus, Joey Weiss. Thanks for your thesis as a formatting guide for mine, and especially thanks for making me feel less awkward at conferences by sitting with me and not feeling obliged to go and mingle all the time. Fred, your constant fascination with NMR continues to be an inspiration to those who feel like they have lost their way, and I'm sure someday you will find a metal song I can endure for longer than you're around to make me listen. Kevin, I love listening to your stories, and it has been great getting to know you the last year. We need to plan many more Bryce Lab trips/outings, even when I'm gone. Jaz, it has also been really great becoming your friend since your return from Paris, and I appreciate your filling Liz's vacancy as my awesome female friend in the lab. I always know if I'm bored that you're there to distract me (unless Dave is reading this, in which case get back to work!) and I appreciate that. I know it's intimidating considering being in the office with Kev and Fred once Becky and Cory leave, but they're good guys, I'm sure it won't be so bad! Whose poster got 2nd place at CSC 2011? I rest my case. Jess, while your time in the lab was short-lived, I wouldn't be where I am today if it wasn't for our many days spent loudly singing in the lab, and I know I'm a better performer now because of that. I wish you all the best in your academic as well as musical endeavours. Becky and Cory, of all of the grad students, in all of the labs, in all of Marion and D'Iorio, you two stand alone. While I didn't spend very much time with either of you, probably mostly due to my insistence on keeping my awesome desk in the lab, I am extremely appreciative of all the help you've given me over the years. There was never

a problem of mine that one of you couldn't solve (except NQR) and my experiments would not have been nearly as successful without such great NMR role models in the lab.

Finally, I would like to thank Dr. Dave Bryce, the supervisor to rule all supervisors. If not for the opportunity you gave me at the end of 3rd year to work for the summer in your lab, I would certainly be a very different person today. All of your guidance and assistance with my projects and schooling were essential to my success as both an undergraduate and graduate student. When I was considering leaving grad school, you convinced me that should stick with it and finish what I started, and it's for that reason that I'm writing these words today. Your insistence on celebrating achievements and milestones is a huge part of what makes you great, and if I am ever given the opportunity to advise or counsel those a few rungs behind me on any ladder, I will be sure to pay my debt to you forward in kind. Since joining your group, I have really come to appreciate a good, strong beer and I have also learned that being thorough in every aspect of life will pay off in the end. I cannot thank you enough for all of your kindness and advice, try as I might to put that gratitude into words. I challenge anyone to find a better, more caring supervisor than Dave.

There were also a few other people worth mentioning who have helped with some of the actual hard work which has gone into this thesis. Ilia Korobkov deserves my thanks for performing x-ray crystallography on the two compounds mentioned in this thesis, as well as putting up with my rather hectic schedule whenever my turn in the queue was up. Tara Kell should be recognized at least briefly for providing me with powder x-ray training, even though I never used it after the training. Glenn Facey was always very helpful with any problems in the NMR department, and for his tireless hours keeping up all the NMR instruments at the University. Cheryl McDowall, as Glenn's assistant, kept the nitrogen tanks full at all times, and

we always seemed to run into one another during these weekly fills. I'd like to thank Eric Ye and Victor Terskikh at the Ultrahigh-Field NMR Facility for Solids (which by the way is not a catchy name) for all of their assistance while I was at the facility using the 900. I'd like to especially thank Eric for helping me by running a few chlorine-35 MAS spectra when I had a very busy day and couldn't make it to the NRC campus, and then for making sure to get the samples back to me safely with excellent data.

I would also very quickly like to thank all the students I TAed last year. Your shining faces provided me with some much needed motivation and your excitement about science and learning (and having fun in that environment) has renewed my faith in first years, I don't know how I got so lucky to have so many great students. If any of you ever want to grab a beer (you're all legal by now, right?) let me know! I never imagined that TAing first years could be so fun and rewarding.

Finally, I would like to thank a few people who have come into my life more recently than many of those mentioned so far, but who still deserve mention for their help with my state of mind as well as for listening to my gripes and stories about my research. Cait (OMal'z), you have provided me with so many great things since we met, and have always been quick to boost my spirits with your sassiness, and then keep me grounded by turning the sass against me. I appreciate it, and I'm glad I can attribute 'Science Rob' to you. I really hope that we can continue to become better friends, and we simply must go on a bike ride together soon. I mean how have we not? Sydney, I may not fully understand you, but I appreciate your kindness and friendship more than you know. Knowing that you are downstairs and always willing to talk is very reassuring, and I look forward to much more Workaholics in the future with you. We need to hang out more than we have been of late. Jacquie, you have finally moved back into the

neighbourhood and out of Sketchville. Of course at the exact same time as that happens I would crawl into a thesis-y hermit hole for a month, but I look forward to spending lots more time with you once this magical adventure is over. Harry Potter Marathon anytime you want, I downloaded them all (I mean bought, I bought them all). Now that you live nearby again there is no good excuse for not hanging out. Valery, I cannot in good conscience write this without at least mentioning your influence on my master's experience. Thanks for spending time with me while I was getting accustomed to graduate life, and for keeping me grounded while I was trying to figure out how to mark 40 labs a week while taking a class and TAing 6 hours a week. Though we haven't talked in a while now, I haven't forgotten about you. I sincerely do hope that you're doing well and hope that someday we'll see each other again, you're pretty awesome.

Julia, I think you have been the most supportive of anyone during this degree. It wasn't always easy, especially coming up to the end of it, when I'm basically spending every waking minute thinking about the next part of my thesis which needs doing. It can't be easy, especially being so busy yourself. You always seem to know what I'm going to need or want to feel better, even though it's kind of cheating that the answer is Mike & Ike's almost every time. Thanks for putting up with all my crazy the last couple of months; I'm sure it wasn't easy. Bippity boppity!

Finally, I think it's probably important that I acknowledge Matthew Staroste, my very good friend and faithful roommate. Through all my time spent working on this project and thesis, working and writing, you have always been around to talk to, for a beer, for breakfast, or as in some cases, both of those at once. You have always been an open ear to any issue. You're my wingman, my confidante, my fellow furniture aficionado. I joke around a lot about you, but know that in all seriousness I have so much respect for the things you do and who you are. You may be scrawny and clothes from the regular Gap and Gap Kids may not fit you quite right, but

you do a lot of other things right. You've seen me at my best, and you've definitely seen me at my worst (man they need to make Pabst more expensive…oh wait), but through it all you've shown me that roommates can be friends. We may not always be happy with one another (and I promise to leave the house more in October than I did in September), but living with you is an awesome experience. I have to call you my oldest friend overall, nursery buddies for life! And finally, Summer of George!! We really lived it up this time. That is what summer is supposed to be.

Finally, I'd like to thank Marianas Trench. Yes, they are a band, but in the last 2 years or so they have given me so much to think about, to sing along with, and to enjoy. I hope to meet you some day, so I can teach you all a little something about solid-state NMR.

Okay, so that **wasn't** short. It was actually much longer than I expected. I hope there is something in this little novel for everyone, and if I have forgotten to include you here, it doesn't mean that you did not impact my life, I just set myself a 5000 word limit.

ps. There are 10 glaring typos spread randomly throughout the accompanying work. If you think you've found them all, please contact me for a special surprise!

Table of Contents

Table of Figures

Table of Tables

List of Abbreviations

B3LYP	Becke, three-parameter, Lee-Yang-Parr
CPMG	Carr-Purcell-Meiboom-Gill
CT	Central Transition
CS	Chemical Shift
CSA	Chemical Shift Anisotropy
DFT	Density Functional Theory
DFS	Double Frequency Sweeps
EFG	Electric Field Gradient
FID	Free Induction Decay
GIPAW	Gauge-Including Projector-Augmented Wave
XB	Halogen Bonding
HF	Hartree Fock
HMQC	Heteronuclear Multiple Quantum Coherence
HB	Hydrogen Bonding
IUPAC	International Union of Pure and Applied Chemistry
MAS	Magic Angle Spinning
MQMAS	Multiple Quantum Magic Angle Spinning
NMR	Nuclear Magnetic Resonance
NQR	Nuclear Quadrupole Resonance
ONIOM	Our own N-layered Integrated molecular Orbital and molecular Mechanics
ppm	Parts per million

PAS	Principal Axis System
QCPMG	Quadrupolar Carr-Purcell-Meiboom-Gill
QI	Quadrupolar Interaction
RF	Radio Frequency
STMAS	Satellite Transition Magic Angle Spinning
SEDUCE	Sequence for Selective Composite Pulse Decoupling Using Shaped Pulses
STREAQI	Slow Turning Reveals Enormous Anisotropic Quadrupolar Interaction
SSNMR	Solid-State Nuclear Magnetic Resonance
TTF	tetrathiafulvalenes
VDW	van der Waals
VOCS	Variable Offset Cumulative Spectrum
WALTZ	Wideband Alternating-Phase Low-Power Technique for Zero Residual Splitting
WURST	Wideband, Uniform Rate and Smooth Truncation

Abstract

The results of a systematic ^{35}Cl, ^{81}Br, and ^{127}I SSNMR spectroscopic study of a series of halogen-substituted anilinium halide salts are presented. Solid-state NMR of these nuclides, bromine-/81 and iodine-127 in particular, is not well established. Twenty-one compounds thought to exhibit halogen bonding were prepared based on modified literature procedures, and two crystal structures were solved. Experiments show that collection of SSNMR spectra of the anions is feasible, though ultrahigh magnetic fields (21.1 T) and variable offset data acquisition were found to be essential. Electric field gradient and chemical shift tensors are measured experimentally for all 21 compounds, significantly expanding the body of data for the quadrupolar halogen nuclei. Quadrupolar coupling constants for chlorine-35 ranged from 2.12 to 6.04 MHz, for bromine-81 from 12.3 to 45.3 MHz, and for iodine-127 from 57.50 to 152.50 MHz. Gauge-including projector-augmented wave density functional theory (GIPAW-DFT) calculations were used to provide insight as to how the NMR parameters vary with local environment and long-range crystal packing. Overall, calculations reproduced the experimental trends in quadrupolar coupling constants and chemical shift tensor span (Ω) but failed to provide quantitative agreement within experimental error. Experimental and computational data were analyzed in order to provide insight into how halogen bonding influences NMR parameters. Several trends were elucidated from this study, including an inverse correlation between Ω and the length of the shortest halogen-halide contact (*d*). In selected bromine compounds, for example, Ω (^{81}Br) was measured to increase from 120 to 240 ppm as *d* decreased from 3.838 to 3.443 Å. In summary, this study has demonstrated the feasibility and utility of quadrupolar halogen SSNMR, and that these techniques may prove useful in characterizing halogen bonding interactions in solids.

Chapter 1

General Introduction & Objectives

1.1 Definitions

Nuclear magnetic resonance is a spectroscopic technique whose use has become ubiquitous in chemistry and biology, as well as in many industrial and medical applications.[1] Development of this method continues to flourish in the scientific community, and many nuclei on the periodic table are conducive to study by nuclear magnetic resonance (NMR). However, different nuclei exist in vastly different chemical environments and are susceptible to a variety of physicochemical phenomena. Each nucleus presents a unique set of challenges and affords different information on its surroundings. The quadrupolar halogens, chlorine, bromine, and iodine, are all important in modern chemistry, and the database of NMR spectra of these halogens, especially in the solid state, is still fairly small. The primary purpose of this thesis is to describe the results of an NMR and computational study of a series of organic halide salts, the haloanilinium halides. This chapter will discuss the basic mathematics and theory describing the NMR interactions which are pertinent to the description and interpretation of chlorine, bromine, and iodine solid-state nuclear magnetic resonance (SSNMR) spectra. This section will also describe the scope of this thesis as well as objectives of the experiments which were performed as part of this study.

Quadrupolar nuclei will be the focus of all the NMR experiments in this thesis; these are nuclei which have a nuclear spin larger than 1/2. There are three important interactions which need to be considered when commencing an NMR study on one or several quadrupolar nuclei. The Zeeman, magnetic shielding, and quadrupolar interactions are all important to the

observation and de-convolution of SSNMR spectra of quadrupoles, and each interaction gives a different but important subset of information. Combined, these data give a very detailed understanding of the environment in which the nucleus of study exists.

The first interaction to be considered, the Zeeman interaction, forms the basis for NMR spectroscopy. This interaction exists as a result of the nucleus' placement in an external magnetic field, B_0. Quadrupolar nuclei can occupy one of several different quantum spin states according to values in this series:

$$m_I = -I, (-I + 1) \ldots I \qquad \textbf{[1.1]}$$

where m_I is the magnetic quantum number and can take integer values between the positive and negative value of the spin quantum number *I*. This formula indicates that in the case of spin 3/2 nuclei like chlorine-35 and bromine-81, four energy levels are possible, and six levels are possible in the case of the spin 5/2 nucleus of iodine-127. In the absence of a magnetic field each of these levels is degenerate and so none is favoured. When a magnetic field is applied, the spins of the nuclei in different energy levels will prefer certain alignments with respect to the field. In so doing, just more than half of the spins (those in the lower energy levels, see Figure 1.1) will lower their energy by aligning favourably with the field and the remaining spins will oppose the field and will therefore have a higher energy. This population difference follows the Boltzmann distribution, and so the energy gap dictates the relative populations of the energy levels. This difference between energy levels stays the same between each set of levels, and so in considering only the Zeeman levels, an NMR signal will always be a single line at an energy

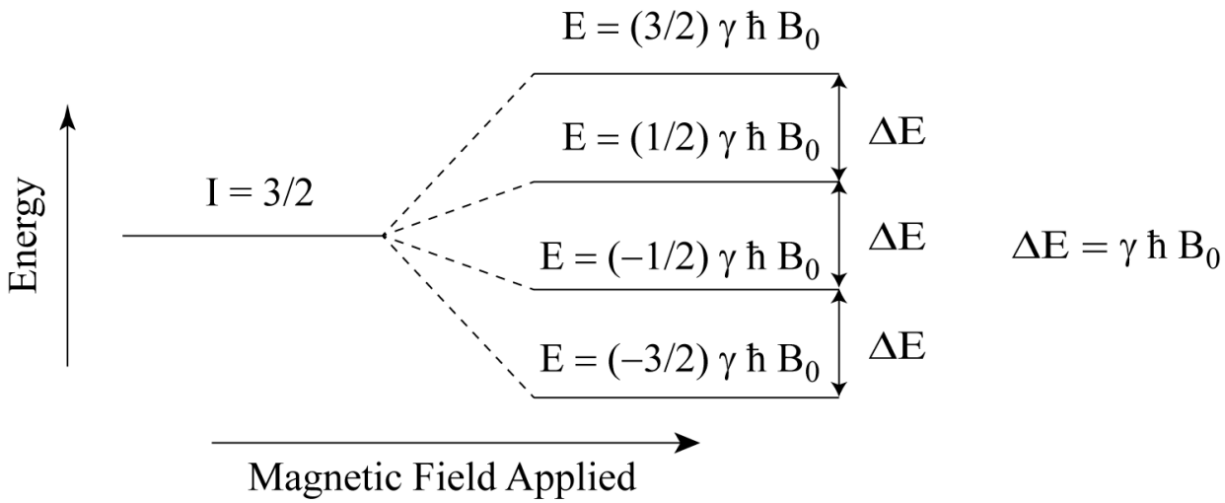

Figure 1.1. Zeeman interaction for a spin-3/2 nucleus.

equivalent to ΔE. For the purposes of this work, the other two interactions will act as perturbations to the Zeeman interaction.

In Figure 1.1, the equation for the energy gap depends on γ, the magnetogyric ratio of the nucleus in question, $\hbar$ which is the reduced Planck constant, and B_0 which is the magnetic field strength. It is this interaction which gives rise to the NMR signal, and in fact the exploitation of the energy level splitting between different spin states is the goal of NMR. Let us consider a nuclear spin system (assume a large group of isolated spin-3/2 nuclei which have a negligible quadrupole moment for the purpose of this discussion) which has been split into its respective energy levels by a magnetic field as described by Figure 1.1. These nuclei, if allowed to equilibrate, will reach a state wherein the higher energy levels become slightly under-populated, according to the Boltzmann distribution:

$$\frac{N_i}{N} = \frac{g_i \exp\left(-\frac{E_i}{kT}\right)}{\sum_j g_j \exp\left(-\frac{E_j}{kT}\right)}. \qquad \textbf{[1.2]}$$

This difference in population leads to a measurable net magnetization of the nuclear spins, wherein the spins aligning with the field will exist in larger numbers than those opposing it. The nuclear spin magnetization, being in an external applied magnetic field, will precess around the external magnetic field axis. This precession happens at a very specific frequency for a given nucleus, called the Larmor frequency:

$$\nu_L = \frac{\gamma B_0}{2\pi} \qquad \textbf{[1.3]}$$

which is proportional to the energy gap mentioned in Figure 1.1 and depends on the external field B_0 as well as the magnetogyric ratio γ, which is different for each nuclide or isotope. This precession is essential to NMR as it is what is detected in the radiofrequency coil in an NMR probe. Since the net magnetization is pointing directly along the axis of the main field, this precession will be undetectable, and therefore useless for the purposes of spectroscopy. A secondary electromagnetic field is required to perturb the magnetization, and to detect the strongest possible signal from the precessing spins, they should be perpendicular to the field. Since it is unfeasible to quickly apply and then remove a secondary external

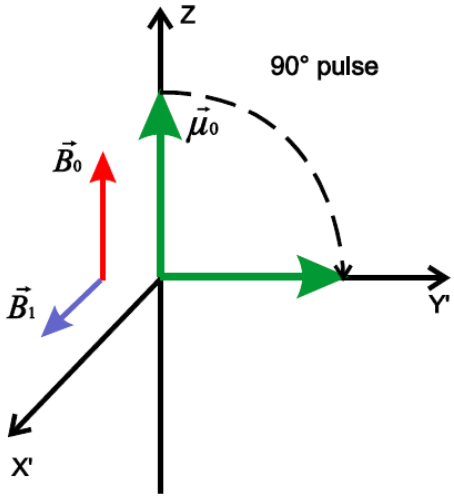

Figure 1.2. Net magnetization during a 90 degree pulse.[2]

field to the spins, a pulse of electromagnetic energy is used to excite the bulk magnetization. In practise, the energy required to rotate the spins about a secondary axis falls in the radio frequency (RF) portion of the spectrum. In SSNMR experiments, a solenoid coil is used to deliver high-power RF energy to the sample at its Larmor frequency, which causes the spins to precess about the new magnetic field created by the RF pulse. In the simplest of NMR experiments, this pulse is timed to cause the spins to rotate 90 degrees from the axis of the external magnetic field, leaving the magnetization perpendicular to said field (see Figure 1.2). This so called transverse magnetization is easily detectable by NMR, at least in simple NMR experiments like those performed on ^{1}H and ^{13}C where high magnetogyric ratios don't pose any further complications.

The second interaction which will be considered applies to any nucleus as well, and is called magnetic shielding. This interaction arises from interactions a nucleus has with electrons surrounding it. Protons can be viewed as having the same properties as small bar magnets, while electrons moving through space nearby give rise to currents which cause small magnetic fields around them. These small fields will act in a perturbatory manner to the main external field, disrupting the isotropic environment in which the nucleus would otherwise find itself. These shielding electrons will behave differently depending on the orientation of the external magnetic field, so in a powder this interaction will be anisotropic. The magnetic shielding tensor is symmetric, at least to a good approximation, and has a non-zero trace, which means that 6 independent components are required to fully describe its magnitude and orientation. It is important to mention that though magnetic shielding is the phenomenon which occurs at the nuclear level to perturb nuclei, experimentally we are not able to directly measure this shielding.[3]

Instead what we measure is called a chemical shift, and is related to magnetic shielding according to the following formula:

$$\delta_{ij} = \frac{\sigma_{ref} - \sigma_{ij}}{1 - \sigma_{ref}} \qquad \textbf{[1.4]}$$

This formula will convert each of the nine components of the magnetic shielding tensor:

$$\boldsymbol{\sigma} = \begin{bmatrix} \sigma_{11} & \sigma_{12} & \sigma_{13} \\ \sigma_{21} & \sigma_{22} & \sigma_{23} \\ \sigma_{31} & \sigma_{32} & \sigma_{33} \end{bmatrix} \qquad \textbf{[1.5]}$$

into the analogous component in the chemical shift (CS) tensor.

As mentioned above, the chemical shift tensor is regarded as symmetric, and so only 6 independent components are required to fully describe it. Three of these components can be expressed as angles which relate the orientation of the tensor to the molecular frame, which for the purposes of this discussion is arbitrary and therefore these components will not be considered here. The three important components which remain after the tensor has been diagonalized are called the principal components of the tensor, and are named and ordered as such:

$$\delta_{11} \geq \delta_{22} \geq \delta_{33} \; and \; \sigma_{11} \leq \sigma_{22} \leq \sigma_{33} \qquad \textbf{[1.6]}$$

Note for completeness that the ordering for chemical shift is the reverse of that of magnetic shielding; this difference arises from the math of the conversion. For simplicity, the chemical shift tensor will be used in further discussion. However, when references are made to quantum chemical calculation, note that magnetic shielding is what is calculated, and that an appropriate conversion has been made to give the results in terms of chemical shift. In order to

do this, a calculation must be done on a reference nucleus which is then further compared to very accurate and complex calculations which measure the shielding around a bare nucleus which has no electrons orbiting it.

This ordering system, while convenient, is not the most useful way to describe the components of the chemical shift tensor. The convention used in this work was proposed at the Maryland convention[4] and uses three slightly more useful parameters to describe the tensor. The first and most useful parameter is the average of the three principal components, called the isotropic shift:

$$\delta_{iso} = \frac{\delta_{11}+\delta_{22}+\delta_{33}}{3} \qquad \textbf{[1.7]}$$

This parameter is less important as the spectrum becomes broader, but it retains its usefulness as it gives an indication of the average environment surrounding the nucleus. The next parameter is called the chemical shift span, and is calculated thusly:

$$\Omega \cong \delta_{11} - \delta_{33} \qquad \textbf{[1.8]}$$

The span of a chemical shift tensor is important because it represents the difference in chemical shift of the nucleus between the molecule-fixed principal axis system being oriented parallel to the magnetic field and it being perpendicular. These two values represent the two most extreme chemical shifts the nucleus can experience simply through molecular rotation in the magnetic field.

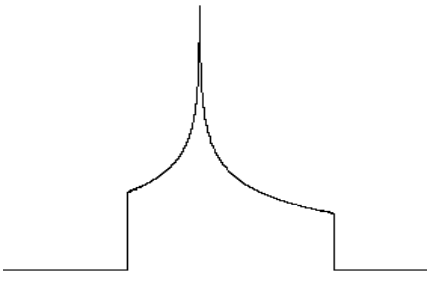

Figure 1.3. Typical CSA line shape (I=3/2) with a skew of 0.3.

The final parameter gives a measure of the asymmetry of the tensor; in other words it is a measure of the distribution of resonance frequencies within the range given by the span. The formula for the last parameter, the skew of the tensor, is below:

$$\kappa = \frac{3(\delta_{22} - \delta_{iso})}{\Omega} \qquad \textbf{[1.9]}$$

This parameter contains a factor of three and refers to each of the other principal components. The skew can take any value ranging from 1 to -1 which represents the fractional position of the greatest percentage of spins which have the same chemical shift (see Figure 1.3). With these three components, it is possible to fully describe the chemical shift tensor of a given nucleus.

The final and most uniquely pertinent interaction to this study is the quadrupolar interaction (QI). The QI arises from the coupling of the nuclear quadrupole moment (*Q*, which is a result of an uneven distribution of charge in the nucleus) with the electric field gradient (EFG) at the nucleus, which can also be described by a second rank tensor. Since this tensor is symmetric as well as traceless, it does not require all three of its principal orthogonal components: $|V_{33}| \geq |V_{22}| \geq |V_{11}|$, to fully describe it. This particular tensor can be described by 5 independent components, three of which can be expressed as angles relating the tensor to another frame, which can, for example, be the magnetic shielding tensor frame. The magnitude and asymmetry of the EFG can now be described in a very simple way, with only two independent parameters relating to the principal components of the tensor. These two parameters are the quadrupolar coupling constant (C_Q) and the quadrupolar asymmetry parameter (η_Q). The equations describing these parameters are below:

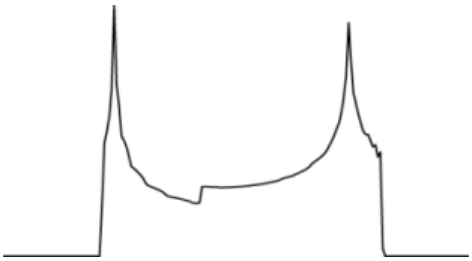

Figure 1.4. Typical quadrupolar line shape (I=3/2) with an asymmetry of 0.1

$$C_Q = \frac{eV_{33}Q}{h} \qquad \textbf{[1.10]}$$

$$\eta_Q = \frac{V_{11}-V_{22}}{V_{33}} \qquad \textbf{[1.11]}$$

where *e* is a fundamental unit of charge and *h* is Planck's constant. The asymmetry of the interaction, η_Q, necessarily ranges from 0 to 1, with a value of zero corresponding to axial symmetry (see Figure 1.4).

The final set of important parameters which are important in quadrupolar NMR are the Euler angles, which relate principal axis systems (PAS) to one another. As the QI and CS interactions are second rank tensor quantities, three of these angles are necessary, as shown in Figure 1.5. For example, the crucial PAS in NMR is the molecular PAS, the one which holds the molecule or atom in question rigid while interactions are considered in three dimensions around it. This PAS is related to the main magnetic field, which is defined as being aligned with the z axis. From that definition, any molecule in the field can be related to the magnetic field based on the Euler angles. In NMR experiments, the Euler angles are traditionally only used to relate PASs to one another. For example, in the figure below, the relation the

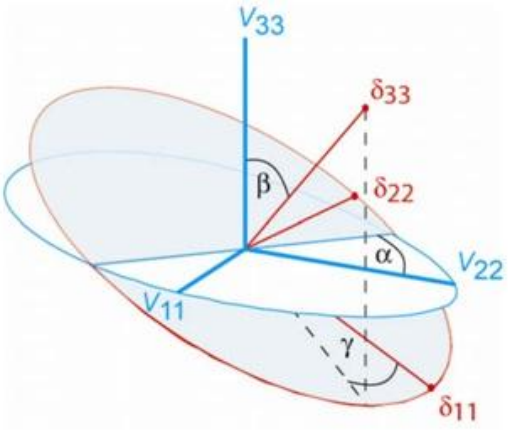

Figure 1.5. The three Euler angles and how they are viewed. α is the rotation of δ about V_{33}, β is the rotation about the new δ_{22}, and γ is a further rotation about the new δ_{33}.[21]

Euler angles describe is the rotation of the CS tensor in the EFG tensor's frame.

In nuclei such as the quadrupolar halogens which form the basis of this study, both of these interactions are present simultaneously and their separate effects are not inherently discernible in spectra, rendering the parametrization of these spectra quite difficult. There are, however, other ways of separating or separately altering the extent to which these interactions perturb the spectrum. The simplest method for doing this is called magic angle spinning (MAS).[5] In this experiment, the sample is spun rapidly at 54.74° with respect to the magnetic field (the "magic angle"), which causes the chemical shift interaction to be averaged to zero. While this is only the case when the sample can be spun at a higher frequency than the width of the spectrum, it is nevertheless a useful technique and is simple to implement if the compound in question fits within the capabilities of the hardware required to spin the sample. This technique has the effect of removing the anisotropic effects of the chemical shift interaction. MAS also removes the quadrupolar interaction to first order, as well as reducing second-order quadrupolar broadening by 2-3 times, greatly simplifying the spectrum and allowing for its fitting with only a few parameters.

1.2 Scope of Thesis and Objectives

This work aims to characterize and describe the chlorine-35 and bromine-81 EFG and CS tensors in a series of haloanilinium halide salts. Succinctly, the two key objectives are: (i) to record benchmark NMR data for these compounds and describe the data in the context of other related NMR data, and (ii) to investigate the possible relationships between the NMR parameters and the halogen bonding environment. Quadrupolar halogen SSNMR is a field which has been developed by a few groups in the last 5-10 years, but continues to allow many opportunities for study. Several studies have been conducted on organic chloride salts,[6] while bromide ions in reasonably low symmetry sites remain largely unexplored. There are several instances in literature where SSNMR has been used in determining strength and directionality of hydrogen bonding, which is present in this series of compounds. These compounds also contain short halogen-halide contacts which are referred to as halogen bonds which will be the focus of one section (see Chapter 3 for literature review) of this thesis. Pairing the experimental NMR data with x-ray diffraction data in the literature and acquired in the course of this work allows for even more detailed understanding of the types of interactions in which these halide ions are involved. With x-ray diffraction data comes the required experimental atomic coordinates to perform quantum chemical calculations (see Chapter 5 for background and theory) with a much greater degree of accuracy than would otherwise be possible. Quantum calculations are a helpful tool for assisting with understanding the electronic basis for a given set of NMR parameters and how those parameters relate to molecular structure. Two types of calculations have been used to assist in the complete description of the halide environment. Gauge-including projector-augmented wave density functional theory GIPAW-DFT[7] calculations necessarily use x-ray crystal data to approximate actual crystal environments in a lattice framework. Conversely,

Gaussian software which uses molecular orbital theory, molecular mechanics, and ONIOM[8] (our own n-layered integrated molecular orbital and molecular mechanics) whose algorithms allow for a less rigid, much less defined structural motif. This allows more freedom when building molecular structures, but restricts realism as full crystal structures are not modeled.

The second chapter of this work introduces the more specific topic of solid-state quadrupolar halogen NMR, and the challenges and nuances of performing experiments on those nuclei (chlorine, bromine, and iodine). A literature review of the last 10 years in the study of these nuclei will also be presented in this chapter, along with some insights which will help with the current study.

The third chapter contains a definitive description of halogen bonding, which comprises a large part of the discussion in the chapters following it, as well as a thorough review of the recent literature surrounding the halogen bond. Also in this chapter is a brief history of halogen bonding, as well as an overview of a few of the applications of halogen bonding in solid- and liquid-state chemistry and some of the important advancements in those fields which can be attributed to it.

Chapter 4 contains the new x-ray crystallographic data obtained in the course of this work as well as the ^{35}Cl and ^{81}Br SSNMR data obtained both at the University of Ottawa as well as at the Ultrahigh-Field NMR Facility for Solids in Ottawa. This chapter also contains experimental details pertaining to synthesis as well as to the NMR experiments. The end of this chapter discusses the relationship between NMR parameters and structural features from the crystal structures. Chapter 5 explores a variety of calculations which were undertaken to correlate NMR parameters directly to specific structural features. Comparisons of these calculations are also

made to experimental values to test the efficacy of the calculations as well as their accuracy. A thorough computational exploration of the possible relations between halogen bonding and NMR parameters is also presented in this chapter, ending with one specific trend which shows promise as a probe of halogen bond strength in these types of compounds.

Finally, chapter 6 gives some conclusions which can be gleaned from the experimental and computational data, and about the testing of halogen bonding in these types of compounds. The end of this chapter describes directions future projects could go in pursuit of a more complete description and understanding of the competition between hydrogen and halogen bonding in these types of compounds, and suggests some topics for studies which could further that knowledge.

SSNMR can provide information on local structure in a compound which is not possible with any other spectroscopic technique. Very subtle changes in structure from one compound to the next can lead to drastic changes in SSNMR parameters. This is one important aspect of the study of a group of distinct but related compounds. In this study specifically, studying compounds which are similar and exist in groups of three which vary in a predictable way allows for a solid foundation on which conjectures and theories can be based. These theories can be further tested with calculations and either supported or refuted based on the results of those calculations. With the recent advances in NMR technology, specifically probe design and ultrahigh magnetic fields, new experiments which could not be considered previously are now becoming possible. New pulse sequences are also being developed which can lead to signal enhancement and can considerably shorten experiment time at the expense of some spectral

resolution. These pulse sequences, while reportedly time-saving and useful, are not explored in this study. More reliable, time-tested methods are used instead (*vide infra*).

Chapter 2

Introduction to Solid-State Quadrupolar Halogen NMR

2.1 Background

Nuclear magnetic resonance (NMR) spectroscopy is a decades-old technique which measures subtle changes in the magnetic and electronic environment at and surrounding a given nucleus. These changes can arise from bonding electrons or non-bonding electrons from a nearby nucleus, and also from nuclei and charged ions in the crystal lattice. Important chemical information can be gained from these experiments, which are also very sensitive to even minute changes in structure. While liquid-state NMR is excellent for determining average environments of nuclei in solution, it is not helpful for solid applications, and for heavier nuclei or those which bond in more complex ways. A solution-state NMR spectrum consisting of a singlet gives only a fraction of the information which SSNMR can provide. Solid-state NMR (SSNMR) spectroscopy allows a much larger range of information to be extracted from nuclei, since structural constraints are not averaged out by molecular tumbling. Also, minor interactions such as dipolar and *J* coupling, which are not discussed here, can impair resolution or prevent assignment of peaks in solution. These couplings often have a reduced impact on the line shapes in solids due to the breadth of the signals. In the case of most quadrupolar nuclei, and for all of what will be seen in this work, line shapes are broad enough that these interactions can be ignored entirely.

A solid-state NMR experiment can be as simple as a regular 90 degree pulse and Bloch decay.[9] There are, however, issues which complicate the acquisition of these spectra with a one-

pulse experiment (*vide infra*). The halogens in this study are all quadrupolar, and so their detection will require advanced NMR techniques.

Quadrupolar nuclei (those with a nuclear spin quantum number I greater than ½) often have very short free-induction decays (FIDs) which may decay to below the level of noise before the receiver has an opportunity to recover from the high-power RF pulse and begin detection. This fast decay is a result of the nuclear spins' interactions with their surroundings. Therefore, since the decay constant of the FID and the breadth of the frequency domain spectrum are reciprocal, in the case of halogen NMR the spectrum can be extremely broad (e.g., several MHz or tens of thousands of ppm depending on the applied magnetic field strength and the nuclear environment).

Chlorine, bromine, and iodine are commonly found in two important forms, as covalently bound atoms typically on carbon chains, and as negatively charged ions in salts. Both of these forms are useful in their own rights, though in terms of NMR responses they are complete opposites. On one hand, collection of SSNMR data for ionic chloride is typically straightforward, as the line shapes tend to be narrow enough to require only a single echo experiment. Conversely, attempts to collect SSNMR data for covalent chlorine atoms is often met with either a large time expenditure or a complete inability to collect signal due to the extreme broadness of the lines. For bromine, line shapes tend to be about 5-10 times broader than those for chlorine, and so collection of data for ionic bromide systems is still feasible. However, collection of data for covalent bromines is completely unreasonable, as powder patterns can span several hundreds of MHz, which would require several days or even weeks to acquire. Bearing these facts in mind, it is not surprising that data for these nuclides is quite sparse compared to common organic nuclei in solids such as ^{13}C and ^{15}N.

When compared to simple NMR experiments such as those involving ^{1}H or ^{13}C, quadrupolar halogen NMR does present some complications. First, the difficulty inherent to chlorine NMR is the fact that it has a small magnetogyric ratio (see Table 2.1). This leads to low sensitivity of nuclei to the NMR experiment, and since strong pulses are required, probe ringing can also be an issue. In this case, echo experiments are necessary to acquire any signal in almost all chlorine NMR experiments. In an echo experiment, probe ringing issues are avoided by using a second pulse at a time after the 90 degree pulse (see Figure 2.1). This pulse, which can be either 90 or 180 degrees, is called an echo pulse, because it reverses the direction of the nuclear spins' dephasing. It is this dephasing which causes such rapid loss of signal, and the application of this second pulse will cause the spins to rephase. At a time equal to the delay between the two pulses, the echo delay, the rephasing of the spins will cause them to realign, giving rise to a temporally symmetrical signal identical to the original signal but without any probe ringing.

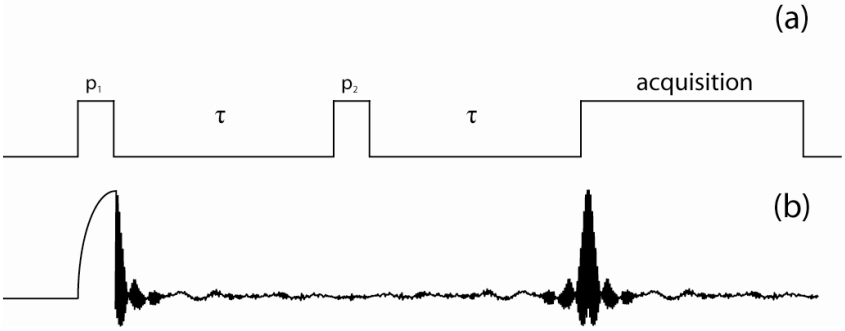

Figure 2.1. Echo pulse: (a) Pulse sequence for the echo experiment (b) Visualizing the time-domain response, if it were possible to acquire for the entire sequence.

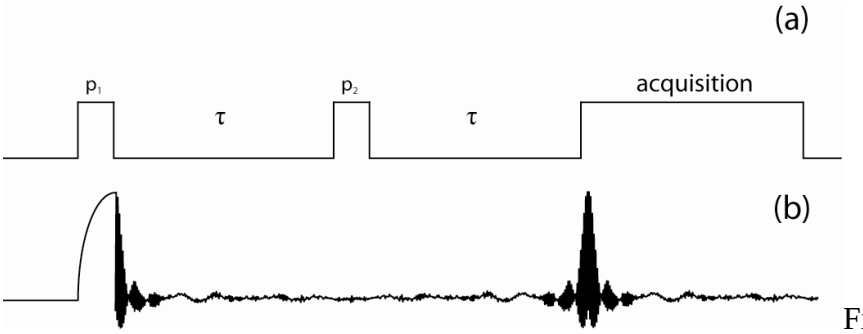

Chlorine-35, the nuclide which is central to the chlorine portion of this study, has a natural abundance of just over 75 %, which is very useful because its low sensitivity would otherwise preclude efficient NMR experiments. Bromine-81, the nuclide central to the bromide portion of this study, has an average magnetogyric ratio, similar to that of carbon-13. This is convenient because most NMR probes are already designed to tune to this frequency. The complication with bromine is the much larger quadrupole moment of the nucleus, which leads to a large broadening of resonances, to the point where complete spectral acquisition is only possible in extremely symmetric environments. The variable offset cumulative spectrum[10] (VOCS, see Figure 2.2) acquisition method is used in cases where the line shape is broader than the receiver is capable of collecting in one shot. This method involves setting the receiver at equally spaced intervals across the breadth of the pattern in order to acquire its complete line shape. After collecting a series of spectra with the same number of scans and identical pulses and delays, at properly spaced intervals (whose distance apart depends on the power and length of the pulses used, see Figure 2.3), the spectra can be Fourier transformed and processed separately as usual. The final step is to co-add all the pieces onto a flat baseline to give the complete spectrum in the frequency domain.

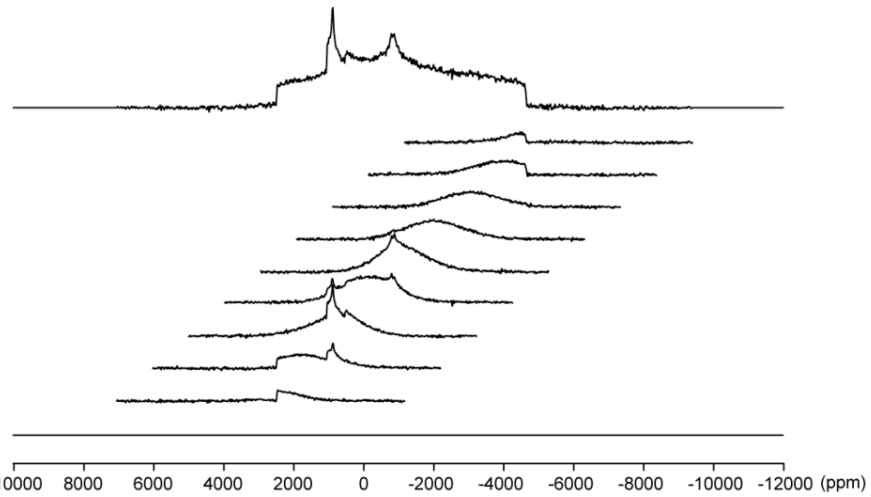

Figure 2.2. Variable offset cumulative spectrum method.

Once the final spectrum has been produced, the next step is to fit the spectrum to a set of parameters which match the experimental line shape. Depending on the type of spectrum and NMR techniques used, the required parameters will differ. For the static experiments on quadrupolar nuclei like the halogens, the parameters for the quadrupolar interaction (QI) and CSA will be used, since those are the interactions which affect the spectrum. In MAS experiments, the CSA is averaged by rapid spinning, and so the only parameters which are required to fit these spectra are the quadrupolar coupling constant (C_Q) and the quadrupolar asymmetry parameter, as well as the average, or isotropic chemical shift (see Chapter 1).

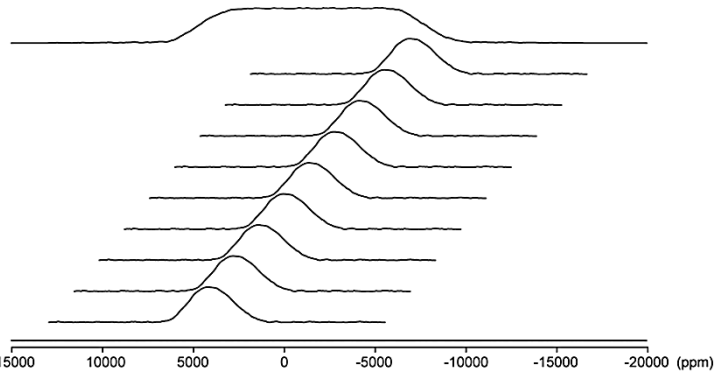

Figure 2.3. Co-adding Gaussian shapes to get a flat baseline can be used to calculate how large transmitter frequency steps should be. In this case the Gaussian peak is about 650 kHz broad and the steps have been optimized at 150 kHz apart.

At low magnetic field, the QI is the dominant interaction, whereas using an ultrahigh field such as exists at the National Ultrahigh Field Facility for Solids in Ottawa provides the ability to capture the CSA effects as well, which is of the reasons why the facility is so useful for ultrawide line shapes. The breadth of the central transition arising from the QI, to second order, scales inversely with magnetic field strength[11]:

$$\Delta\upsilon_{CT} = \frac{25+22\eta_Q+{\eta_Q}^2}{144}\left[\frac{\left(3C_Q\right)^2}{\left((2I)(2I-1)\right)^2}\right]\left[\frac{I(I+1)-\frac{3}{4}}{\nu_L}\right] \qquad \textbf{[2.1]}$$

hence the powder pattern becomes narrower at higher fields. The breadth of the central transition depends inversely on the Larmor frequency, ν_L of the nucleus, which itself scales with

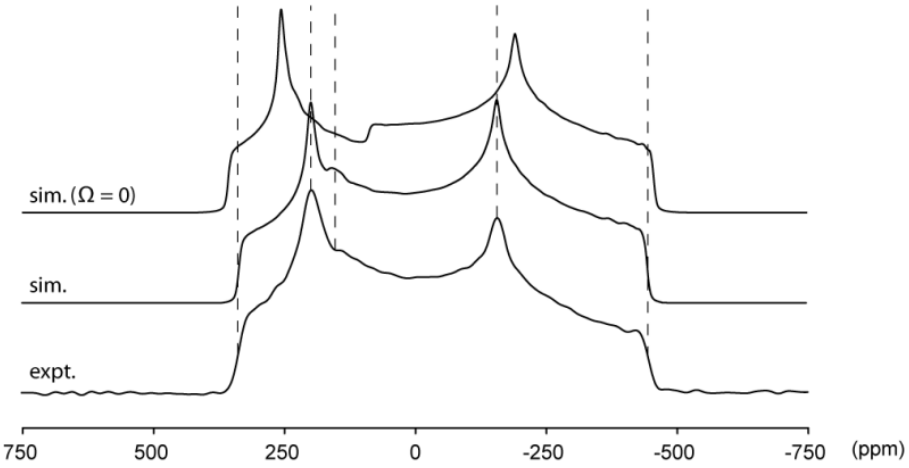

Figure 2.4. Visualizing changes in SSNMR powder patterns with and without CSA

magnetic field. The spectrum acquired at higher magnetic field will have a stronger dependence on the chemical shift tensor (which scales with B_0, in Hz, see Chapter 1) and chemical shift anisotropy will be much easier to detect at this field, whereas at low field the line shape will be almost entirely due to the QI.

Especially with quadrupolar nuclei, there are many different parameters which may produce similar effects on the line shape, so when there are CSA and quadrupolar effects present simultaneously, the spectra can be very difficult to simulate with any confidence. In total there are 8 parameters used to fit the spectrum. One way to increase the reliability of the results is to acquire the spectra at multiple magnetic field strengths. Therefore, in the present work, at 9.4 T, changes in line shape due to CSA will be very difficult to see, whereas at 21.1 T, CSA effects will be visible in the spectrum (see Figure 2.4).

Another method for increasing certainty in the fitted parameters is to acquire spectra from other isotopes of chlorine and bromine. This technique is not broadly applicable, but both bromine and chlorine have a second stable isotope with a Larmor frequency not unlike their more abundant partner. Chlorine-37 and bromine-79 SSNMR are generally performed if the fit of a spectrum is in doubt or if another magnetic field is not available. These nuclides have properties which are similar to the conventional halogen NMR nuclides but are not always used

either for reasons of sensitivity or for overlap with other more common nuclei. Chlorine-37 is about three times less abundant than chlorine-35, and has a smaller magnetogyric ratio, which is difficult to tune to on even low-frequency probes, and causes even more issues with respect to low sensitivity. Bromine-79 on the other hand, has properties which are quite similar to bromine-81, but its spectrum tends to overlap with carbon-13, and since that nucleus is many times more sensitive and typically quite abundant in samples, bromine-79 NMR is typically not the first choice. There is also the minor fact that bromine-79 gives lines which are approximately 20 percent broader than those of bromine-81. The nuclear properties of the quadrupolar halogens which are the subject of this study are tabulated in Table 2.1 & Table 2.2:

Table 2.1. Nuclear properties of the quadrupolar halogens[12]

	I	**N.A. (%)**	**$\gamma/10^7$ (rad T^{-1} s^{-1})**	**ν_0 @ 9.4 T (MHz)**	**Q (10^{-30} m^2)**	**Relative CT Linewidth[a]**
^{35}Cl	3/2	75.78	2.624198	39.19	-81.65	1.34
^{37}Cl	3/2	24.22	2.184368	32.62	-64.35	1.00
^{79}Br	3/2	50.69	6.725616	100.21	313	7.70
^{81}Br	3/2	49.31	7.249776	108.02	261.5	5.01
^{127}I	5/2	100	5.389573	80.03	-710	11.44

[a] Central Transition line width for a powder sample.

Table 2.2. Larmor frequencies for halogen isotopes at all pertinent magnetic fields

B_0 Field	**Chlorine ν_0 (MHz)**		**Bromine ν_0 (MHz)**		**Iodine ν_0 (MHz)**
Isotope	**35**	**37**	**79**	**81**	**127**
9.4 T	39.19	32.62	100.21	108.02	80.03
11.7 T	48.99	40.78	125.27	135.03	100.04
21.1 T	88.18	73.40	225.48	243.05	180.06

2.2 Literature Review of Quadrupolar Halogen SSNMR

There have been several studies performed by our group[6,12,13] involving various organic hydrochloride salts and alkali and alkaline earth metal chlorides, as well as studies of similar environments concerning ionic liquid chlorides,[14] organometallic chlorides,[15] and group 13 chlorides.[16] Bromine SSNMR has not been explored as extensively as chlorine, but there are some data, also mainly for near-symmetrical environments. For example, alkali and alkaline metal earth bromides have been explored in detail,[17] as well as some simple organic bromides[18] and ionic liquids[19]. Organic hydrobromides are a largely unexplored area, as well as other inorganic metal bromides.

The alkali metal and alkaline earth salts for chlorine and bromine have been studied, and the iodine salts studies are in progress or have recently finished.[13] Most of those give narrow spectra (on the order of tens to hundreds of ppm) which are measurable in one piece, especially at high field. The field of chlorine SSNMR is well behind carbon and the other common half-integer nuclei but there are some data for chloride-containing organic salts[20] for comparison. These spectra are also narrow for the most part, although some do have the complication of containing more than one magnetically non-equivalent site, resulting in overlapping line shapes. In terms of bromine-79/81 SSNMR spectra of bromide-containing compounds, considerably less data are available,[21] since these spectra tend to be broader, due to a larger quadrupole moment (Table 2.1), and therefore piecewise data acquisition can be necessary (*vide supra*). Iodine-127 SSNMR is the least studied of the three in terms of the amount of data, since iodine-127 has a very large quadrupole moment, which tends to lead to extremely broad spectra in most cases. There are advantages and disadvantages associated with data collection of all three halides (see Table 2.1), but with the right series of compounds all three can be compared and contrasted.

Another useful method of collecting SSNMR data is through 2D NMR experiments. These experiments, like multiple-quantum MAS[22] (MQMAS) and satellite transition MAS[23] (STMAS), allow for the separation of the SSNMR line shape from its isotropic shift in MAS spectra. This technique is very useful in compounds with multiple sites, as the two-dimensional nature of the experiment allows for the separation of peaks with different isotropic shifts and gives exact values for isotropic shifts without fitting. In MQMAS, quadrupolar broadening is removed in one dimension through excitation of multiple quantum coherences followed by a transfer of this magnetization to the central transition for detection. STMAS works in much the same way, but uses magnetization transferred from the satellite transitions in order to increase the population difference between the central transitions energy levels. However, the usefulness of these experiments is limited for the quadrupolar halogens, since spectra for these compounds typically are not narrow enough to render MAS feasible. There has only been one report of chlorine MQMAS in the literature,[24] measuring some chlorine containing sodalite compounds.

Another interesting experiment which can be applied to the SSNMR study of quadrupolar halogens is QCPMG, [26] the quadrupolar version of the Carr-Purcell-Meiboom-Gill pulse sequence. This experiment is used to enhance sensitivity, and it does so by collecting the signal from the line shape into a series of spikelets at evenly spaced intervals (see Figure 2.5). This behaviour of the line shape stems from the acquisition process, wherein a series of echoes are collected, as

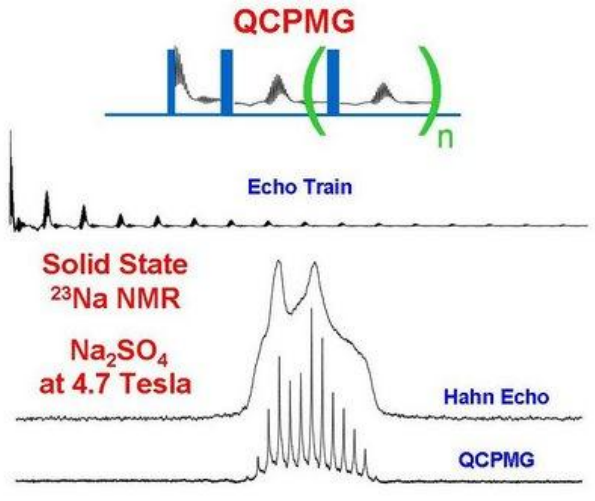

Figure 2.5. QCPMG pulse sequence, FID and resulting spectrum.[25]

opposed to the single echo in a typical SSNMR experiment. This so-called echo train contains many duplicates of the same signal with decreasing intensity, as this signal depends on the actual transverse relaxation time (T_2) of the nuclei, and not the reduced transverse relaxation time (T_2*) which is affected by local magnetic field inhomogeneities. By virtue of this fact, the amount of total signal which can be gained from QCPMG is much higher than from just a single echo experiment. There are really only two major downsides to QCPMG; the first being that it takes considerably longer to set up than a traditional echo experiment due to the complexity of the pulses and powers involved. The other downside is that while the gathering of signal into spikelets does drastically increase apparent signal to noise, the spikelets are prone to distortion and artifacts which can lead to misreading the spectrum and unnecessary complication in already difficult to fit spectra. There is also the issue of setting the separation frequency between the spikelets; too large and there won't be enough data to properly fit the spectrum, too small and the inherent sensitivity gain will be lost in the sheer number of spikelets. QCPMG can be considered a useful alternative to echo experiments provided setup is done carefully and the spectrum is not too complicated.

Some other less common SSNMR experiments which can be used for the signal enhancements of wider line shapes include double-frequency sweeps (DFS)[27] and hyperbolic secant pulses,[28] both of which use more complicated pulse sequences and pulses of varying frequency or phase to increase sensitivity and therefore signal in wider line shapes.

Putting new data into context with existing data is an important step in any fundamental study, and having some idea of what the results of an experiment will be before it begins begets an advantage to the spectroscopist. For chlorine SSNMR, there is a decently large data base to work with, with a wide range of compounds in various fields having been studied.

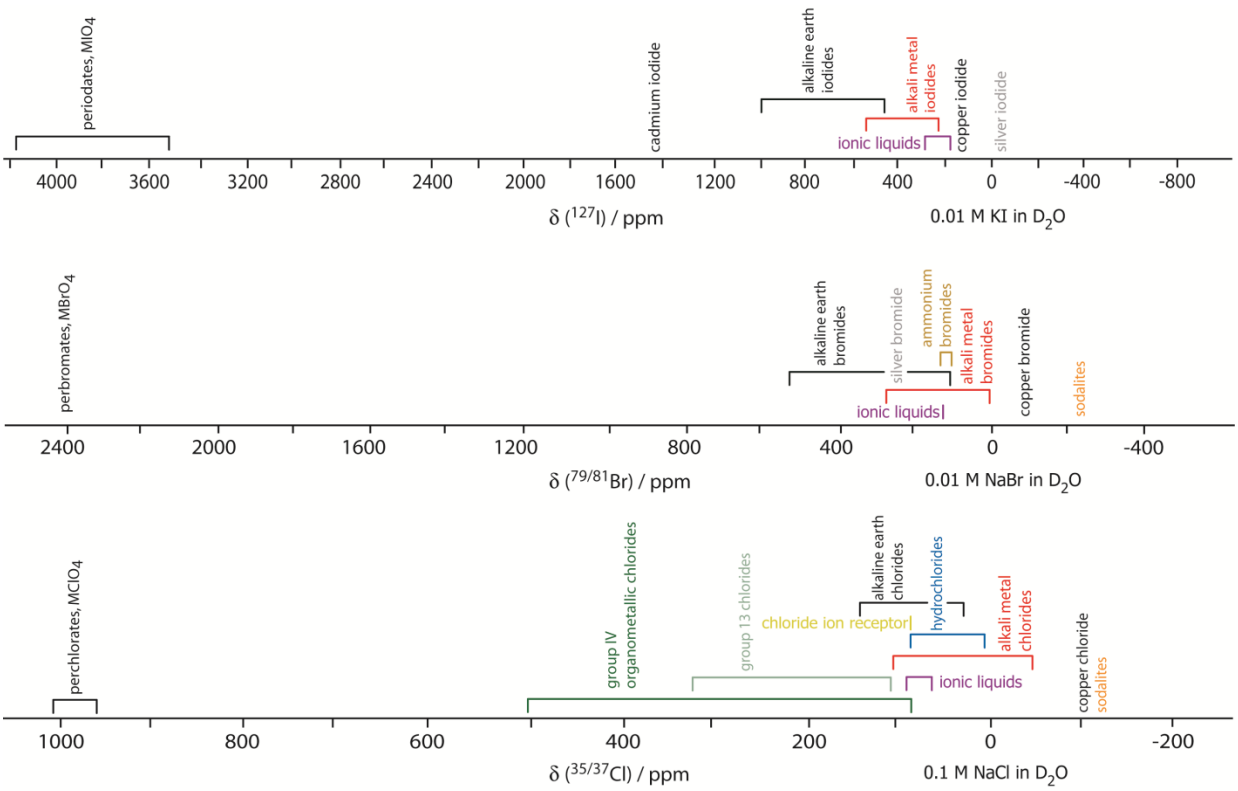

Figure 2.6. Chemical shift ranges in the solid state for known chlorine, bromine and iodine compounds.[21]

Unfortunately, such a large data set is not available for bromine and iodine in terms of EFG and CS tensor parameters, though some information can still be gleaned from the data which does exist in terms of what to expect from a new series of compounds (see Figure 2.6 for chemical shift ranges).

As mentioned above, there have been a variety of studies done on materials containing chloride ions, ranging from biological molecules to glasses. The known chemical shift range for chlorine goes from -78.06 ppm for CuCl up to 1049.3 ppm for $KClO_4$ (referenced to NaCl(s)). While this is a very large range, other than the perchlorates, most of the chlorines have isotropic shifts which fall between -100 and 500 ppm. These compounds also tend to have a wide variety of EFG and CS tensor parameters, with C_Q values ranging from about 1 MHz up to about 36

MHz, and chemical shift spans of up to 200 ppm. Though this is a very large C_Q range, if only data from compounds of an organic nature are considered the range shrinks from about 1 to 10 MHz, so this range is what is to be expected. There have been fewer reports of bromide and iodide tensor parameters outside of the cubic salts, though with the few reports of amino acid bromides the expected range of bromide for chemical shifts is -200 to 600 ppm. The C_Q values for organic bromide compounds are also expected to range from about 10 up to 50 MHz. The values which exist for iodide ions are based on alkali and alkaline earth metals, which are in environments which are quite different from the ones being studied, but will nevertheless give the only real comparisons to existing data which is possible for iodine. The C_Qs in these compounds range from about 50 MHz up to over 200 MHz, and there have been two reported spans, of 120 ± 80 and 300 ± 100 ppm. Given the lack of SSNMR data for this nucleus, it is difficult to say for certainty that the new data will fit into the existing range, but given its fairly large size, it is a good assumption. There are also some data for bromine and iodine pertaining to the perhalogenates[29] which are shifted to much higher frequency, but since these compounds are of little relevance to the current study, no further mention will be made of them.

The latest techniques to be applied to bromine and iodine SSNMR are called STREAQI[18] (Slow Turning Reveals Enormous Anisotropic Quadrupolar Interaction) and WURST [30] (Wideband, Uniform Rate, and Smooth Truncation) NMR, and they are useful for dealing with ultrawide line shapes. STREAQI is a 2D NMR technique which uses slow MAS to map out a correlation between the solid line shape and the isotropic shift. WURST is an extremely useful pulse sequence for solids because it is capable of capturing a much larger bandwidth using shaped pulses than a typical echo experiment is able to with one shot. This pulse sequence is typically combined with QCPMG to capture a wide bandwidth with an increased signal to noise

ratio. Whether or not this technique will continue to be applied to quadrupolar halogen SSNMR in the future remains to be seen.

Chapter 3

Halogen Bonding

3.1 Definitions

Halogen bonding is an interaction between a covalently bound halogen atom and a Lewis base, anything which can donate electron density. This bonding paradigm draws comparisons to hydrogen bonding, and the two can be considered somewhat analogous. The strict definition of a halogen bond is currently under investigation, but a good definition for the time being is as follows: a halogen bond is formed when the distance of the donor-acceptor interaction is shorter than the sum of the van der Waals (VDW) radii of the atoms forming the bond.[31] This definition is valid for any bond, and there is an equation which defines the orbital overlap accompanying the formation of a halogen bond:[32]

$$R = \frac{d}{r_X + r_D} \qquad \textbf{[3.1]}$$

where *d* is the bond distance and each of the *r* values represent the van der Waals radii of the atoms involved. *R* is therefore a measure of the degree of overlap of the atomic orbitals, where a value less than 1 indicates an interaction, while a value above 1 shows that the atomic orbitals do not overlap significantly. There is, however, a slight complication forming a firm definition. In hydrogen bonding, there is clearly a bond formed when a hydrogen atom attached to a heteroatom is pointing at a lone pair of electrons (see Figure 3.1). For halogen bonding though, there are two possible atomic arrangements which can allow for van der Waals overlap.

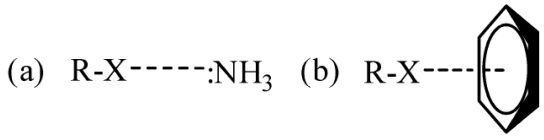

Figure 3.1. Typical Lewis bases for a halogen bond. (a) lone pair, (b) delocalized π-electrons. [33]

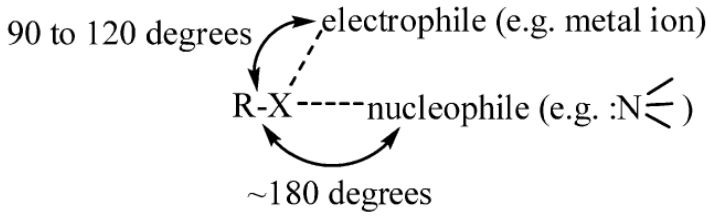

Figure 3.2. Possible halogen bonding modes.[33]

The first, and most common is the linear halogen bond, which as explained above is comparable in geometry and electronics to a hydrogen bond. The second and less common angular orientation is where there is an atom or group which forms a bond with the halogen at 90 degrees with the covalent bond[33] (see Figure 3.2). This type of halogen bonding requires an electrophile perpendicular to the covalent halogen bond to accept electron density, because of the band of negative electrostatic potential around the halogen when it is covalently bound.

The reason halogen bonding happens at all is due to the changing electron density around the halogen nucleus when the covalent bond forms (in typical applications this is a carbon-halogen bond). Because of the large number of electrons around halogen atoms, the entire surface of the halogen's electrostatic potential is typically negative. However, when connected covalently to a molecular system which is sufficiently electron-withdrawing, something unexpected will occur. On the side of the halogen atom opposite the covalent bond, if the molecule bound to the halogen is electron-withdrawing enough, an area of positive electrostatic potential can appear (seen in red, Figure 3.3). This spot is referred to as a sigma hole,[35] because the

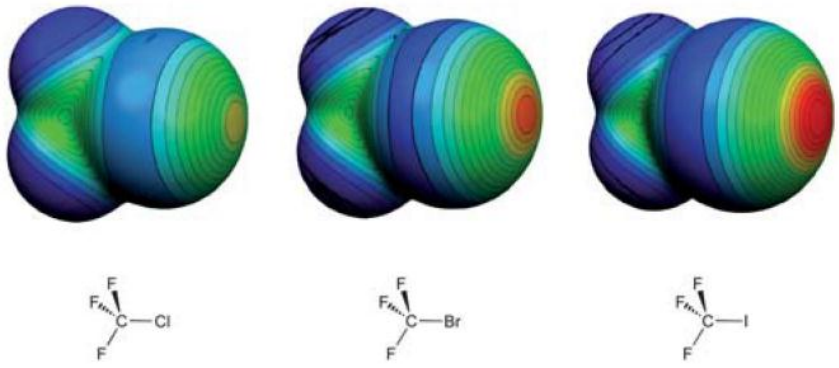

Figure 3.3. Enlargement of the sigma hole moving down the halogen series. Blue represents negative electrostatic potential, red represents positive potential, or the sigma hole.[34]

covalent bond is sigma type.

Typically this kind of anomaly is not seen for covalently bound fluorine compounds, because the atom is simply too electronegative. However, with the right combination of electron-withdrawing groups on the molecular frame, and a larger halogen atom, a sigma hole will inevitably appear.[36] In a straight comparison of chlorine, bromine, and iodine, the sizes of the sigma holes, and thus the strengths of the halogen bonds, increase moving down the column.

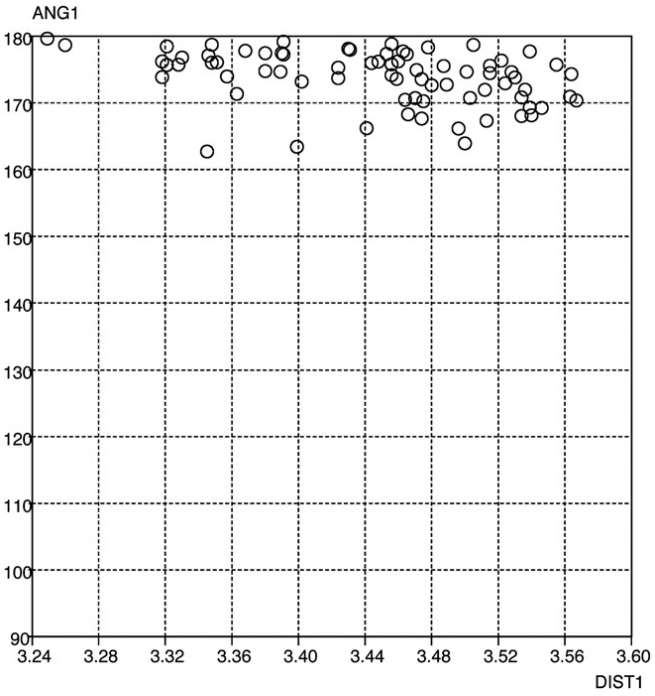

Figure 3.4. Correlation between halogen bond angle vs bond length in iodine-iodide halogen bonding paradigm.[38]

Strong halogen bonds are not always formed by chlorine, as has been shown and confirmed by experiment and in computational studies.[37] In cases where a true impactful halogen bond is desired in crystallographic studies, synthetic chemists will normally choose iodine as the halogen bond acceptor. This is because it is well known that iodine forms the strongest halogen bonds and also that the bonds it forms are the most linear[38] (see Figure 3.4) and the shortest.[38] Another common technique to induce strong halogen bonds in compounds which are chosen in crystal engineering is to perfluorinate the surrounding carbons, e.g., *p*-diiodotetrafluorobenzene. In so doing, the whole structure is made much more electron-withdrawing, pulling electron density from the covalent halogen bond, and enlarging the sigma hole.

The strengths of halogen bonds vary widely depending on the substituents on either side of the halogen, with theoretical strengths of the interaction having an upper bound of 180 kJ/mol (the I_2-I^- interaction in I_3^-), which is actually a very strong non-covalent bond.[39] This is under ideal circumstances with the strongest molecular fragments arranged in perfectly linear fashion, but still gives a good idea of the kinds of strengths these bonds will have under normal conditions. When compared to the hydrogen bond, which has been shown to exist with strengths of anywhere from about 5 kJ/mol (anything less than that is not enough to realistically be considered stable), to 155 kJ/mol,[40] the two interactions seem quite competitive. Compared to compounds where the halogen bond is a binding molecular interaction in the solid state, where the strongest halogen bond was found to have a more realistic measured strength of 153 kJ/mol,[41] the two interactions seem about on par with one another. In compounds where only hydrogen bonding exists, the addition of a halogenated compound could be all that is required to change the geometry to a point where a halogen bond begins to impact the lattice structure.[42]

3.2 Early History

Though the field of halogen bonding as it is currently being studied is only 10 to 15 years old and saw a fairly slow start, the fundamental interactions involved in the bonding have been known for quite a bit longer. The first publication to mention what we now call a halogen bond is a report by Frederick Guthrie in 1863.[43] Among many other compounds, he created an adduct of ammonia and molecular iodine from a mixture of ammonium nitrate and iodine. This compound has a short nitrogen-iodine distance, the first of many compounds with this particular configuration, though being 1863, the exact geometry and conformation of the interaction was not known. It was only upon decomposition of the material to form ammonia and molecular iodine that Guthrie decided he had formed $H_3N{\bullet\bullet\bullet}I_2$. Regardless, this is the first record of such a compound being found or created, and was the first of many compounds to be categorized as having a donor-acceptor interaction involving a halogen atom accepting electron density.

Though many compounds were discovered in the intervening time,[44] the theory behind halogen bonding remained largely undeveloped until the 1950s. At this time, Robert Mulliken devised a classification system for all donor-acceptor complexes which included a full description of halogen bonding,[45] though at the time the exact reasons for halogen bonding specifically were not yet known. At the same time, German chemist Odd Hassel began compiling x-ray data for many compounds,[46] a number of which contained halogen bonds. The first, and most well-known of these compounds is a complex containing 1,4-dioxane and molecular bromine in a 1:1 ratio. This compound formed in chains with significant overlap between the bromine and electrons from the oxygen atoms on the dioxane. In this compound, the bond is quite strong and the angle of the interaction is almost exactly 180 degrees, allowing for optimal overlap.

3.3 Review

Since the 1950s there have been many new compounds formed which include short halogen-donor interactions, and they have appeared and found uses in a variety of fields. Given the almost infinite array of possible combinations which can form involving covalent halogen atoms, it is no surprise that reports of compounds exhibiting these interactions are scattered across the literature, appearing everywhere from medicine, to liquid crystals and even in molecular magnets. The tunable nature of these compounds also allows for simple modifications to structure which lead to fine changes which can be useful in tweaking parameters in the crystal structure.[47] There are many literature reports of crystal structures which contain hydrogen bonds, but crystallographic studies for their own sake are not nearly as useful as ones which are applicable to other fields, and so applications will be the focus of this section. There is great interest in quickly and unambiguously determining halogen bonding distances and angles, without resorting to crystallographic studies if that is possible. Several possibilities for doing this have been proposed, just as similar methods have been developed for hydrogen bonding. The first method which will be discussed is using solid-state NMR in order to detect the presence and possibly strength of a donor-acceptor interaction, if it exists.

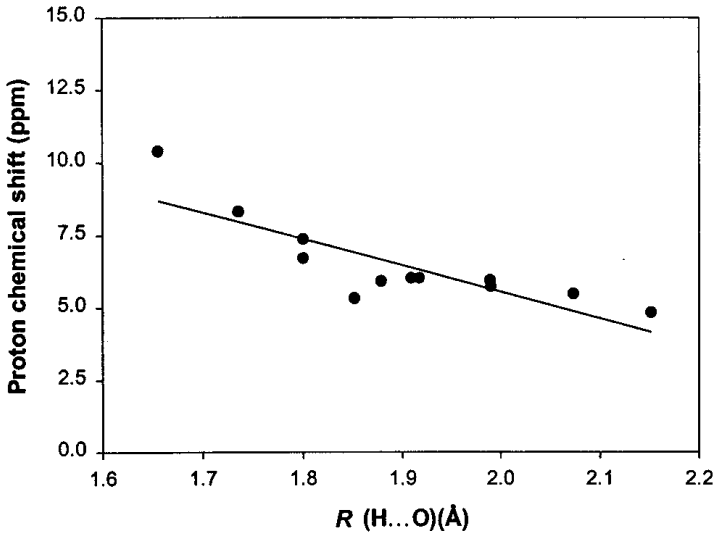

Figure 3.5. Experimental proton chemical shifts plotted as a function of the H•••O distance determined from X-ray crystallography for a series of metal and organic hydrates.[48]

In the hydrogen bonding realm, there have been several

attempts to characterize the number, orientation and strength of many hydrogen bonds in relevant or interesting systems. In 1998, Gang Wu et al.,[48] measured the proton SSNMR spectra of a variety of organic and inorganic hydrates in order to quantify any relationships which may exist between the geometry of the hydrogen bonding environment in those compounds and the NMR parameters measured by experiment. It was found that the trend in these compounds with respect to proton chemical shift was a decreasing shift with a lengthening hydrogen bond. This parameter held as a trend for a series of 11 relatively unrelated compounds (see Figure 3.5), and so attempting to apply it more broadly is not out of the question. Perhaps halogen bonding strength or at least bond length could be quantified by NMR in much the same way.

A second NMR related study which concerns halogen bonding directly this time was performed by Piotr Tekely et al.[49] in 2008. This study used an indirect halogen bonding probe (the halogen atom itself was not the nucleus of study) to determine N-I distances in a solid organic material (see Figure 3.6). Dipolar couplings can be related to bond distances through a set of simple calculations, the equation for which is here:

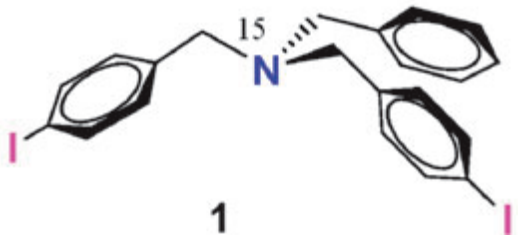

1

Figure 3.6. Structure of benzyl-di(4-iodobenzyl)-amine, subject of reference 49.

$$D_{12} = -\frac{\mu_0}{4\pi}\frac{\gamma_1\gamma_2\hbar}{r^3{}_{12}} \qquad \textbf{[3.2]}$$

and so halogen bond distances can be determined using ^{15}N SSNMR. With this in mind, a 1D ^{15}N SSNMR spectrum was collected and simulated. First, the spectrum was fit to a set of parameters which did not include any sort of dipolar effects. This spectrum was very close to fitting to the experimental spectrum (see Figure 3.7; bottom spectrum), but did not model it

perfectly. The top spectrum includes the effects of CSA as well as those of dipolar coupling to a would-be iodine atom. In this spectrum, the simulation can be fit perfectly to experiment, which is taken as proof that there is indeed a short nitrogen-iodine contact in the molecule. While this is an indirect probe of halogen bonding, in theory it nevertheless shows that dipolar coupling measurements could be a valid technique for measuring for the presence of halogen bonding as well as specific bond distances.

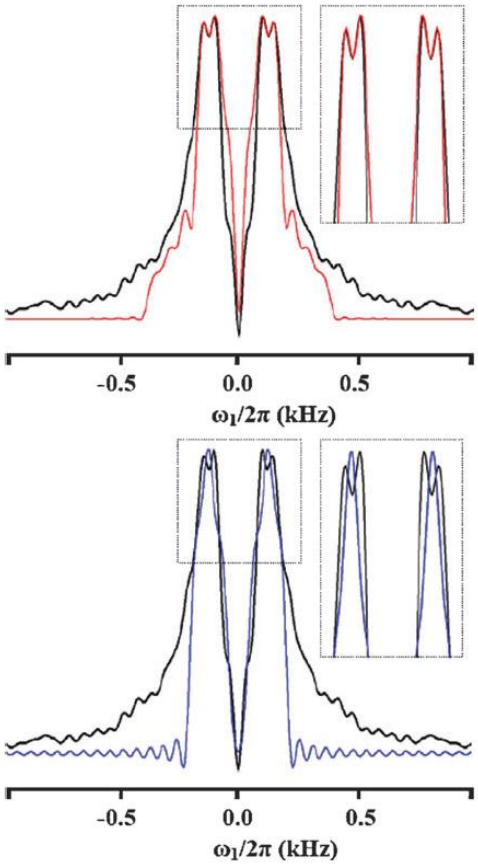

Figure 3.7. ^{15}N SSNMR spectra of benzyl-di(4-iodobenzyl)-amine (see Figure 3.6**).** Top spectrum (red) includes dipolar coupling; bottom spectrum (blue) only includes CSA effects. Black line represents experimental spectrum in both fits. [49]

Another interesting and novel use of NMR in the measurement of bond geometries was performed by Vitali Tugarinov et al.[50] in 2010. This study looked at *D*-labelled ubiquitin, a protein which is found in almost every tissue in the body. By labelling specific amino acids with deuterium, the chemists were able to measure quadrupolar coupling constants (QCCs, see Chapter 2) for those atoms which were involved in hydrogen bonds. The study used a Carr-Purcell-Meiboom-Gill (CPMG) sequence for deuterium to reduce measurement times and improve signal to noise in the spectra, while SEDUCE and WALTZ-16

decoupling sequences were included to decouple carbon and deuterium respectively. In these compounds, the deuterium QCC tends to decrease along with decreasing hydrogen bond distances, though the relationship is not linear (see Figure 3.8). As shown in Figure 3.8, the relationship is linear when compared to the inverse cube of the hydrogen bond distance; the reason for this comparison rather than using the bond distance directly is due to the EFG's inverse cube dependence on *r* as well. This methodology does show that it's possible to use QCCs to probe hydrogen bonding, and so it should be possible to transfer these ideas to halogen bonding.

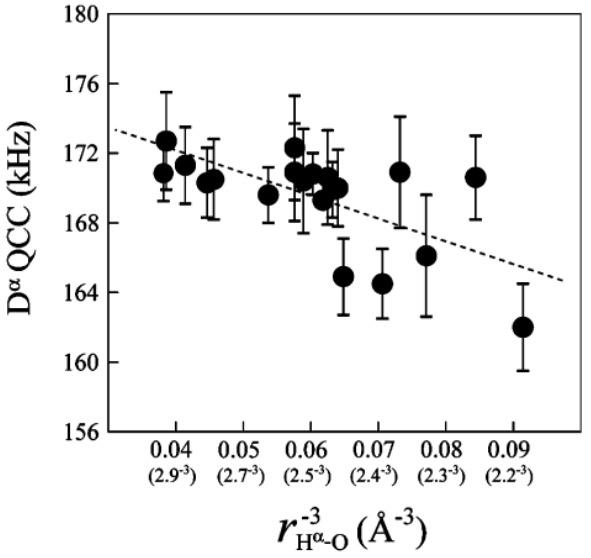

Figure 3.8. Relationship between the deuterium QCC and hydrogen bond lengths in ubiquitin.[50]

Another study, done by Jerome Boisbouvier et al.[51] in 2010 used a different technique to attempt to measure and correlate NMR parameters to structure. In this case, proteins were once again the subject of the study, though this article brings much more obscure interactions into consideration to measure weak hydrogen bonding. Hydrogen bonding is fundamentally between a hydrogen atom attached to an electronegative atom and a source of electron density, and weaker interactions than hydrogen bonding are still possible. In the case of this study, the interactions being measured are between CH groups in amino acids and the π-electrons on nearby side chains (see Figure 3.9). Heteronuclear multiple quantum coherence (HMQC) is a two-dimensional NMR technique which allows for the correlation of protons and carbon atoms which are close in space but are not necessarily bonded. In the 2D spectrum, a cross peak will

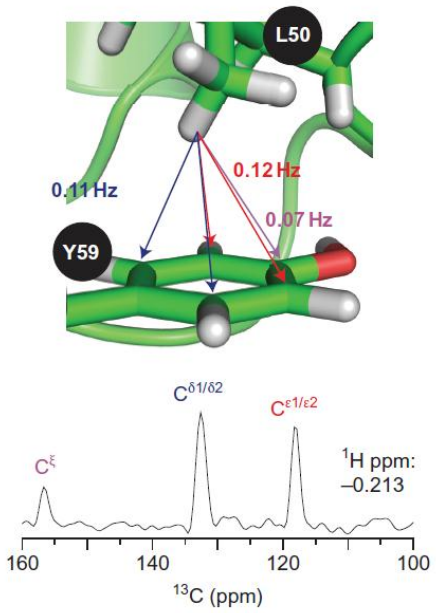

Figure 3.9. Sample geometry of CH-π interactions between a leucine residue and a nearby aromatic tyrosine ring in a labelled protein.[51]

form if the atoms are interacting, and so J coupling between the two involved atoms implies that they are at least weakly interacting. The strength of the coupling is therefore a good indication of the strength of the interaction. In the proteins from the study, there were over a hundred different small J couplings which were found, in addition to the normal ones which typically appear when performing J coupling measurements. This shows that there are more subtle effects than hydrogen bonding and π-stacking on protein folding and overall structure. This technique is very useful primarily because it isn't restricted to only certain nuclei, although the J coupling in larger and quadrupolar nuclei is much less obvious due to the width of those lines, especially when J couplings in the spectra presented are on the order of tenths of Hz.

As can be seen from the above cases, donor-acceptor interactions can be measured in a variety of ways using NMR-based techniques. Given this plethora of methods for probing hydrogen or halogen bonding, it would seem as though finding bonding trends in new sets of compounds wouldn't be very difficult, and applying the current methods more broadly should at least prove useful.

3.4 Applications

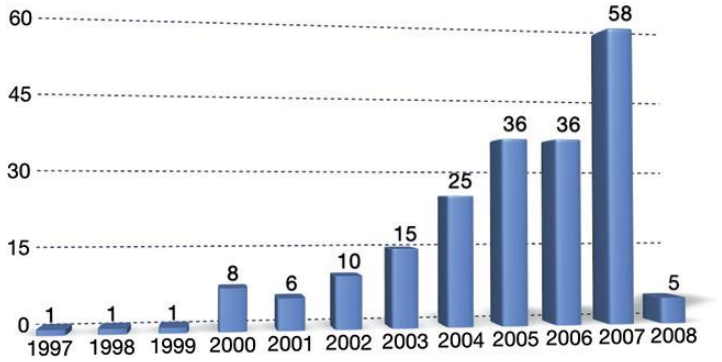

Figure 3.10. Papers with halogen bonding in the title from 1997 to early 2008.[38]

Halogen bonding is a field which has been around for almost two centuries, yet for a long time almost nothing was known about the way this bonding actually worked. However, in the last 10 to 15 years, this has definitely not been the case. Since the years 1997-9, when there was only one publication mentioning halogen bonding in each year, the number of papers on the topic has begun to grow exponentially (see Figure 3.10). Now papers on halogen bonding number in the hundreds per year, and show no signs of slowing down. In fact, this summer an IUPAC committee met in Spain to discuss halogen bonding in an attempt to more solidly define its parameters. As mentioned in the previous section, halogen bonding has found a variety of applications from the solid state as well as in solution, and in many different subject areas. There have been numerous reports of compounds containing halogen bonds which are being used as receptors for various ions, in self-assembly with halogen bonding driving selectivity, and even in areas of biology for protein complex formation and enzymatic catalysis.

In each of the above-mentioned topics, hydrogen bonding has been a commonly used tool of chemists to perform many selective tasks. In some cases though, hydrogen bonding has either not been up to the task, or alternatives were needed, and halogen bonding offers the variety to assist in this endeavour.

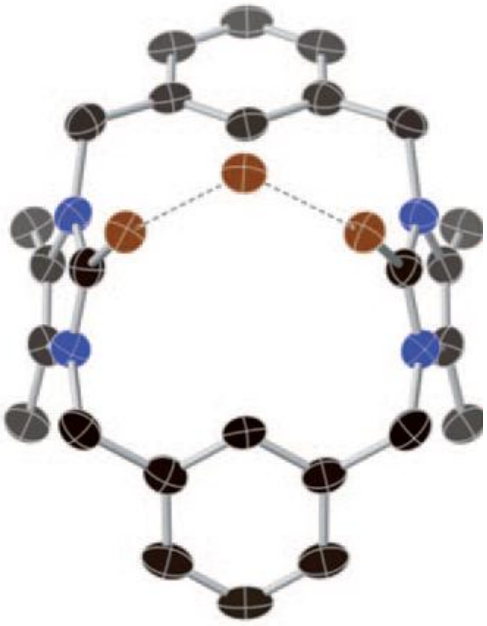

Figure 3.11. Bromoimidazoliophane receptor binding bromide.[52]

In the instance of an article from Beer et al., a bidentate receptor was prepared with a bromoimidazoliophane backbone.[52] This receptor had a *syn* and *anti* conformation, and was tested with bromide ions as well as with hexafluorophosphorus to assess binding qualities. The result of the experiment was that of the four possible outcomes (two anions, two conformations), the *syn* configuration binding bromide was the only stable one (see Figure 3.11). This is because in this configuration the two covalent bromine bonds pointed to the area in between them which was the perfect size for a bromide anion. The stable compound has two linear halogen bonds with bromide as the Lewis base holding the molecule in this conformation.

In another example of halogen bonding directing site-selective binding, a rotaxane system [53] was fitted with an iodine atom in the centre where the rotation of the macrocycle actually occurs (see Figure 3.12). The macrocycle itself features several hydrogen bond donors, and when a halogen atom was included in the space between the iodine on the dumbbell of the molecule and the hydrogen bond donors on the macrocycle, it was found to bind quite strongly, with a linear halogen bond formed between the iodine and an anionic bromide, as well as 3 hydrogen bonds being formed from the macrocycle. It was also noted

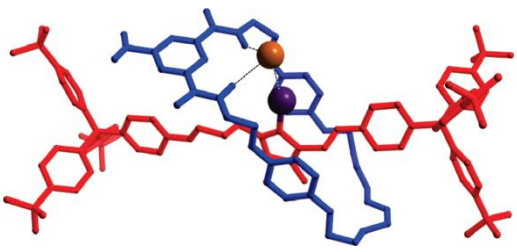

Figure 3.12. Rotaxane system exhibiting anion recognition.[53]

that the type of halide ion affected the binding affinity of the ion. The larger the halide ion, the more strongly bound it was to the system, with about a ten-fold increase from chloride to bromide and bromide to iodide.

In terms of systemic biological activity, halogen bonds are not the first thing which come to mind, as the human body is 80 % water and in aqueous media hydrogen bonding should be the prevalent interaction to be considered. However, when considering the ways in which the human body deals with chemicals for which it was not specifically designed, or which it is not typically exposed to very often, considerations other than those involving typical animal-based organic material (such as drug molecules) must be made. The primary use of a structural study[54] published in 2011 was to assess the structural features of halocarbon-protein complexes across all fields of medicine and biology. The main category of these interactions involves medications which contain covalent halogen atoms, typically chlorine. Since protein is rich in electron donor sites, there are many possible binding options for drug molecules. Hydrogen bonding is very commonly used to bind drugs, and so halogen bonding could be used in a similar fashion. Methionine seems to be a very common binding site for these drugs, since the lone pairs on sulfur are prime targets for halogen bonds. Also, when disulfide bridges form in proteins, these areas become a large site for halogen bonding. In one particular protein, it was found that a halogen bond was actually formed between chlorine and the disulfide bond itself, which is of course an electron rich area, so this is not too surprising. There is also a separate case which showed a single bromine atom on a drug molecule bonding with an amino acid in the traditional more linear fashion and at a right angle with an adjacent water molecule. This type of study is important primarily because knowing where drug molecules reside in the body once injected or

ingested is extremely useful in knowing the activity of the molecule, and knowing that halogen bonding can influence the binding of drugs to proteins is important for drug design.

The last important application which will be discussed here is probably also the broadest of all the applications so far, self-assembly of crystal systems and nanoparticular systems. Metrangolo and Resnati have put together a comprehensive overview[55] of all things halogen bonding, and a brief summary of its content will be provided here. The first chapter of the book deals with halogen bonding in conducting materials. Included in this section is a short account of some halogen-halide interactions such as will be discussed in the remaining chapters of this text, but there is also mention of halogenated nitroxides with radicals, and halogenated tetrathiafulvalenes (TTFs). These compounds show that halogen bonding is important in the description of the electronic structure of solid materials, and by transmitting magnetic interactions. This transmission indicates that part of the spin density is delocalized onto the halogen atoms involved in halogen bonding. The second chapter of the book describes how the competition between halogen and hydrogen bonding. It goes on to discuss the structure and chemistry of both the halocarbon and the Lewis base partner, and is an important read for anybody doing this type of chemistry. It also discussed supramolecular architectures in 1, 2, and 3 dimensions containing halogen bonding. Halogen bonding has been shown to be capable of driving specific site selection, and even the choice of halogen atom itself is even important in these systems.[47]

In an account published in Supramolecular Chemistry in 2011,[56] Resnati et al. showed that a diiodoperfluorooctane combined with a tetraazahelicene was able to self-assemble into 2D sheets which contained fluoroalkanes stacked with iodines at each end connecting them to the azahelices via a pair of halogen bonds. This is another excellent example of halogen bonding

being applicable to a field where normally it is hydrogen bonding which gets the spotlight. Chapters 3-7 of the halogen bonding book are less applicable to the scope of this work, but they describe dihalogen and interhalogen bonding, liquid crystal applications of the halogen bond, gas phase energetics comparisons of the hydrogen and halogen bond, theoretical trends in halogen bonding, and x-ray structures of π-halogen complexes with halogen bonds. Many articles in journals across inorganic chemistry display the work of Metrangolo and Resnati, and they continue to be the group to follow in advancing this exciting field.

Chapter 4

Experimental Results and Discussion; X-ray Crystallography and Solid-State NMR Spectroscopy

4.1 Introduction

This chapter consists of the experimental data associated with a quadrupolar halogen SSNMR and x-ray crystallographic study of mono-halogenated anilinium halide salts. SSNMR was performed in all cases on the ionic halide atom, and as part of this study, x-ray crystal structures for 2-bromoanilinium chloride (compound **2**) and 3-chloroanilinium bromide (compound **13**) were also collected (see Table 4.1). Of the 27 possible permutations of monohaloanilinium halides, data are reported here for 21 compounds (see Table 4.2). Discussion of the structures, halogen SSNMR parameters and their relation to both the structure as well as to halogen bonding will also be discussed.

4.2 Synthetic Details

All 9 monohaloaniline compounds were purchased from Sigma-Aldrich with purities of 97-99 % and used without further purification. Hydrohalic acids also came from Sigma-Aldrich, with concentrations in water of 37 % for HCl, 48 % for HBr, and 57 % for HI. Compounds are stable in the air and preparation was performed in open air in a fume hood. All compounds were prepared using a procedure adapted from the literature.[57] Synthesis consisted of mixing each haloaniline with an excess of each hydrohalic acid in turn followed by a period allowing the salt to precipitate from an ethanol solution and dry completely. Crystals were grown from ethanol by slow evaporation over several days and their identities confirmed by single-crystal X-ray diffraction. Crystals were powdered prior to solid-state NMR studies. Before NMR experiments, all samples were powdered and packed tightly into 1.3, 2.5, or 4 mm o.d. zirconium oxide MAS rotors.

Scheme 4.1. General molecular structure of monohaloanilinium halides. X is an electron density acceptor and D is a donor of electron density. X = Cl, Br, I. D = Cl^-, Br^-, I^-.

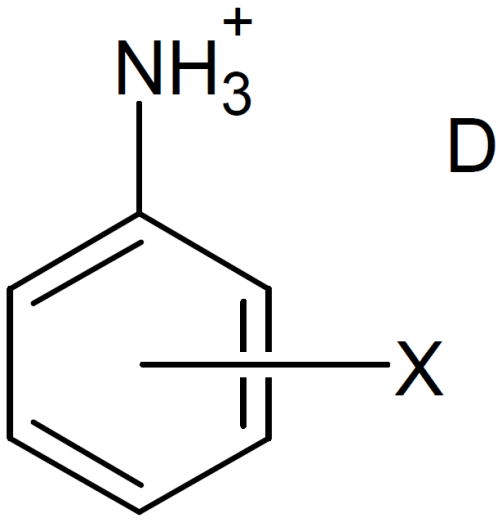

4.3 Experimental: X-ray Crystallography

Ilia Korobkov at the University of Ottawa performed the x-ray crystallography. The crystals of **2** and **13** were mounted on thin glass fibers using paraffin oil. Crystals of both compounds were cooled to 200.15 K prior to data collection. Data were collected on a Bruker AXS SMART single crystal diffractometer equipped with a sealed Mo tube source (wavelength 0.71073 Å) APEX II CCD detector. Raw data collection and processing were performed with APEX II software package from BRUKER AXS.[58] Diffraction data for both samples were collected with a sequence of 0.5° ω scans at 0, 120, and 240° in φ. Initial unit cell parameters were determined from 60 data frames collected for different sections of the Ewald sphere. Semi-empirical absorption corrections based on equivalent reflections were applied.[59] Systematic absences in the diffraction data set and unit cell parameters were consistent with orthorhombic **P***ca2*$_1$ (№29) for both compounds. Solutions in the non-centrosymmetric space group for all compounds yielded chemically reasonable and computationally stable results of refinement. Due to the non-centrosymmetric group and presence of heavy atoms, "floating origin restrain" was automatically generated during the refinement. The structures were solved by direct methods, completed with difference Fourier synthesis, and refined with full-matrix least-squares procedures based on F^2. In the structures of both compounds, halogen anions and anilinium cations are situated in general positions. All non-hydrogen atoms were refined anisotropically with satisfactory thermal parameter values. Positions of all the hydrogen atoms were obtained from the Fourier map analysis, however all hydrogen atoms were treated as idealized contributions. All scattering factors are contained in several versions of the SHELXTL program library, with the latest version used being v.6.12.[60] Crystallographic data and selected data collection parameters are reported in Table 4.1.

Table 4.1. Crystallographic data and selected data collection parameters for 2 and 13

compound	2-bromoanilinium chloride (**2**)	3-chloroanilinium bromide (**13**)
empirical formula	C_6H_7BrClN	C_6H_7BrClN
formula weight	208.49	208.49
crystal size, mm	0.32 x 0.25 x 0.21	0.22 x 0.21 x 0.18
crystal system	Orthorhombic	Orthorhombic
space group	**P***ca2*$_1$ (№29)	**P***ca2*$_1$ (№29)
Z	4	4
a, Å	15.606(2)	16.1551(5)
b, Å	5.4026(7)	5.5958(2)
c, Å	8.7865(11)	8.4538(2)
α, °	90	90
β, °	90	90
γ, °	90	90
volume, Å^3	740.80(17)	764.23(4)
calculated density, Mg/m^3	1.869	1.812
absorption coefficient, mm^{-1}	5.816	5.638
F(000)	408	408
Θ range for data collection, °	2.61 to 28.31	3.49 to 28.28
limiting indices	h = ±20, k = ±7, l = ±11	h = ±21, k = ±6, l = ±11
reflections collected / unique	5679 / 1695	8717 / 1871
R(int)	0.0246	0.0378
completeness to Θ = 28.32, %	98.5	99.1
max. and min. transmission	0.3747 and 0.2576	0.4302 and 0.3702
data / restraints / parameters	1695 / 1 / 82	1871 / 1 / 82
goodness-of-fit on F^2	1.084	1.017
final R indices [I>2σ(I)]	R_1 = 0.0239, wR_2 = 0.0614	R_1 = 0.0253, wR_2 = 0.0599
R indices (all data)	R_1 = 0.0259, wR_2 = 0.0623	R_1 = 0.0267, wR_2 = 0.0606
absolute structure parameter	0.019(14)	0.038(9)
largest diff. peak/hole, e·Å^{-3}	0.282 / -0.719	0.778 / -0.758

4.4 Experimental: SSNMR details

Data were acquired at the University of Ottawa on 9.4 and 11.7 T wide-bore magnets and the National Ultrahigh-field NMR Facility for Solids in Ottawa at 21.1 T with a standard-bore magnet. Experiments at 9.4 and 11.7 T used a 4 mm Bruker HX MAS probe with a low-frequency capacitor insert for chlorine, while experiments at 21.1 T used a 4 mm HX MAS probe for bromine and iodine, a 4 mm static X probe for chlorine, as well as a 2.5 mm HX MAS probe for chlorine and 1.3 mm HX MAS probe for bromine. Spectra were referenced to 0.1 mol/dm^3 NaCl in D_2O, 0.01 mol/dm^3 NaBr in D_2O and 0.01 mol/dm^3 KI in D_2O respectively. Secondary standards used were solid NaCl (-41.11 ppm) or KCl (8.54 ppm), solid KBr (54.51 ppm) and KI (192.62 ppm). Pulse widths (π and $\pi/2$) were determined using the secondary standard and selective CT pulse scaling factor calculated using the expression $1/(I + ½)$, where I is the spin of the nucleus. The scaling factor for chlorine and bromine is ½ and is ⅓ for iodine compared to the cubic salt. SSNMR signals for $^{35/37}$Cl, ^{81}Br and ^{127}I were acquired using the Solomon (90/90) and Hahn (90/180) echo pulse sequences. For the chlorine compounds at 9.4 and 21.1 T sweep widths of between 250 and 1000 kHz were used, with acquisition times ranging from 1 to 4 ms with proton decoupling where possible. Recycle delays of 2-5 s were used between scans and $\pi/2$ pulses of 2.5 to 4.5 μs with 36 to 80 μs echo delays were used in the acquisition of the spectrum. 25000 to 55000 transients were collected for these spectra.

For bromine and iodine, sweep widths of 2 MHz were used for all compounds, with acquisition times ranging from 180 to 301 μs, with proton decoupling used only at 21.1 T. Recycle delays for these experiments were 0.25 to 0.5 s, with echo delays ranging from 20 to 40 μs and 90 degree pulse lengths ranging from 1.15 to 1.6 μs. 3000 to 10000 transients were collected for each piece for these spectra.

VOCS (Variable Offset Cumulative Spectrum) data acquisition was used when required for chlorine, bromine and iodine. Offsets were set to 250 kHz for the 90/90 and 90/180 piecewise experiments. Resulting spectra were coadded in the frequency domain to produce the final spectrum.

SSNMR line shapes were fitted using the WSolids, simulation software which allows for analytical modelling of CSA and quadrupolar effects simultaneously. All simulated spectra include only the effects of the central transition. Spectra were fitted using all EFG and CSA parameters, as well as the Euler angles representing the relative orientations of the two interactions. Spectral simulation is impacted by the positions of spectral discontinuities rather than relative intensities of different line shape components. Errors are estimated by manual heuristic iteration of parameters individually until significant variance from optimal parameters is beyond the point-by-point resolution of the experimental spectrum.

4.5 Results and Discussion: X-ray Crystal Structures

The crystal structures of 2-bromoanilinium chloride (**2**) and 3-chloroanilinium bromide (**13**) were solved during the course of this study and some relevant crystallographic and structural parameters are summarized in Table 4.1 & Table 4.2. Also shown in Table 4.2 are the space groups and some geometrical information pertaining to the halogen bonding environment in a larger series of monohaloanilinium halides. The crystal structures of some of these compounds, as well as the topic of halogen bonding in monohaloanilinium halides have been discussed previously, most notably by Rissanen and co-workers[74] and by Gray and Jones.[57] We therefore focus our brief discussion of crystallographic aspects on how the data for the two new crystal structures fit into the overall trends. This discussion also reviews relevant structural features which will be useful in the interpretation of the halogen NMR data (*vide infra*). Despite the chemical similarity within the series of compounds shown in Table 4.2, they crystallize from ethanol in a variety of space groups. The majority of these compounds feature near-linear C-X•••D contacts (X = Cl, Br, I; D = Cl^-, Br^-, I^-). It is useful to discuss these contacts in terms of a normalized distance parameter,[61]

$$R = \frac{d}{r_X + r_D} \qquad \textbf{[4.1]}$$

where d is the observed X•••D distance and r_X and r_D are the van der Waals' radii[62,63] of the halogen (X) and halide (D), respectively. The structures of **2** and **13** exhibit R values near the two extremes of all the values shown in Table 4.2, at 0.91 for **2**, and 1.03 for **13**. The latter compound, while exhibiting an approximately linear C-Cl•••Br^- angle of 164.7°, therefore does not exhibit notable halogen bonding due to the large value of R. The strongest halogen bonding interaction is seen for **21** (R = 0.88), which is not surprising as it involves iodine as the electron

Table 4.2. Compound numbering and some crystal structure and local halogen bonding geometrical information for monohaloanilinium halides for which either single-crystal X-ray diffraction or halogen solid-state NMR data are available

compound[1]	compound name	space	crystal	C-X / Å	X•••D / Å[2]	C-X•••D / °	R[3]
1	2-chloroanilinium chloride	$Pca2_1$	57	1.740	3.412	170.6	0.96
2	2-bromoanilinium chloride	$Pca2_1$	this work	1.899	3.314	170.3	0.91
3	2-iodoanilinium chloride	-	-				
4	3-chloroanilinium chloride	$P2_1/n$	57	1.745	n/a	n/a	n/a
5	3-bromoanilinium chloride	-	-	-	-	-	-
6	3-iodoanilinium chloride	-	-	-	-	-	-
7	4-chloroanilinium chloride	$P\ 1\ 2_1/c\ 1$	57, 72	1.742	3.635	166.6	1.02
8	4-bromoanilinium chloride	$P2_1/c$	73, 74	1.892	3.587	165.9	0.98
9	4-iodoanilinium chloride	$P2_1\ a\ b$	74	2.102	3.405	169.8	0.90
10	2-chloroanilinium bromide	$Pca2_1$	75	1.742	3.589	170.0	0.97
11	2-bromoanilinium bromide	$Pca2_1$	57	1.893	3.443	170.2	0.90
12	2-iodoanilinium bromide	-	-	-	-	-	-
13	3-chloroanilinium bromide	$Pca2_1$	this work	1.742	3.838	164.7	1.03
14	3-bromoanilinium bromide	P-1	57	1.895	n/a	n/a	n/a
16	4-chloroanilinium bromide	-	-	-	-	-	-
17	4-bromoanilinium bromide	-	-	-	-	-	-
18	4-iodoanilinium bromide	P-1	74	2.102	3.704	158.4	0.94
19	2-chloroanilinium iodide	-	-	-	-	-	-
20	2-bromoanilinum iodide	-	-	-	-	-	-
21	2-iodoanilinium iodide	$P2_1/c$	57	2.101	3.692	170.2	0.88
24	3-iodoanilinium iodide	$P\ 1\ 2_1/m\ 1$	57	2.104	3.782	174.2	0.90

[1] Compounds **15**, **22**, and **23** are not listed as we do not report NMR data for them and to our knowledge there is no information on their crystal structures.

[2] Distance of shortest contact. Here, "X" is the covalently bound halogen and "D" is the anionic halide (donor of electron density); X and D may be different elements.

[3] Relative XB distance, $R = d/(r_X+r_D)$, where d is the X•••X- distance and r_X and r_D are the van der Waals' radii of the electron density acceptor and donor.

density acceptor. It is well-known that iodine typically forms the strongest halogen bonds within a given series. The C-X•••D angles range from 158.4° in **18** to 174.2° in **24**. The most linear contact is again observed when iodine is the electron density acceptor. However, overall it is clear that the halogen bonding interaction in monohaloanilinium halides is rather weak compared to the more pronounced cases observed when the electron density acceptor is *p*-diiodotetrafluorobenzene or other related perfluorinated compound. As noted previously,[57] two compounds in the series for which there are X-ray crystallographic data (**4** and **14**) do not exhibit any halogen bonding interaction; this is of interest in the context of the present study to assess whether this difference is manifested in any of the NMR parameters (*vide infra*).

It is important to consider that the halide ions in these compounds are typically involved in various hydrogen bonding interactions with NH groups, in addition to participating in a halogen bond. As an example, we show in Figure 4.7 the local halide ion environment for **2** and **13**. The interactions seen are typical of many of the compounds in Table 4.2 in that a single near linear C-X•••D contact is present, along with three hydrogen bonds to the halide.

4.6 Results and Discussion: Chlorine-35, Bromine-81 and Iodine-127 Solid-State NMR of Haloanilinium Halide Salts

Figure 4.1, Figure 4.2 and Figure 4.3 contain the ^{35}Cl NMR spectra of powdered samples of compounds **1** through **9**, acquired under stationary conditions. The central transition, (m_ℓ = ½ ↔ -½) of the ^{35}Cl nucleus in the chloride anion is observed in each case. The ^{35}Cl quadrupolar and chemical shift tensor parameters determined through simulation of the spectra are presented in Table 4.3. Given the number of parameters required to fully fit the spectra, several steps must be taken in order to be confident in the accuracy of the parameterization. Spectra should be acquired at more than one field (9.4 and 21.1 T) and static and MAS spectra (where possible) will allow for greater confidence in the fits. In the case of chlorine and bromine, there is also a second isotope of the nucleus (^{37}Cl, ^{79}Br) which gives the same parameters with a slightly different QCC, due to the different quadrupole moment. This influence, along with a different magnetogyric ratio, gives rise to a different Larmor frequency (see Table 2.2). Because MAS removes the effects of CSA from the spectrum, these spectra can be fit using only the isotropic chemical shift (δ_{iso}), quadrupolar coupling constant (C_Q), and quadrupolar asymmetry parameter (η_Q). These spectra are much easier to be fit because they are defined by only 3 parameters, as seen in the top rows of Figure 4.1, Figure 4.2 and Figure 4.3. A spectrum acquired at the second field also increases confidence in the spectral fit because effects of the quadrupolar interaction and the chemical shift scale differently with the applied magnetic field.

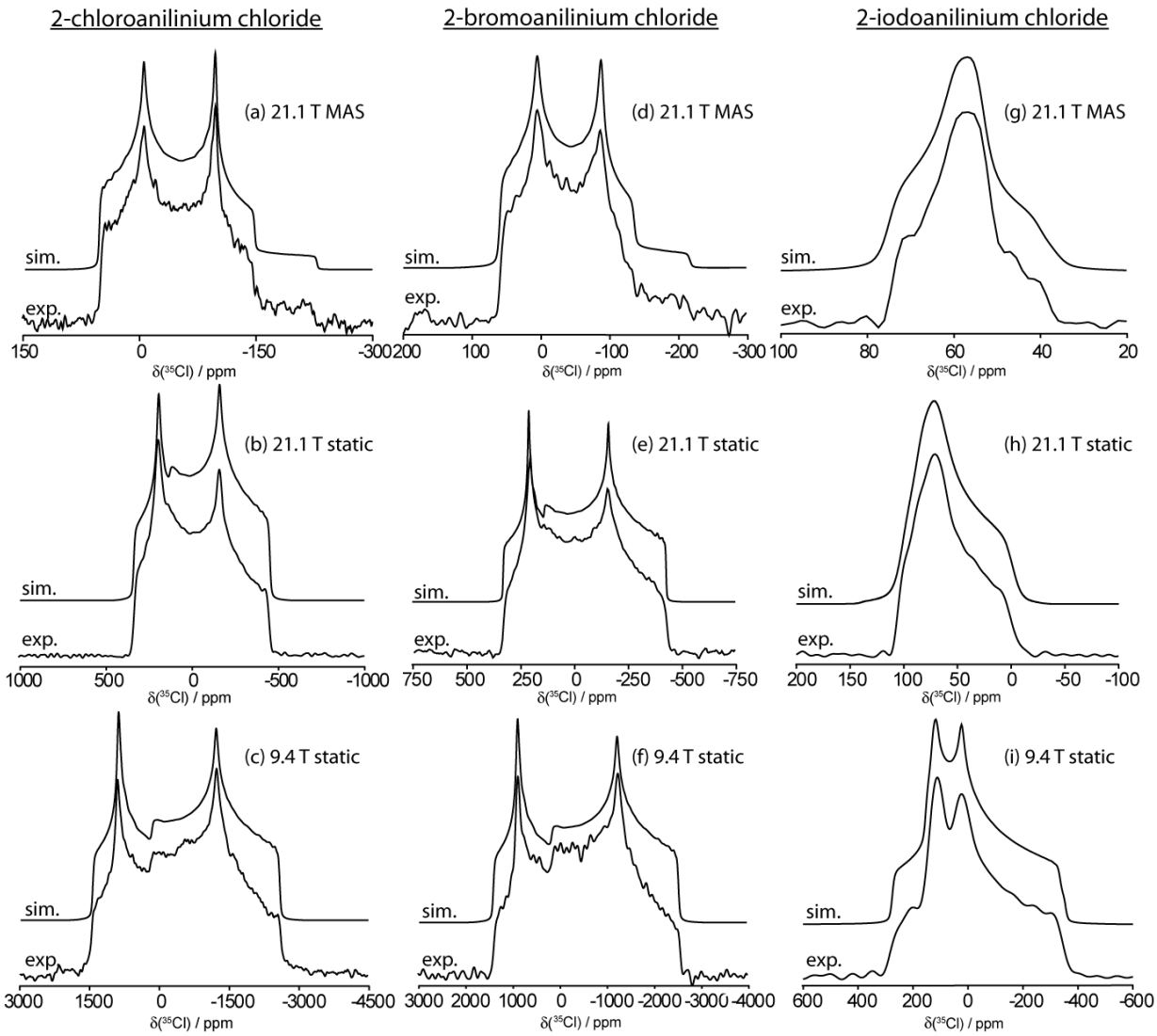

Figure 4.1. Chlorine-35 SSNMR spectra of **1**, **2**, and **3**.

Several important points may be made concerning the ^{35}Cl NMR spectra. These spectra can span up to several thousand ppm at 9.4 T (as in Figure 4.3 (c)). An increase in the applied magnetic field strength going from 9.4 to 21.1 T results in a narrowing of the spectrum and an increase in signal-to-noise given the same number of scans. As shown in Table 4.3, the value of $C_Q(^{35}Cl)$ ranges from 2.12 MHz in **3** to 6.04 MHz in **1**, which fits in the range for known

hydrochloride compounds. The range for these compounds is anywhere from near zero to approximately 10 MHz (7.1 MHz in aspartic acid HCl[64]). Isotropic ^{35}Cl chemical shifts for the chloride compounds range from 67 ppm in **8** to 88 ppm in **4**, and chemical shift tensor spans range from 40 ppm in **3** up to 120 ppm in **9**. These data also fit within the known ranges for hydrochloride salts in the literature.

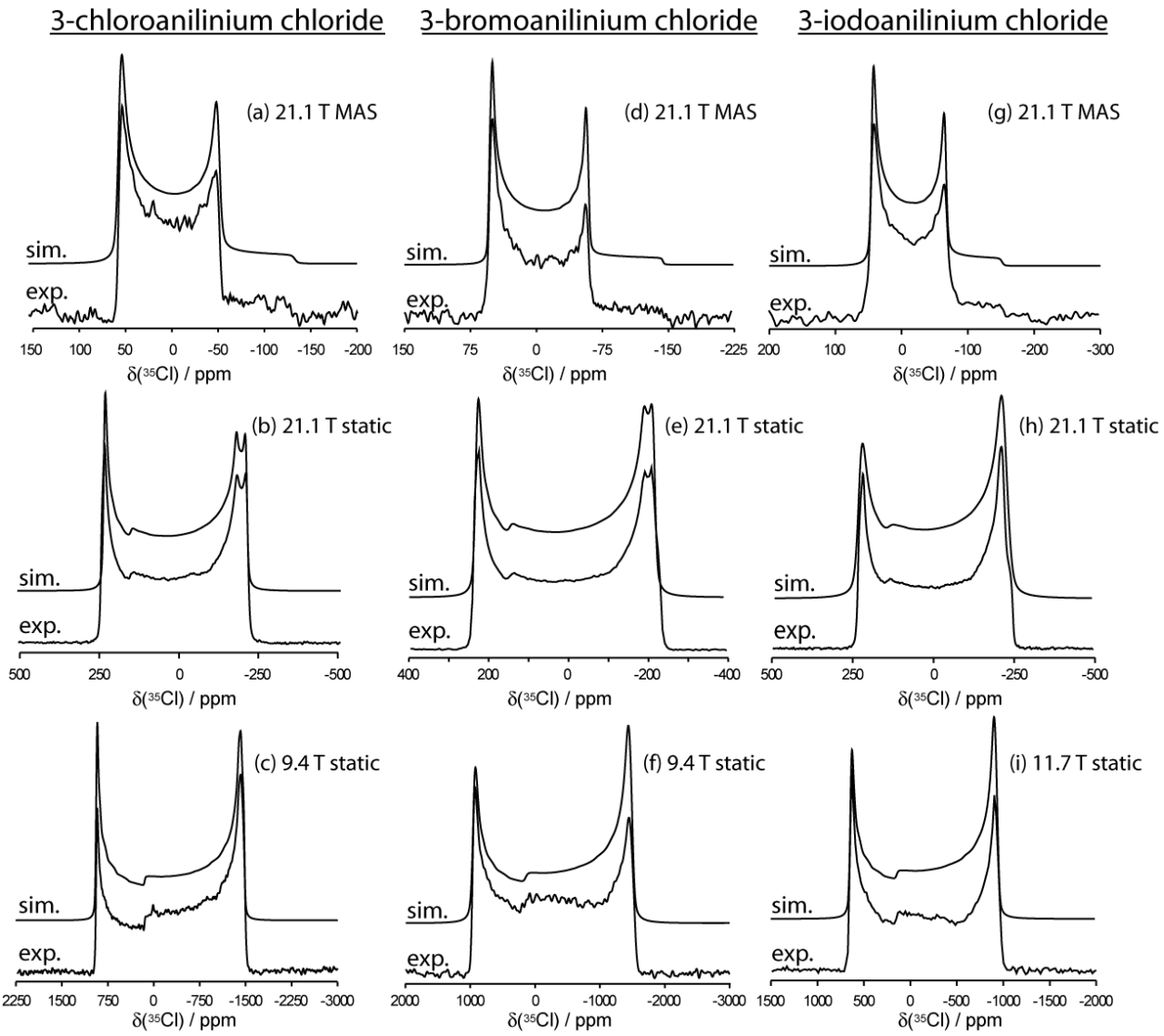

Figure 4.2. Chlorine-35 SSNMR spectra of **4**, **5**, and **6**.

From these data, it is clear that for this series of compounds, there is no inherent SSNMR parameter that describes or signifies whether or not a halogen bond is present. In these compounds there are several effects in competition which affect the spectrum. This is not at all surprising, considering that using the electron density donor as an indirect probe means that any evidence of halogen bonding is going to be subtle. The only applications of SSNMR to halogen

bonding thus far[48-50] have used dipolar or J couplings of the Lewis bases involved in halogen bonds to determine interactions and/or their strengths. No general correlations between bond angle, distance, or *R* value (a measure of the overlap of the interactions' van der Waals radii, see Chapter 3) were found for these compounds. Compound **4**, for example, doesn't contain any halogen-halide VDW overlap (see Table 4.2), but there is nothing particularly distinctive about its ^{35}Cl NMR parameters.

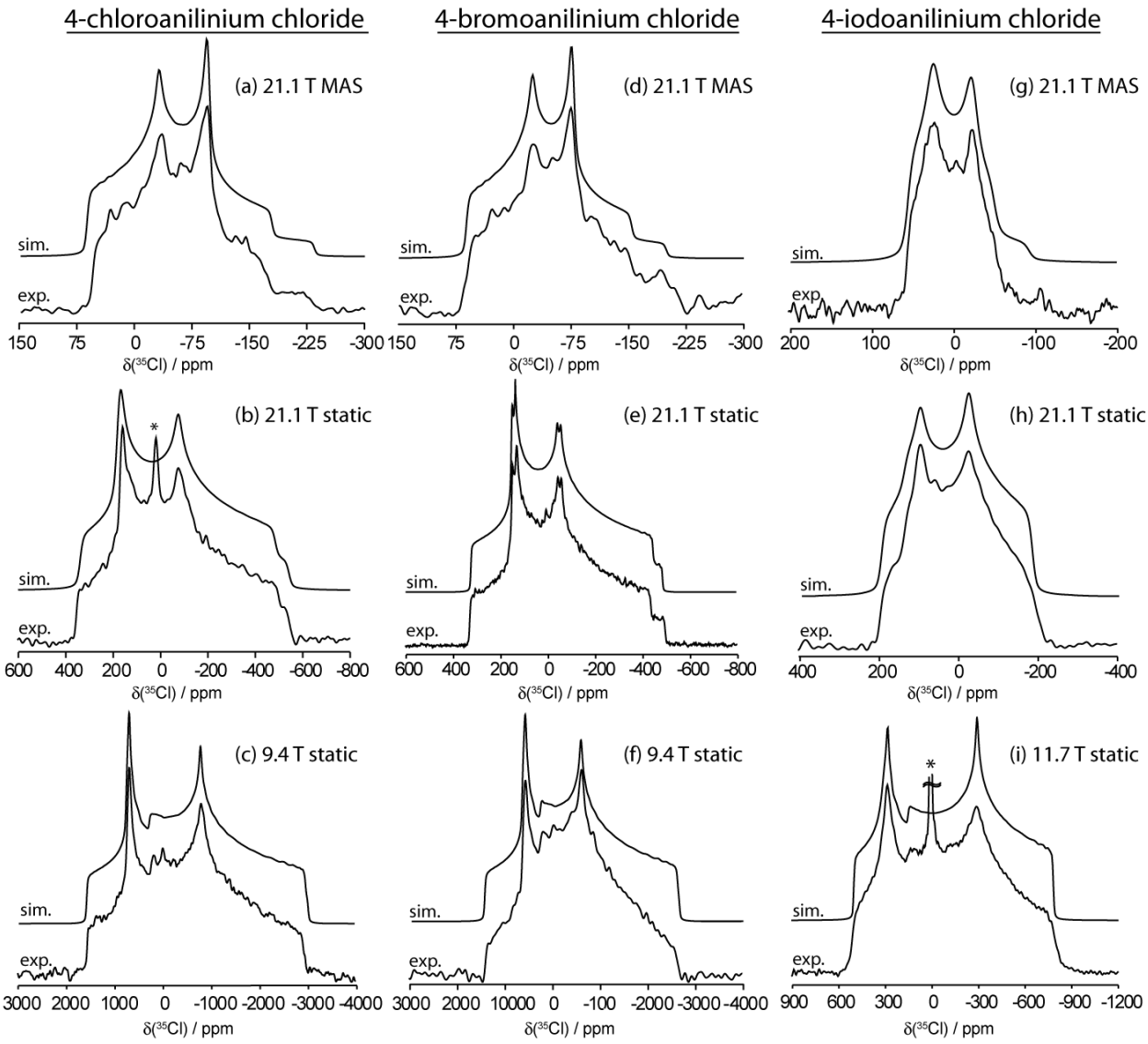

Figure 4.3. Chlorine-35 SSNMR spectra of **7**, **8**, and **9**.

Table 4.3. Experimental ^{35}Cl quadrupolar and chemical shift tensor parameters

compound	$\lvert C_Q(^{35}Cl)\rvert$ / MHz	η_Q	δ_{iso} / ppm	Ω / ppm	κ	α / °	β / °	γ / °
1	6.04(3)	0.34(1)	70(1)	95(5)	-0.2(2)	90(20)	90(5)	0(5)
2	6.01(1)	0.330(5)	79(1)	95(5)	-0.5(2)	90(20)	90(2)	0(2)
3	2.12(2)	0.76(1)	75(1)	40(5)	-0.1(2)	20(10)	85(5)	0(5)
4	5.30(5)	0.025(5)	88(1)	100(5)	-0.8(1)	0(5)	81(2)	0(2)
5	5.37(3)	0.025(5)	85(1)	95(10)	-1(0.1)	0(15)	83(2)	0(2)
6	5.39(5)	0.02(2)	77(1)	90(5)	-0.5(2)	0(0)	85(3)	5(3)
7	6.02(5)	0.56(1)	69(1)	115(5)	-1(0.1)	20(20)	90(5)	10(5)
8	5.60(5)	0.60(1)	67(1)	90(5)	-0.4(1)	75(10)	78(2)	12(2)
9	4.33(7)	0.38(1)	71(1)	120(5)	0(0.1)	55(10)	90(5)	0(5)

[a] Error bounds are in brackets. Parameter definitions can be found in Chapter 1 & Chapter 2.
[b] Although C_Q may take any real value, $|C_Q|$ is measured using SSNMR experiments.

Inspection of data acquired for the bromide compounds shows that this series had a larger C_Q range than the corresponding chlorides, even taking into account the larger quadrupole moment of bromine, which would only account for a proportionally larger C_Q range. C_Q values in the bromine compounds in this series range from 12.3 to 45.3 MHz, which is also in the range expected for bromide salts.[18] Isotropic chemical shifts for the 8 compounds range from 100 to 250 ppm, which falls in the typical range for bromides as well. Finally, spans for the series started at 75 ppm ranging all the way up to 340 ppm, which is quite high, fairly atypical of hydrobromides, whose shifts normally occur up to about 250 ppm.[21]

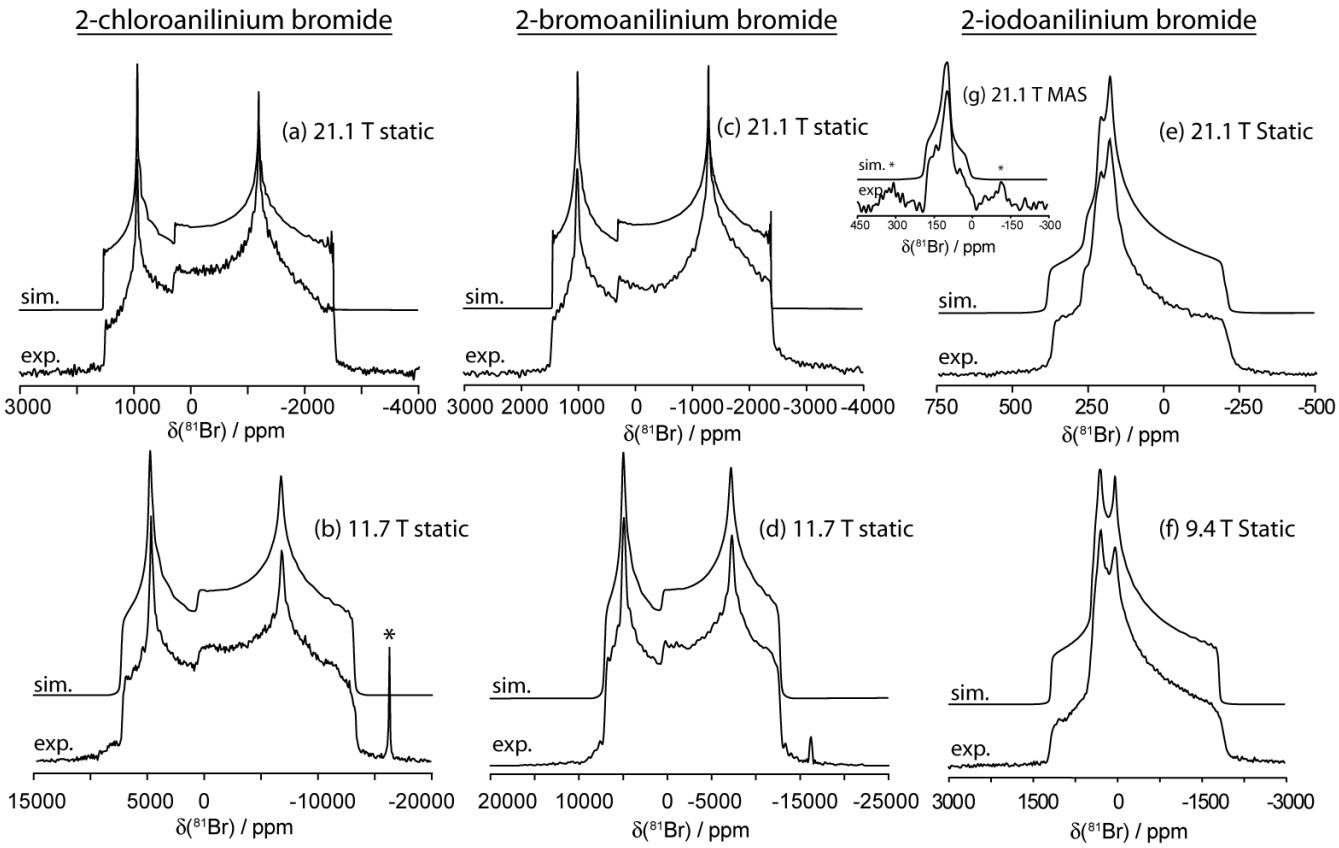

Figure 4.4. Bromine-81 SSNMR spectra of **10**, **11**, and **12**.

Broadening due to the quadrupolar interaction between the electric field gradient and the quadrupole moment of ^{81}Br dominates the NMR spectra. The quadrupolar coupling constants, C_Q(^{81}Br), are notably larger than those obtained for other organic hydrobromides where halogen bonding is absent (C_Q < 20 MHz) (except L-Leu HBr).[18] The identical values of 38 MHz for the two 2-substituted anilinium salts, when contrasted with the value of 45.4 MHz for the 3-substituted salt within the space group $Pca2_1$, and the increased value of η_Q for the latter, demonstrates that the ^{81}Br quadrupolar tensor is sensitive to this differing substitution which increases the bromide-halogen distance and slightly decreases the C_{Aryl}-X•••Br^- angle (see Table 4.2).

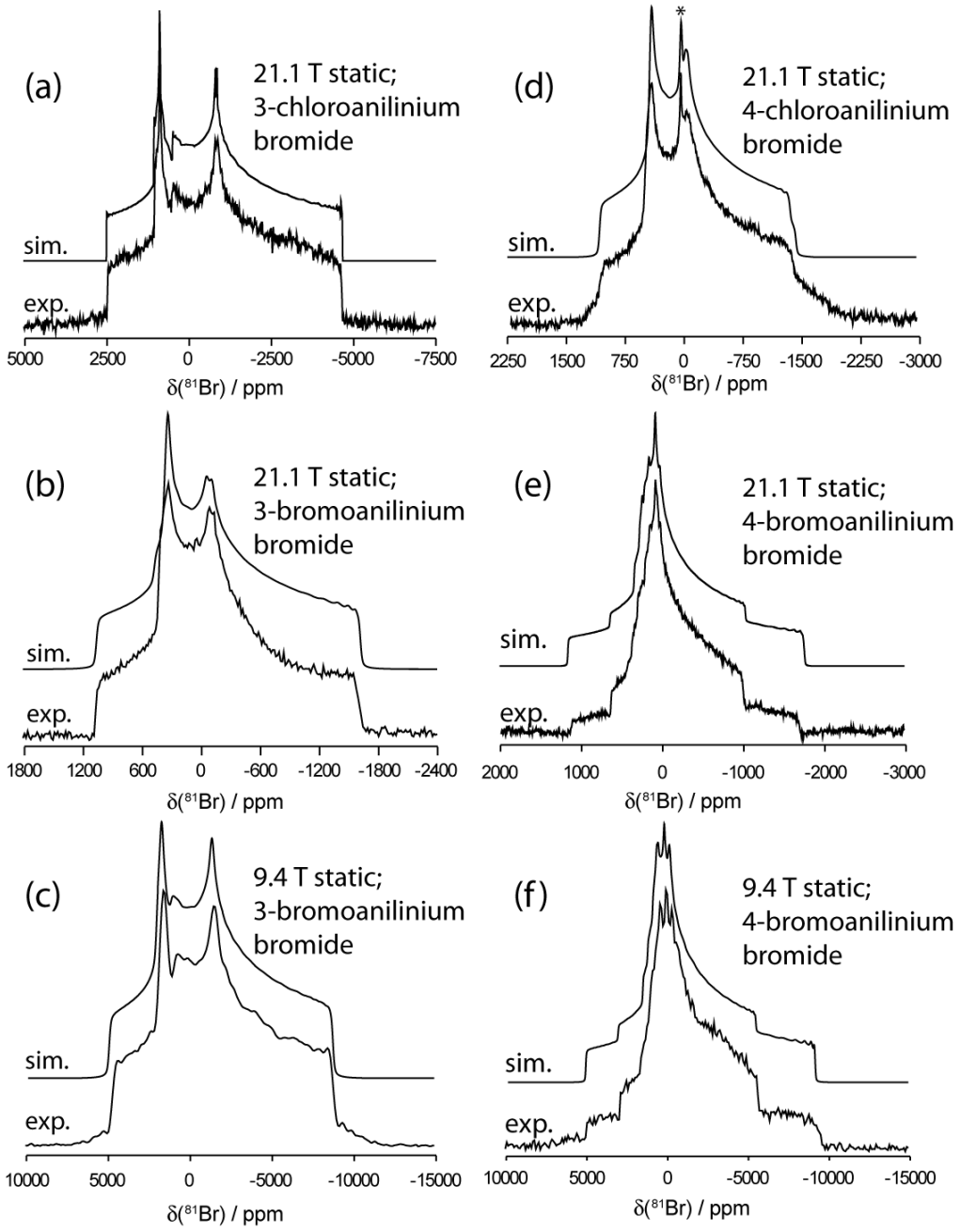

Figure 4.5. Bromine-81 SSNMR spectra of **13**, **14**, **16**, and **17**.

Table 4.4. Experimental ^{81}Br quadrupolar and chemical shift tensor parameters

compound	$\lvert C_Q(^{81}Br)\rvert$ / MHz	η_Q	δ_{iso} / ppm	Ω / ppm	κ	α / °	β / °	γ / °
10	37.95(3)	0.31(5)	135(3)	210(20)	0.2(1)	90(25)	90(5)	0(2)
11	38.0(2)	0.27(1)	155(10)	240(10)	0.0(5)	45(2)	90(2)	0(10)
12	12.3(2)	0.85(1)	187(5)	75(10)	0.2(2)	65(3)	85(5)	0(5)
13	45.3(1)	0.665(5)	130(10)	120(30)	-0.7(2)	0(25)	75(10)	0(15)
14	27.7(2)	0.67(5)	250(10)	340(10)	-0.2(1)	90(5)	90(10)	0(2)
16	26.2(1)	0.66(1)	230(10)	220(30)	0.4(1)	90(5)	80(5)	15(10)
17 (site 1)	20.0(1)	1.0(1)	100(10)	-	-	-	-	-
17 (site 2)	26.2(1)	0.92(2)	150(10)	190(20)	-1.0(1)	5(3)	10(3)	12(3)

[a] Error bounds are in brackets. Parameter definitions can be found in Chapter 1 & Chapter 2.
[b] Although C_Q may take any real value, $|C_Q|$ is measured using SSNMR experiments.

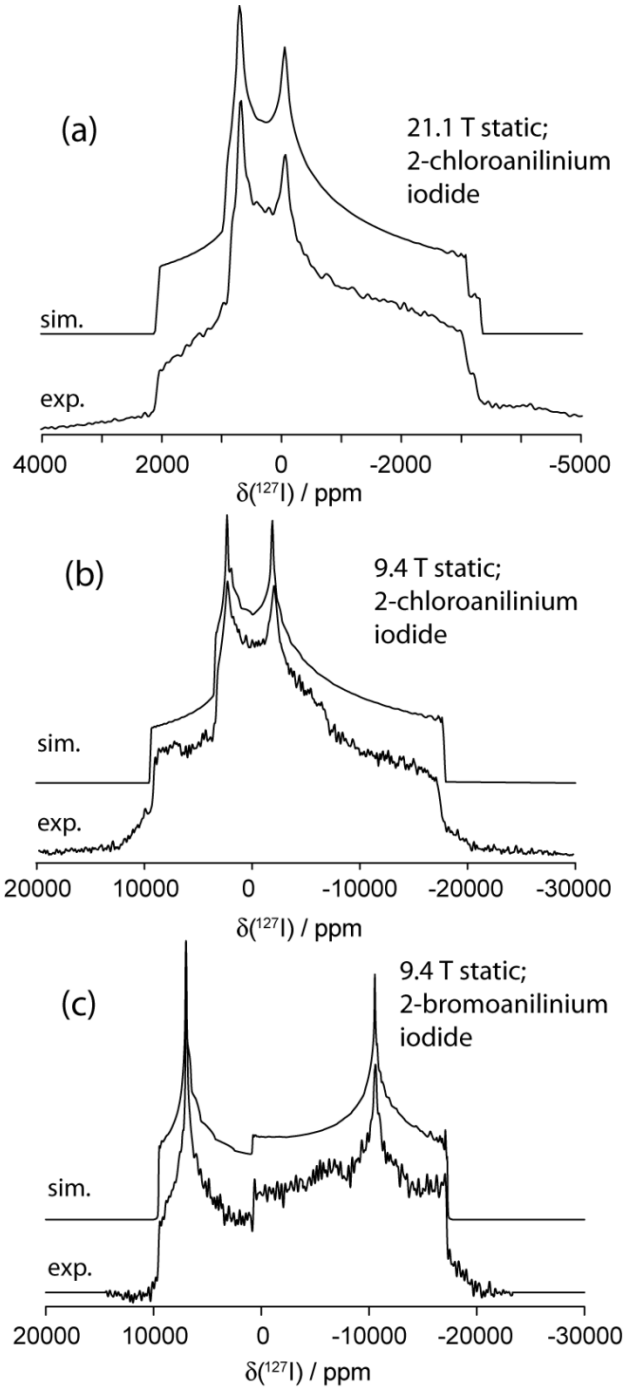

Figure 4.6. Iodine-127 SSNMR spectra of **19** and **20**.

Table 4.5. Experimental ^{127}I quadrupolar and chemical shift tensor parameters

compound	$\lvert C_Q(^{127}I)\rvert$ / MHz	η_Q	δ_{iso} / ppm	Ω / ppm	κ	α / °	β / °	γ / °
19	57.50(75)	0.775(20)	340(10)	300(100)	-1.0(0.3)	0(0)	85(5)	25(5)
20	152.50(25)	0.235(20)	250(35)	500(25)	-1.0(0.3)	90(15)	90(20)	0(5)

[a] Error bounds are in brackets. Parameter definitions can be found in Chapter 1 & Chapter 2.
[b] Although C_Q may take any real value, $|C_Q|$ is measured using SSNMR experiments.

As for the iodine compounds, there are only representative spectra for two compounds to show that data can be collected for iodide ions in halogen bonding environments. The iodine compounds were unstable over time and difficulty was had in forming a powder with iodide as the halide. The two spectra collected have vastly different parameters, with C_Q's of 57.5 and 152.5 MHz, isotropic chemical shifts of 340 and 250 ppm, and spans of 300 and 500 ppm respectively for 2 and 3-chloroanilinium iodide.

4.7 Discussion of experimental data in terms of structure

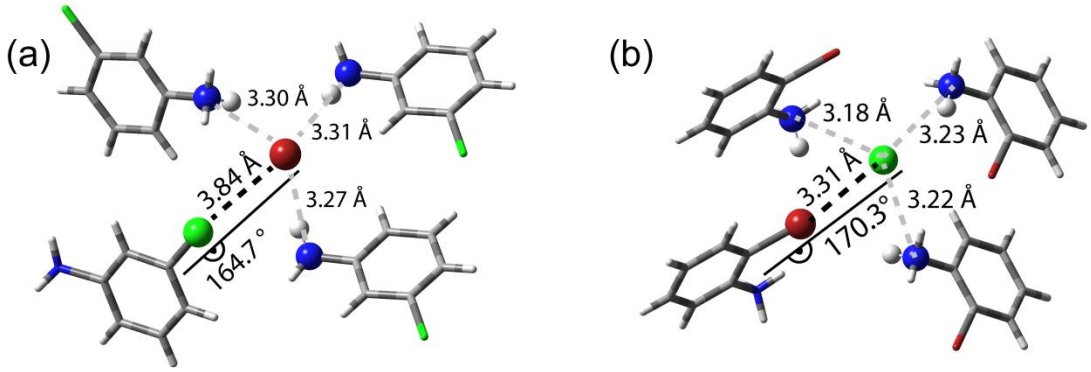

Figure 4.7. Important distances and angles around the halide ion in (a) 3-chloroanilinium bromide (**13**) and in (b) 2-bromoanilinium chloride (**2**). Shown are the C-X•••D angle, the halogen-halide distance, and the halide-nitrogen distances.

An analysis of various trends in the NMR parameters in the context of some of the known crystal structure data (see Figure 4.7 for examples) reveals useful insights into how these parameters are sensitive to chloride ions which participate as halogen bond electron density donors.

Since the crystal structures are not yet known for all 21 compounds which comprise this study, rationalizations must be made for the time being based on comparison to structures which are known. The crystal structures for **1** and **2** are known, whereas **3**'s structure is yet unknown, so it is possible that their crystal structures could be similar. Compounds **1** and **2** have the same crystal structure and pack in the same space group, $Pca2_1$, and the two compounds have identical SSNMR parameters values within experimental error. The only difference between the two spectra is that there is a 9 ppm shift difference between **1** and **2**, with the larger of the two shifts belonging to compound **2**, which has the stronger halogen bond as characterized by its *R* value

(see Table 4.2). That being said, compound **3** gives a spectrum which is vastly different from the other two compounds. Its spectrum is much narrower, i.e., C_Q = 2.12 MHz (vs 6.04 and 6.01 MHz for **1** and **2**) and η_Q = 0.76 (vs 0.34 and 0.330 for **1** and **2**). The span of the chlorine CS tensor is also substantially different for **3** (40 ppm) compared to **1** and **2** (95 ppm) and compound 3 has an α angle of 20° whereas **1** and **2** have α angles of 90°. This suggests that compound **3** belongs to a different space group than the other two. This strongly implies that **3** packs in a space group other than *P*ca2$_1$, and indeed that the halogen and hydrogen bonding environment about the chloride ion is different from that found in the isostructural **1** and **2**. Taken together, the data for the series (**1**, **2**, and **3**) show that the NMR parameters reflect crystal symmetry and packing, and also hints that the slightly different XB environment may be reflected in the value of δ_{iso} for **1** and **2**. Compound **3** cannot fairly be compared to **1** and **2** in terms of δ_{iso} or quadrupolar parameters since they pack in different space groups, so there will be more than slight differences in halogen bonding to affect the parameters.

Chlorine-35 NMR spectra for the 3-halosubstituted chloride series **4**, **5**, and **6** are presented in Figure 4.2. The spectra as well as the NMR parameters determined through spectral simulations (Table 4.3) strongly imply that these three compounds pack in the same space group and exhibit similar halogen bonding geometries. The three spectra also look very similar, giving further credence to the idea that all three compounds have very similar crystalline structures. The values of $C_Q(^{35}Cl)$ vary over a small range, from 5.30 MHz for **4** to 5.39 MHz for **6**. The quadrupolar asymmetry parameter for the three compounds is identical within experimental error (Table 4.3). The CS tensor parameters are also very similar for the three compounds, with small variations in δ_{iso}. Among this series, a crystal structure is only available for **4**. This compound

packs differently from **1**, **2** and **3**, in the $P2_1/n$ space group. The NMR data point to two important points. First, it is probable that compounds **5** and **6** are isostructural with **4**, pack in the $P2_1/n$ space group, and do not exhibit halogen bonding. Second, assessment of all data in Table 4.3 shows that the values of C_Q, δ_{iso}, and Ω for **4**, where it is known independently from x-ray crystallography that halogen bonding is absent, are not unequivocally sensitive to halogen bonding such that its presence or absence may be inferred simply by the value of one of these parameters.

The 4-halosubstituted chlorides (**7**, **8**, and **9**) all have known X-ray crystal structures; **7** and **8** pack in the same space group and exhibit similar close contacts around the chloride ion, while **9** packs in a different space group (Table 4.2). This is distinctly reflected in the form of their ^{35}Cl NMR spectra (Figure 4.3) and in the values of $C_Q(^{35}Cl)$ and η_Q. For example, η_Q = 0.56 for **7**, 0.60 for **8**, and 0.38 for **9**. Compound **7** does not feature a significant halogen bond, as quantified by the *R* value of 1.02, while **8** features a long halogen bond (*R* = 0.98) and **9** features a slightly more substantial halogen bond (*R* = 0.90). The small difference in *R* value for the two isotstructural compounds (**7** and **8**) is not enough to manifest conclusively in the value of δ_{iso}.

Overall, for the two series of chloride compounds exhibiting halogen bonding (**1**, **2**, **3** and **7**, **8**, **9**), it is tempting to correlate the value of $C_Q(^{35}Cl)$ with the degree of halogen bonding (as described by *R*). It is seen that within these two small series, larger values of C_Q are observed for weaker halogen bonds. This is a tentative conclusion for various reasons, e.g., other factors can influence C_Q particularly when the compounds pack in different space groups.

To explore whether insight into the HB environment around the bromide ions in these salts may be gleaned from the CS tensor, relationships with various distance and angles characteristic of the Br^- coordination environment were assessed. Since halide ions are often involved in several weak interactions simultaneously, and different crystal packing (i.e., space group) may also influence the NMR parameters, it was essential to study a series of compounds wherein the major structural variable from compound to compound was the halide-halogen distance. 2-chloroanilinium bromide, 2-bromoanilinium bromide, and 3-chloroanilinium bromide satisfy this requirement and they all pack in the $Pca2_1$ space group. A single-crystal X-ray diffraction study was performed as part of this work to determine the structure of the compound **13** (Table 4.1). The bromide ion is involved in three hydrogen bonds whose distances are essentially invariant in the three compounds, i.e., the three shortest unique Br-(H)N distances vary by only 0.03, 0.02, and 0.03 Å over the three compounds. The major feature which changes is the Br^--X distance, which increases from 3.443 Å in 2-bromoanilinium bromide to 3.589 Å in 2-chloroanilinium bromide to 3.838 Å in 3-chloroanilinium bromide. As shown in Figure 4.8, an inverse correlation between the value of $\Omega(^{81}Br)$ of the bromide ion with the shortest halogen-halide contact is observed. The span for 2-chloroanilinium bromide, 120 ppm, is particularly valuable because the Br-Cl distance is comparable to the sum of their van der Waals' radii and so this value is reflective of the limiting case of a very weak HB interaction in this series of compounds.

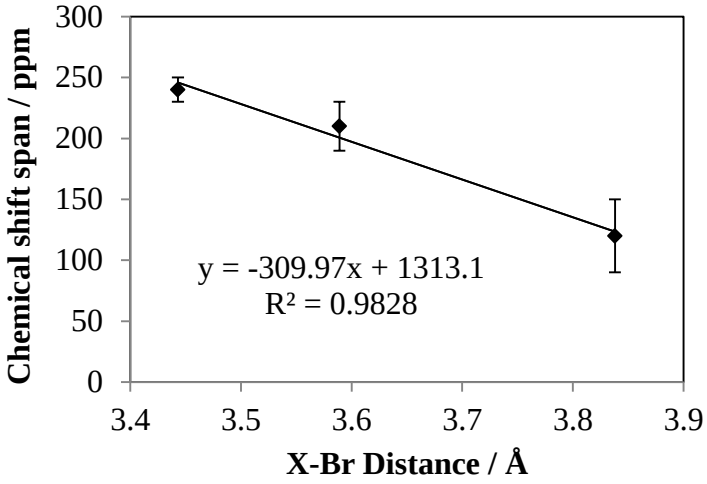

Figure 4.8. Correlation between halogen bond length and experimental chemical shift span in bromine compounds packing in $Pca2_1$ space group.

From the above data, it is clear that x-ray crystallography and SSNMR are very useful tools for determining structure and electronic configurations in the region surrounding an atom, but there is more information still to be gained from this data. The next step in extracting all important information from these compounds is a comprehensive computational study; this will be the focus of the following chapter.

Chapter 5

Computational study of the halide NMR parameters of selected haloanilinium halide salts

5.1 Introduction to GIPAW-DFT and ONIOM methods

Quantum chemical calculation software has become an integral part of modern chemistry in the last 10 years.[65] Due to advances in computer hardware and software, as well as the ubiquitization of the internet, information technology moves faster than ever. With these advances have come great strides towards a more complete and precise understanding of the natural world down to the quantum level. Whether specific computational methods use parameterization or solid theoretical and quantum physics to model interactions or structure, it is important for these models to be capable of properly and accurately reproducing experimental data in order to have any usefulness in chemistry. The ultimate goal of all quantum chemical modelling software is for it to be able to be used predictively, so that experiments can be undertaken without the need for expensive chemicals or lab environments which are subject to experimental or physical errors which can ruin experiments. While there have been great advances in this type of research, the methods are still far from perfect, though in some cases connections can be drawn between experimental data and computed results. There are many different ways of modelling the various interactions chemicals undergo, and as a part of this study two of these were used.

Theoretical molecular orbital calculations use an *ab initio* method (sometimes coupled with other empirical methods) which models small molecular systems with varying possible degrees of accuracy. In this thesis, the software used to run these calculations is called Gaussian '09,[8] and it provides great flexibility in both computational detail and geometric modification.

Gaussian has many uses, including computation of instantaneous energies, optimization of geometries, and electric and magnetic properties. It is this last use which will be the most useful for SSNMR experiments, as NMR is dependent on the electronics surrounding nuclei to measure their magnetic properties. Gaussian software is able to calculate EFG and CS tensor parameters with any of a number of possible basis sets.[66,67,68] The density functional used in this study is called B3LYP,[69] and it is what is called a hybrid density functional. This hybrid functional incorporates electron exchange-correlation into regular Hartree-Fock (HF) theory, leading to a more complete description of molecular electronics than would be possible using HF theory alone. ONIOM, [70] which stands for **o**ur own **n**-layered **i**ntegrated molecular **o**rbital and molecular **m**echanics, is built into the Gaussian software package. It allows for precise control of different methods and different basis sets for different groups of molecules or parts of molecules, which can be useful when one nucleus is of interest but the others do not require as sophisticated a method. Separating the basis sets in this manner is especially important when trying to use as little computational time as possible, which is nearly always the case when dealing with large systems. In the case of this work, however, the systems tested are quite small and thus all atoms were modelled with the same level of theory and basis set. The advantage of this method is its flexibility with regards to the variety of structures which can be used, and the size of the model system is only limited by computational power and time. The biggest disadvantage to the use of a cluster model is that it is very physically unrealistic when modelling real systems because calculations are typically done *in vacuo*, so solvent or crystalline systems can be difficult to model accurately.

The second computational method which will be used to model these systems is implemented in a software package called Materials Studio. Within this package is a piece of molecular simulation software called CASTEP,[71] which is based on the gauge-including projector-augmented wave density function theory (GIPAW-DFT). This software is ideal for modelling the mono-substituted haloanilinium salts, as the method models actual crystal structures very well, which is particularly important for the calculation of EFG parameters for ions as are found in these systems. GIPAW-DFT uses plane wave pseudo-potentials to map out the repeating crystalline structure of typical three dimensional frameworks. It would be extremely computationally expensive to consider a test system large enough to ensure that the atoms of interest are being properly modelled in the context of an infinite lattice, and this is not done. To use minimal computing time, crystalline systems are represented using periodic boundary conditions, which models an infinite lattice repeating the structure of one defined group of atoms. In the case of x-ray diffraction crystal data, because these data are already solved in terms of a three-dimensional unit cell, it is extremely simple to implement periodic boundary conditions. Because of the way plane waves are used in GIPAW-DFT, it is very simple to control the convergence of calculations using only one parameter, the cut-off energy. This parameter can be increased in order to model crystal data with increasing accuracy. With this simple parameter, convergence tests become as quick as increasing the energy cut-off incrementally until no change in parameters or NMR energy values are found. Because of periodic boundary conditions, calculations on crystal data are much more accurate, but there can be downsides to performing calculations with this method. For example, if modifications to the unit cell are attempted, since the structure is repeating and models a crystal system, areas devoid of atoms inside the unit cell are quite small and interactions with nearby molecules will only be

avoided within a small window. Each method has its benefits and drawbacks, and through the use of both, a detailed understanding of molecular environments is possible.

5.2 Computational Details

Calculations were performed on all compounds whose crystal structures were known (see Table 4.2). CASTEP software was used to model all compounds which have crystal structures, and a subset of those compounds were also modelled using Gaussian software to exploit differences between the two types of calculations. GIPAW-DFT calculations were also performed with CASTEP wherein the unit cell parameters were systematically modified from 95 up to 105 % of their experimental values in one percent increments to model differences in intermolecular distances inside a crystal lattice without affecting intramolecular bond lengths or angles. Crystal structures for compounds **1**,[57] **2**, **4**,[57] **7**,[72] **8**,[73] **9**,[74] **10**,[75] **11**,[57] **13**, **14**,[57] and **18**[74] were used without optimization and, in a second set of calculations, with hydrogen atom optimization. Ultra-fine cutoff energies were used for all GIPAW calculations, unless those would not converge, and in those cases fine cutoffs were used. k-point fields for these calculations were predetermined by CASTEP along with the cutoff energies based on unit cell size. The basis sets used for Gaussian calculations were 6-311++G** with the B3LYP hybrid functional. For bromine, to compare magnetic shielding and chemical shift data directly, the calculated SSNMR isotropic chemical shift from KBr was used, since it has a reference chemical shift value for comparison. While this method does allow the comparison of calculations and experiment, ideally the magnetic shielding value for a bare ^{81}Br nucleus would be calculated (as has been done for chlorine-35, see Chapter 2) to give a more explicit comparison between magnetic shielding and chemical shift, though this has not yet been accomplished.

5.3 CASTEP GIPAW and Gaussian B3LYP DFT analysis of the NMR parameters of selected haloanilinium halide salts

Computations using CASTEP and Gaussian software were carried out on all compounds for which crystal structures have been solved. This includes five chloride containing compounds, numbers **1**, **2**, **4**, **8**, and **9**. For the chlorine compounds (see Table 4.3 for experimental data and Table 5.1 for computed data), C_Q is consistently underestimated by CASTEP calculations to approximately 70 % of experimental values. Trends for the quadrupolar asymmetry parameter, chemical shift span and skew are followed with generally good agreement, and isotropic chemical shifts are overestimated systematically by 40-50 ppm from experiment. There is little agreement between experimental Euler angles and ones calculated and parsed from CASTEP calculations.

Table 5.1. Calculated ^{35}Cl quadrupolar and chemical shift tensor parameters

compound	$C_Q(^{35}Cl)$ / MHz	η_Q	δ_{iso} / ppm	Ω / ppm	κ	α / °	β / °	γ / °
1	4.21	0.42	113.2	100.2	-0.41	49.3	85.3	7.1
2	4.25	0.54	132.1	96.2	-0.60	58.4	16.9	18.1
4	3.83	0.13	136.2	94.5	-0.65	108.1	73.4	2.1
7	3.43	0.65	74.0	124.7	-0.38	32.6	74.7	159.7
8	3.91	0.69	102.6	78.1	0.07	140.5	29.3	329.9
9	3.36	0.34	121.0	101.0	0.26	82.9	13.6	209.6

Table 5.2. Calculated ^{81}Br quadrupolar and chemical shift tensor parameters

compound	$C_Q(^{81}Br)$ / MHz	η_Q	δ_{iso} / ppm	Ω / ppm	κ	α / °	β / °	γ / °
10	-30.94	0.61	30.9	203.9	-0.29	53.5	85.6	358.8
11	-35.49	0.23	91.4	213.5	-0.64	190.6	84.9	7.7
13	-38.17	0.87	10.3	179.8	-0.71	184.0	62.6	345.1
14	-14.48	0.68	91.5	235.7	0.22	244.5	83.6	28.7
18	-14.10	0.82	81.6	90.0	0.08	80.8	83.1	10.7

In examining the results of the bromide compounds' calculations, C_Q is again overestimated, although the differences are much less systematic (See Table 5.2). The experimental values for the quadrupolar coupling range from double calculated values (in compound **14**) up to being nearly equal (in compound **11**), showing that there is correlation between these two data types, but precise calculated values are not systematically similar to experimental ones. Trends in experimental quadrupolar asymmetry are also seen in calculated asymmetries, and though some bromide CS tensor spans are overestimated while others are underestimated, overall trends still match (see Table 4.4 & Table 5.2). Because there is no absolute shielding scale for bromine (see Chapter 2), comparison of isotropic shifts between experiment and calculations require a set of calculations performed on a standard compound, in this case $KBr_{(s)}$, and errors from 50-100 ppm are seen for these calculated shifts. Euler angles are no better than for chlorine and show no correlation to experiment (see Table 4.4 & Table 5.2). Comparison between experiment and calculations for iodine is not possible at this time because no compounds in the series have both NMR and crystal data.

Table 5.3. Calculated ^{127}I quadrupolar and chemical shift tensor parameters

compound	$C_Q(^{127}I)$ / MHz	η_Q	σ_{iso} / ppm	Ω / ppm	κ	α / °	β / °	γ / °
21	103.85	0.618	4748.74	209.91	-0.12	93.9	87.6	38.2
24	-363.62	0.198	2168.33	6873.04	0.79	270.0	1.5	180.0

CASTEP data for these compounds also included quadrupolar and chemical shielding parameters for the covalently bound chlorine, bromine or iodine, giving an indication of what

collection of this data would require in terms of spectrometer time and to consider hardware such as probes (which only tune to certain ranges of frequencies). It also gives some indication (based on calculated values) what kind of parameters would be expected should NQR experiments be done. While this data is indicative of possible future SSNMR experiments, the values for these covalent halogens must be taken with a grain of salt, because no experimental data exist to compare these results to. Using the calculated EFG parameters (C_Q = -69.94 MHz; η_Q = 0.101) for compound **1** in an NQR experiment, along with the equation:[76]

$$\nu_Q = \frac{C_Q}{2}\sqrt{1 + \frac{{\eta_Q}^2}{3}} \qquad \textbf{[5.1]}$$

for the quadrupolar frequency gave a value of -35.03 MHz, which is nowhere near the expected quadrupolar frequencies for similar systems,[77] which is around 30 MHz. In performing this NQR experiment, frequencies between 30-45 MHz were sampled, and no quadrupolar resonance signal was found. In this light, calculated covalent halogen parameters were deemed unimportant and were not included in this study.

Comparisons between GIPAW-DFT and Gaussian calculations were made to experimental data to try to establish connections between crystal structure data and NMR parameters (see Figure 5.1). Since NMR experiments for quadrupolar nuclei can be quite time consuming, it is useful to have some indication of the parameters which are to be expected for a given nuclear environment. When multiple sites are involved it can also be beneficial to have some idea of how many sites to expect and the differences in parameters between them. Currently the level of adherence of calculations to experiment is generally good, though some specific deficiencies are known. For example, computed quadrupolar coupling constants for

chlorine underestimate experimental values by about 25 %. It is these issues which continue to restrict the use of crystallographic DFT calculations to being moderately useful as opposed to predictive, though with continued modification and improvements to the software these inconsistencies will one day be a thing of the past. Presented in Figure 5.1 is a series of graphs showing correlation between experimental and computed parameters for quadrupolar coupling constant, chemical shift span and isotropic chemical shift.

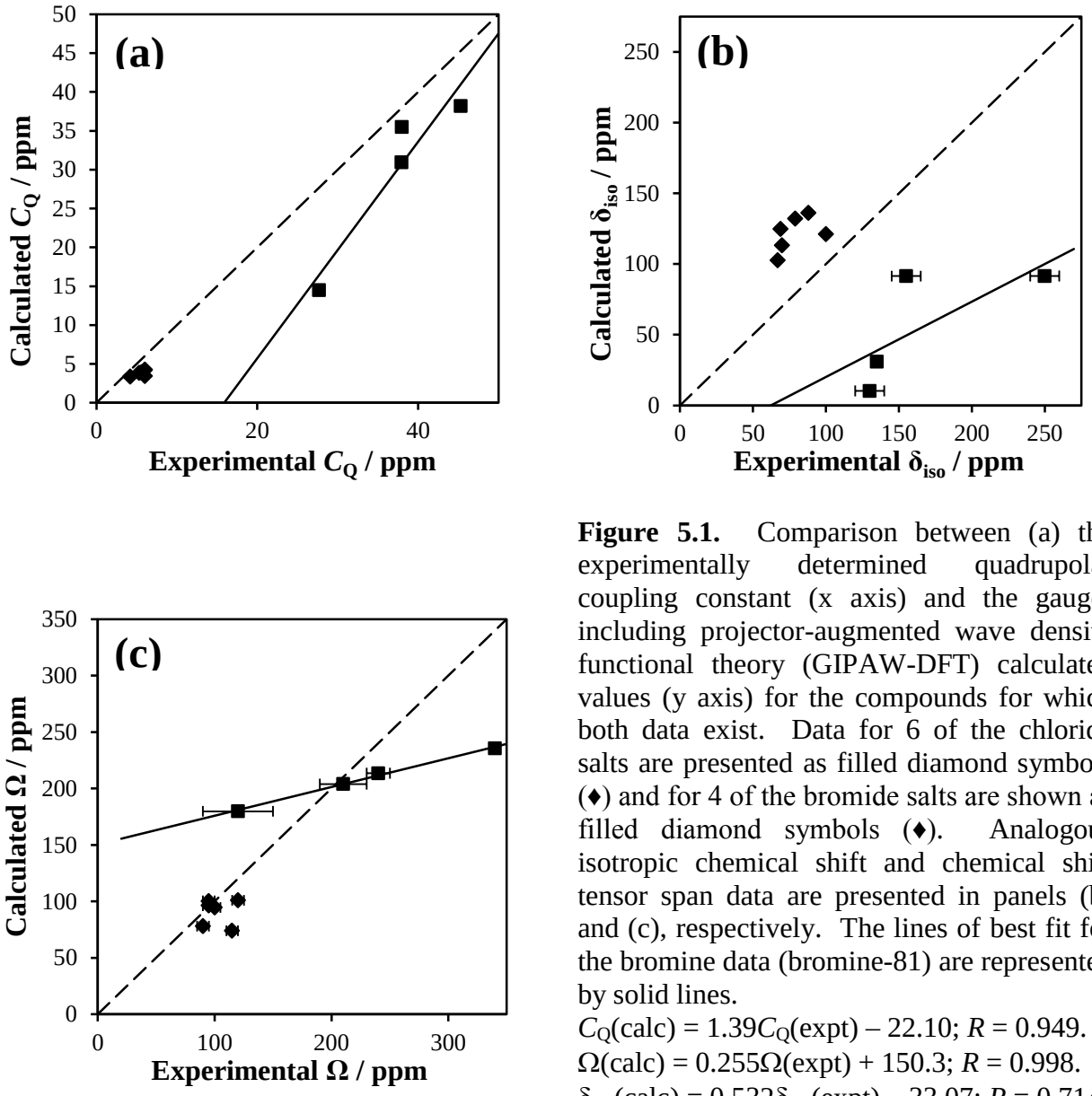

Figure 5.1. Comparison between (a) the experimentally determined quadrupolar coupling constant (x axis) and the gauge-including projector-augmented wave density functional theory (GIPAW-DFT) calculated values (y axis) for the compounds for which both data exist. Data for 6 of the chloride salts are presented as filled diamond symbols (♦) and for 4 of the bromide salts are shown as filled diamond symbols (♦). Analogous isotropic chemical shift and chemical shift tensor span data are presented in panels (b) and (c), respectively. The lines of best fit for the bromine data (bromine-81) are represented by solid lines.
$C_Q(\text{calc}) = 1.39C_Q(\text{expt}) - 22.10$; $R = 0.949$.
$\Omega(\text{calc}) = 0.255\Omega(\text{expt}) + 150.3$; $R = 0.998$.
$\delta_{iso}(\text{calc}) = 0.532\delta_{iso}(\text{expt}) - 33.07$; $R = 0.714$.
The dashed lines represent y = x.

5.4 Trends and insights into correlating structure and SSNMR parameters

From the experimental and calculated parameters for the chlorine and bromine compounds, trends can be pieced together using several series of three compounds varying only one molecular component. In this way, the impact of varying the covalent halogen atom (Cl, Br or I), the position (2, 3 or 4) of the halogen on the aniline ring, and the halide ion which acts as the Lewis base in the crystal structure can be tested. These three changes which can be made are all good indicators of how halogen bonding affects the NMR parameters of the halides. It is well known that halogen bonding gets stronger as the halogen participating increases in size[55] (Cl < Br < I) and so comparing three compounds bearing each of these atoms in sequence should give an indication of whether halogen bonding plays a role in the magnitude or direction of the interactions. Even further along this thread of logic, if a given series of compounds was found to be very similar crystallographically save for minor intramolecular structural differences, any differences in NMR parameters could logically be attributed only to those minor structural changes. In the event, as above, where the changes made to the structure involving different halogens, in effect, changing the halogen bond strength, any changes to NMR parameters can be attributed to a changing halogen bond length or angle. This secondary halogen bond probe (since the atom of study is not strictly the "halogen" in halogen bonding) is a nice handle for gauging halogen bond strength in these systems.

The impact of halogen versus hydrogen bonding was tested with calculations using both GIPAW-DFT and B3LYP hybrid DFT quantum mechanical methods. First, preliminary calculations were performed with unmodified crystal structures and then with hydrogen atom optimized structures, to judge whether hydrogen optimization had any effect, positive or

negative, on the NMR parameters. After these two series of calculations, it was shown that proton optimization of the crystal structures had a negative impact on the calculated parameters (in all cases at least doubling C_Q values and giving worse data than the non-optimized structures), in most cases doubling or tripling the C_Q to the point that the results were meaningless. This probably means that there is an underlying reason why the optimization was ineffective for these compounds, or perhaps there just was not enough time given in the calculation to allow the proton positions to fully optimize. In any case, all further calculations were performed using the un-optimized original crystal structures.

The first set of calculations performed included four sample crystal structures, those of compounds **1**, **2**, **4** and **10**. Using CASTEP (GIPAW-DFT) software inside Materials Studio, the unit cell parameters (a, b, and c) were modified systematically to vary from 95 to 105 % of their original size in increments of 1 %. This change in distances affected only the intermolecular interactions while leaving all intramolecular distances unchanged. Since intermolecular interactions are the desired area of study in the series, this is the first step in isolating the effects of halogen bonding in these systems. Since all intermolecular interactions are varied in the same way, the effects of both hydrogen as well as halogen bonding should get correspondingly weaker or stronger at the same time. Also, in compounds where weaker halogen bonds exist but hydrogen bonds are still relatively strong, it may be possible to watch the effects of the halogen bond shift from strong to weak or from weak to absent.

From these studies, and in Figure 5.3 below, the general trend in chemical shift tensor parameters is that as the intermolecular interactions (the hydrogen and halogen bonds) increase in strength, span and isotropic shift both increase. In other words, as all of the intermolecular

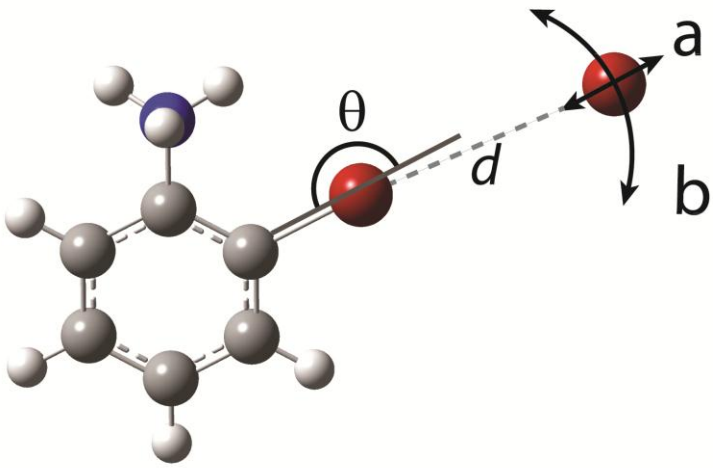

Scheme 2. Sample bonding scheme showing modifications to halogen – halide distance and carbon – halogen – halide angle. Pictured is compound **11** as a sample cluster model with surrounding molecular groups having been removed for clarity. Red atoms are bromine. Modifications corresponding to (a) are shown in Figure 5.4 & Figure 5.5, while those corresponding to (b) are shown in Figure 5.6.

bonds increase in length, span and isotropic shift decrease. With this data set, the effects of hydrogen and halogen bonds on their own must also be measured. In order to do this, a software cluster model was employed.

The effects of intermolecular bonding were tested by creating a cluster model which takes into account the cationic anilinium groups surrounding the halide atom. A model compound was chosen for these calculations, 2-chloroanilinium bromide. The groups are arranged exactly as they are in the corresponding crystal structures, but without the repeating structure. This arrangement allows for the removal or modification of individual aniline rings which interact with the halide atom, allowing for the isolation of effects due to hydrogen and halogen bonding. First, adjusting only the linear halogen bond

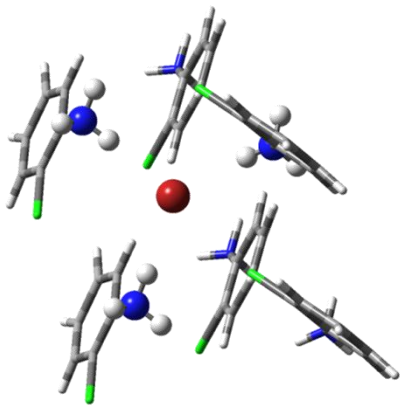

Figure 5.2. Bonding environment surrounding anionic halide in compound **10** with hydrogen bonded NH groups shown in ball and stick form for clarity.

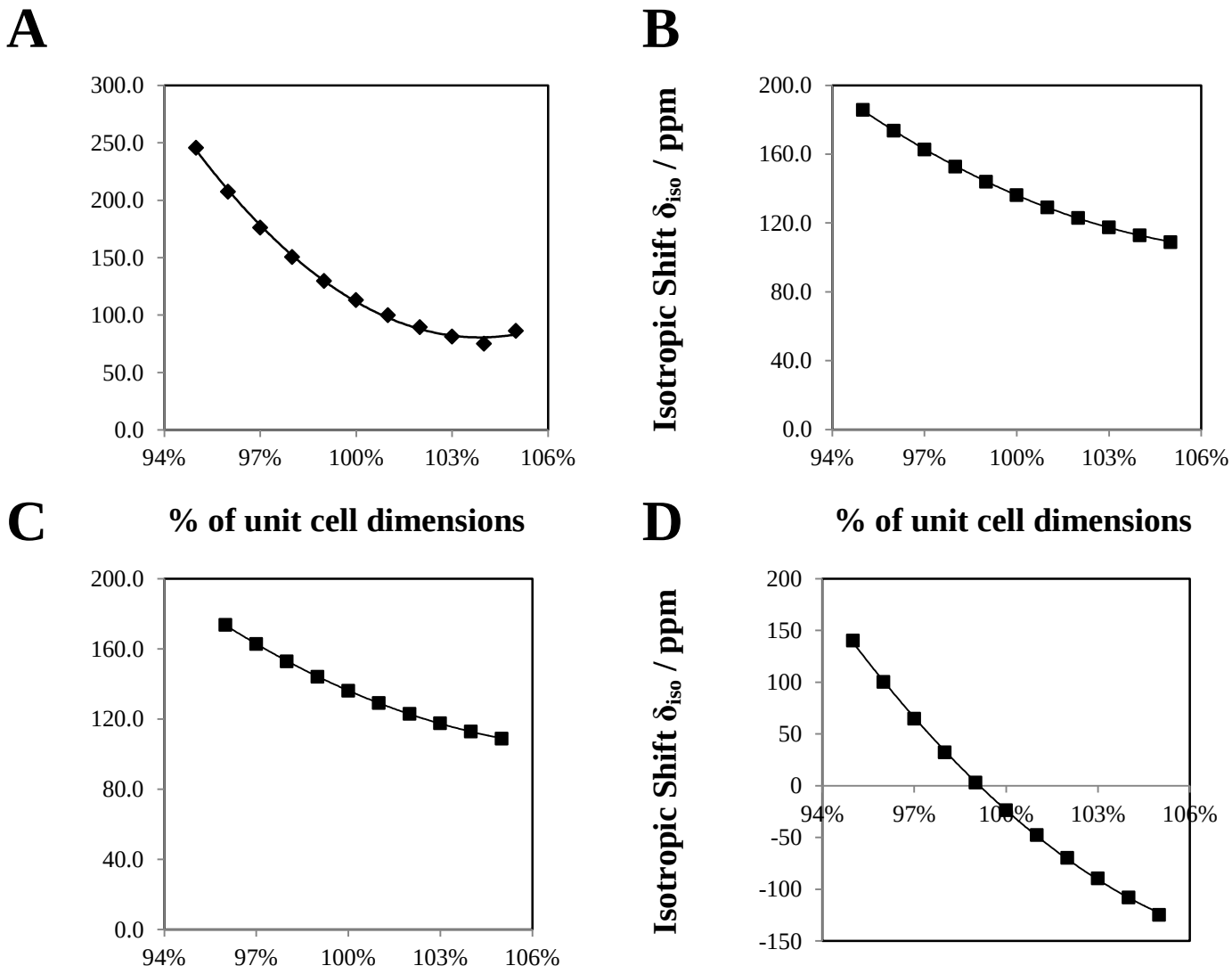

Figure 5.3. Isotropic chemical shift dependence of chloride and bromide compounds based on modified crystal structures based on Scheme **2**(a). Relationship for compound **1** is shown in (A), compound **2** is shown in (B), compound **4** is shown in (C), and compound **10** is shown in (D).

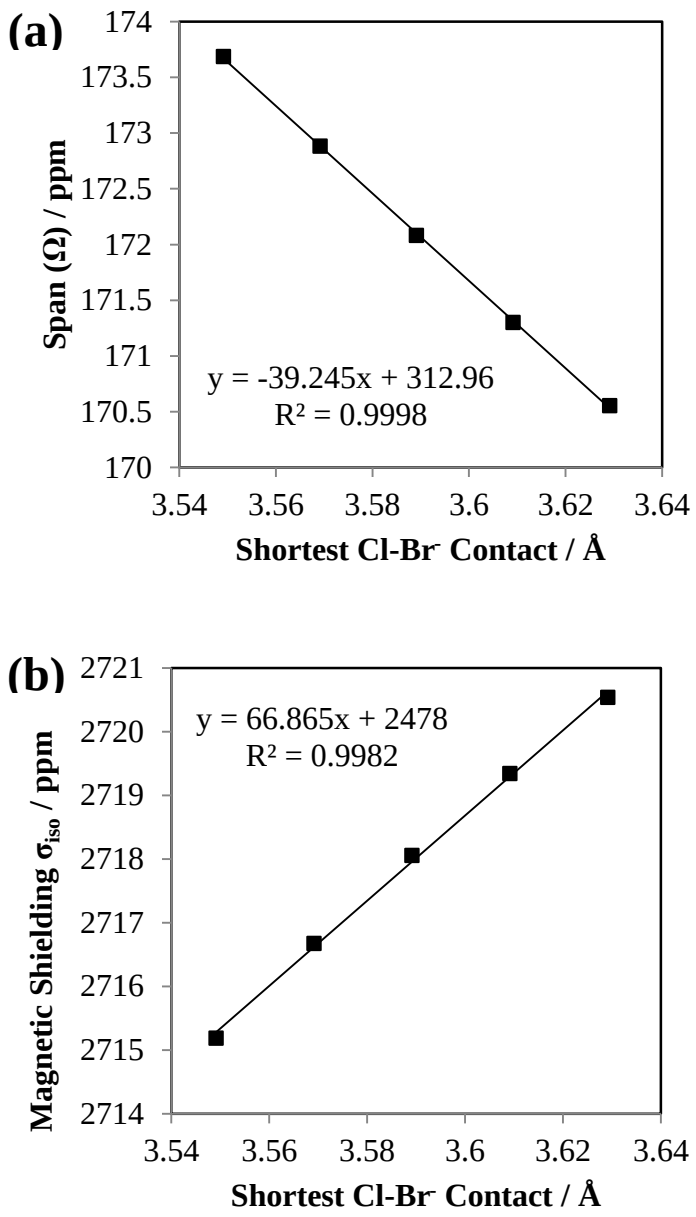

Figure 5.4. Cluster model (Scheme **2**(a)) of compound **11** adjusting only the linear halogen bond length while keeping hydrogen bonds and all angles the same.

length while keeping the angles the same ((a) from Scheme 2), in increments of 0.02 Å, we find that the span and shift follow the same trend as in the CASTEP calculations, with both the span and isotropic shift decreasing by a few ppm over the 0.1 Å range (see Figure 5.4). This trend matches what was seen in the bromide compounds packing in the $Pca2_1$ space group with respect to halogen bond length (see Figure 4.8).

The next set of calculations isolates the impact of the hydrogen bonds in the crystal structure, through the same procedure as above using the B3LYP hybrid density functional method. The difference with these calculations is that since there are three hydrogen bonds in the compound, all hydrogen bonds are modified by 0.04 Å in either direction in 0.01 Å increments, again keeping all bond angles the same. The trend from this series of calculations for both span and isotropic shift also follow the same trend as in the

$Pca2_1$ space group series (compounds **10**, **11**, and **13**) from the crystal structures, which is that both span and isotropic shift decrease with increasing hydrogen bond length (see Figure 5.5).

After all of these calculations trying to find a trend relating NMR parameters to halogen bonding, it seems as though span and isotropic shift are connected to intermolecular bond lengths in crystal structures, though halogen bonding is not the only interaction which affects parameters, as hydrogen bonding also has a noticeable effect on parameters. Ideally these would give slightly different effects, but this is just not the case.

The next step taken in the series of calculations based on these crystal structures brings us back to the GIPAW DFT approach. It was

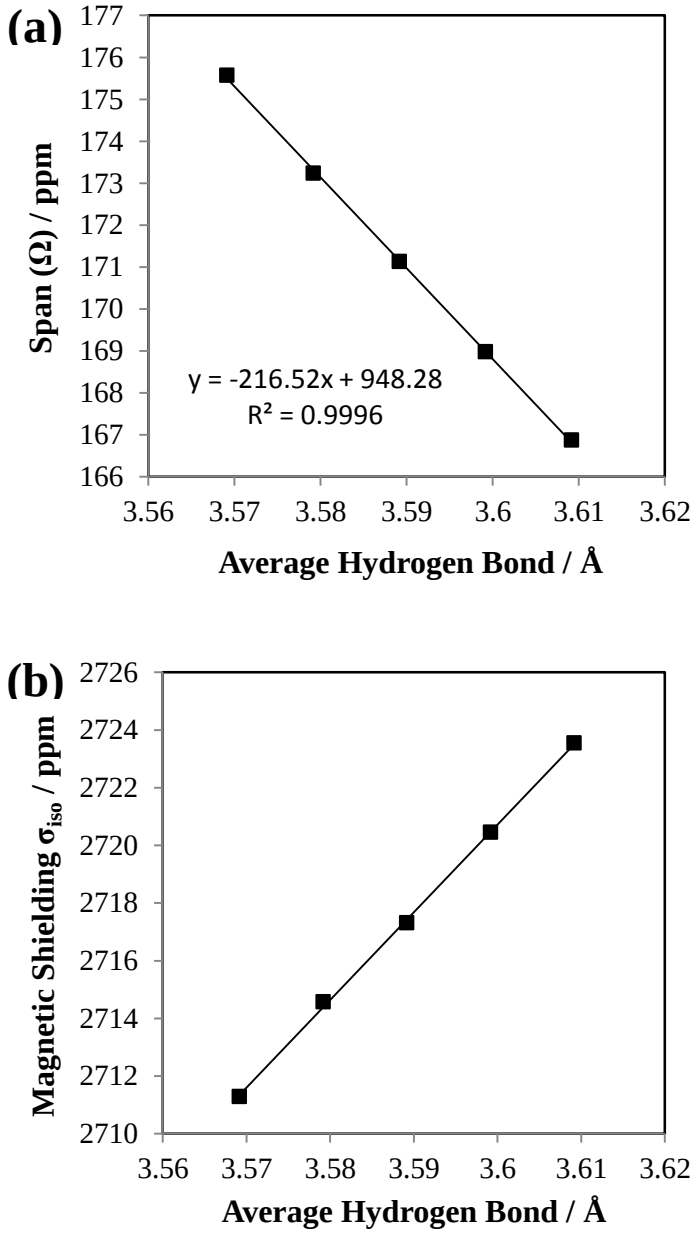

Figure 5.5. Cluster model (Scheme **2**(a)) of compound **11** adjusting only the hydrogen bond length (N-Br) while keeping halogen bond and all angles the same.

suggested that perhaps keeping the unit cell at a constant size and moving the bromide so as to change the angle of the halogen bond would allow some determination of the factors influencing the halogen bonding.

It is well-documented that in halogen bonding cases such as these that the strength of the bond drops off as its angle deviates from linearity[38]. However, in these structures, there is very little empty space to attempt to modify the halogen bond angles and so the unit cells for these calculations have been expanded in all three dimensions to 105 % their original size. With this extra room, it is easy to move the halide in increments of 5 degrees in the plane of the benzene ring ((b) in Scheme 2) over a total range of 10 and 30 degrees in a bromide and chloride compound, respectively, without any interference with adjacent molecular groups.

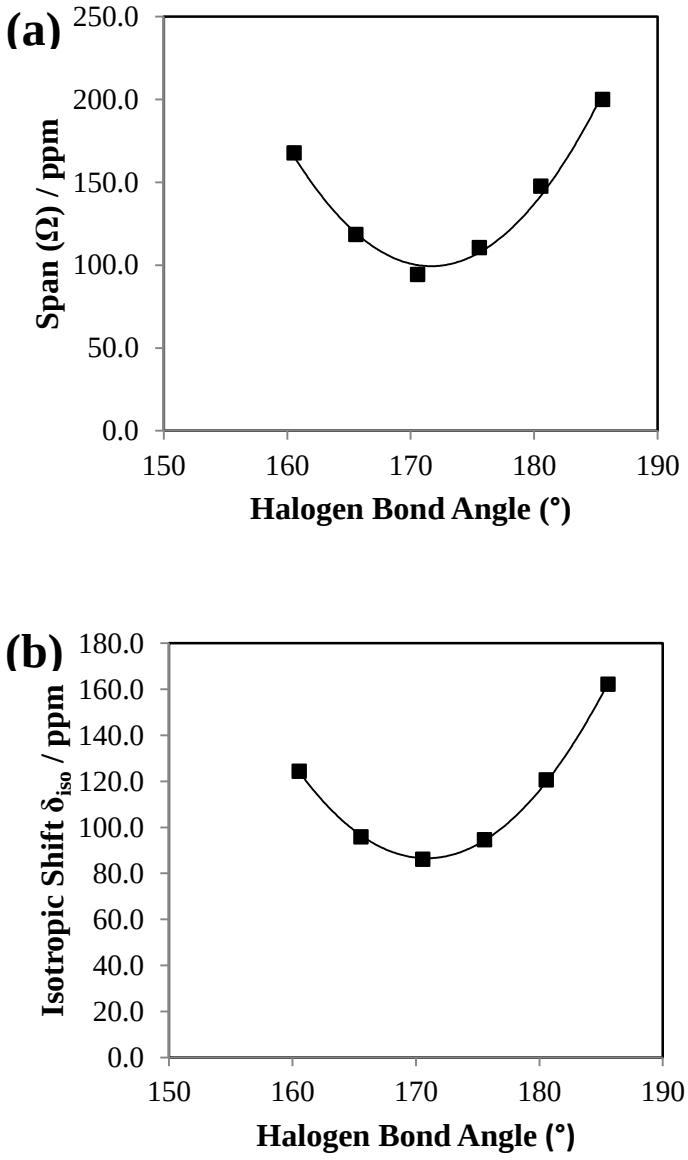

Figure 5.6. Cluster model (Scheme **2**(b)) of compound **11** adjusting the halogen bond angle while keeping halogen bond length and all other angles the same.

From these data (see Figure 5.6), it is clear that there is a strong

dependence of the NMR parameters on the angle of the halogen bond. The NMR energy given as part of GIPAW DFT calculations also show that the structure seems to be the most stable at the actual angle of the halogen bond, and this energy increase with divergence from the optimal halogen bond angle could suggest that a weakening of the halogen bond is the cause of this higher energy.

5.5 Correlation of span and isotropic shift to halogen bonding in *P*ca2$_1$ space group

There are several compounds in this study which pack in the Pca2$_1$ space group (compounds **10**, **11** and **13**, see Table 4.2 & Figure 4.8). These compounds pack in much the same way regardless of the atomic connectivity or the halogen atoms involved. The local environment surrounding the halide ion in the compounds studied consists of three linear hydrogen bonds between amide protons on the aniline and the ionic halide (see Figure 5.2). These hydrogen bonds form a planar equilateral triangle with the halide in the centre; whereas the linear halogen bond in all compounds but **14** range from 160-180 degrees from the covalent halogen and is typically near perpendicular to the hydrogen bonding plane. In theory this perpendicular arrangement between the hydrogen bonding plane and the halogen bond axis should put the two interactions at odds with one another, and should allow for the possibility of comparing the strengths of the competing bonding paradigms. Within the subset of structures which are a part of this space group, the halogen and hydrogen bond lengths change by different amounts. The hydrogen bonds vary in length by only 0.02-0.03 Å between bonds in the same compound, a distance which is almost insignificant even on the molecular scale. On the other hand, halogen bonds in the compounds vary by tenths of Angstroms, up to about a half Angstrom from shortest to longest. These changes even manifest themselves in compounds where the covalent halogen doesn't change, as is the case with the three bromine compounds packing in the Pca2$_1$ space group (compounds **10**, **11** and **13**, see Table 4.2). As shown in Figure 4.8, from the experimental data available so far there is a relation between the chemical shift span of bromide ions as compared to the length of the halogen bonds they participate in. Since the three compounds described all pack in the same space group and have very similar hydrogen bonding

environments, the only remaining factor which seemingly would be able to affect the NMR parameters is the halogen bond.

Given the error bars on the experimental data, we set out to computationally corroborate the experimental findings, and to ensure that the substantial change in $\Omega(^{81}Br)$ is in fact largely associated with a change in the halogen-halide contact. First, the experimental trend was confirmed via gauge-including projector-augmented wave (GIPAW) DFT calculations wherein the crystal structures of the compounds are modeled using periodic boundary conditions.[78] Computed values of $\Omega(^{81}Br)$ are of the correct order of magnitude and clearly follow the experimental trend (Figure 5.7). Computed bromine magnetic shielding constants also substantiate the experimental trend in bromine chemical shifts.

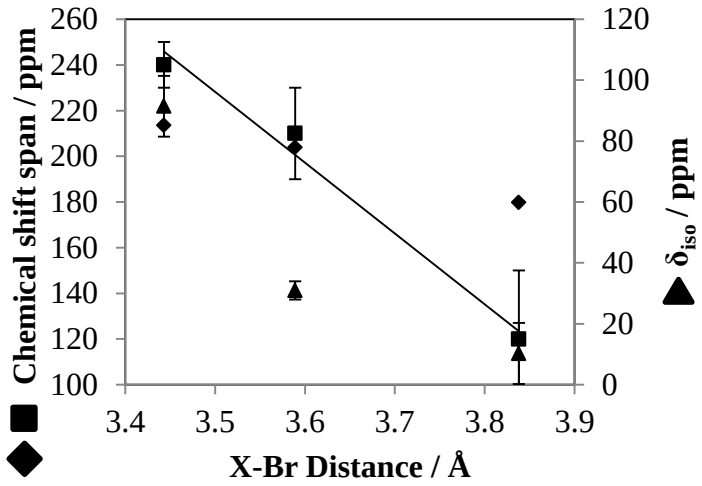

Figure 5.7. Plot of experimental bromine chemical shifts (triangles), bromine chemical shift tensor spans (squares), and GIPAW-DFT calculated spans (diamonds) as a function of the shortest X-Br$^-$ distance (d) in 2-chloroanilinium bromide, 2-bromoanilinium bromide, and 3-chloroanilinium bromide. The line indicates a linear fit to the experimental span data; Ω / ppm = -310d + 1313; R = 0.99.

Next, a cluster model of 2-chloroanilinium bromide, which includes the central bromide ion and the aromatic moieties which are involved in hydrogen and/or halogen bonding with the central ion, was built on the basis of the known atomic coordinates and the bromide-chlorine distance was systematically varied by displacing an intact haloanilinium group, leaving the

remainder of the model unchanged. These results also unequivocally show that $\Omega(^{81}Br)$ and $\delta_{iso}(^{81}Br)$ decrease with increasing bromide-chlorine distance, further substantiating the experimental findings.

This chapter and the one preceding it describe data collected over the course of an SSNMR and computational study of haloanilinium halides and the analysis of that data. Benchmark chlorine-35, bromine-81, and iodine-127 SSNMR data were collected and fit to extract EFG and CS tensor parameters (see Section 4.6). Trends correlating these parameters to space group (see Figure 4.8) as well as to structure are shown. Calculations performed on the compounds in the study for which crystal structures exist show that there are correlations between experimental and calculated values for chlorine and bromine. Further calculations also showed relationships between halogen bonding parameters such as bond length and angle. These trends all show that as the halogen bond gets shorter (and stronger) that chemical shift and span both increase linearly, at least for compounds **10**, **11**, and **13**, where the space group is *P*ca2_1 and so direct comparison is possible. Thus far there is no direct correlation between SSNMR and halogen bonding in general, but the relationship described here (also see Figure 4.8) shows that trends between experimental halogen bonds and SSNMR parameters do exist.

Chapter 6

Conclusions and Future Work

6.1 Conclusions

This study of mono-substituted haloanilinium halides offered 21 compounds which had the potential to employ halogen bonding in their crystal lattices. While some manner of hydrogen bonding was present in all compounds, many did not contain a halogen bond and of those which did, some were quite weak. Benchmark chlorine-35, bromine-81, and iodine-127 SSNMR data were collected and fit for 18 compounds as a part of this study, with all but one (compound **20**) being studied at more than one applied magnetic field. In each case, it was the anionic halide studied by NMR. These data show that collection of SSNMR data from compounds with these types of halide environments can be achieved, due in no small part to the Ultrahigh Field NMR Facility for Solids in Ottawa. With this ultrahigh magnetic field, even ultra-wide line shapes such as those found in these compounds can be properly collected and simulated. Also, at high field the EFG is no longer the dominating influence on the line shape, and CS tensor effects begin to show comparable influence on the spectra.

All of the data for chlorine, bromine, and iodine fit into the known ranges for C_Q, span and chemical shift (see Table 4.3, Table 4.4, and Table 4.5 and Chapter 2 & Chapter 4 for full comparisons), which is not surprising since environments similar to these, such as in the amino acid hydrohalides, have already been studied. In terms of the x-ray crystal structure data, some trends between structure and NMR parameters were found. For example, the experimental chemical shift span was shown to correlate with the shortest halogen bond contact in a series of three bromine compounds which pack in the same $Pca2_1$ space group. It was also shown,

however, that there is no obvious or inherent connection between any of the NMR parameters and the existence of a halogen bond, nor any general trend between any of the parameters and the bonds' strength.

GIPAW-DFT and B3LYP hybrid DFT calculations of the EFG and CS tensor parameters were also performed as part of this study, and these showed that calculations of this type are able to predict trends in most SSNMR parameters. A more complete view of the variation in NMR parameters was gained through CASTEP calculations which looked at each x-ray crystal structure, and with variations in the crystal structure. There were also Gaussian calculations which used a cluster model to simulate different hydrogen and halogen bonding geometries based on both halogen bond distances and angles. Based on these trends, it can be seen that both chemical shift span and isotropic shift can be related to halogen bond length, both in experiment and with calculations.

In summary, this study shows that it is possible to acquire SSNMR data for the quadrupolar halide anions in the haloanilinium halides, and that by simulating these data meaningful EFG and CS tensor parameters can be extracted from the spectra. Crystal structures from these compounds also show that many of them have short halogen bonding-type interactions and that CS tensor parameters are somewhat sensitive to changes in halogen bond length. In addition, DFT calculations performed on the same compounds showed similar trends in CS tensor parameters, but these trends were limited to a series of compounds packing in the same space group, and could not be more broadly applied.

6.2 Future Work

The future of quadrupolar halogen SSNMR has many possibilities to explore, as there are almost an infinite number of compounds available for study with this technique. However, realistically, NMR time is extremely limited, and therefore choices much be made as to which compounds are studied, and so it is up to spectroscopists to decide which series of compounds are pertinent and useful in chemical and physical applications. Since halogen bonding is an important interaction in contemporary structural chemistry, these compounds have been deemed useful for study. Though there are many more compounds which can be studied to describe this kind of bonding better, it would be extremely beneficial to develop a method to use the covalent halogen atom to assess its nuclear environment. It has been proposed that nuclear quadrupole resonance (NQR) be used as a probe of halogen bonding in any important compounds, and at least in theory it seems as though this shouldn't be too difficult, though in practice probe tuning ranges and tedious, time-consuming signal searching must be performed. The reason SSNMR would not work on the covalent halogens in these compounds is that give rise to extremely broad spectra, which take an inordinate amount of time to collect and would have an extremely low signal-to-noise ratio. NQR was attempted on these compounds but no signal was found, due to the low quadrupole resonance frequency of the chlorine nuclei in earth's (zero) magnetic field. Therefore, for the time being, halogen SSNMR seems to remain the best method for determining the effect of the halide atom on halogen bonding in similar environments.

That being said, there are other methods for more closely investigating the halogen bond. First, it is possible to study the *ipso*-carbon by NMR or SSNMR, that being the carbon to which the covalent halogen is attached. Though the changes to the actual carbon-halogen bond itself

may be very small on formation of a halogen bond, NMR is very useful for detecting these small changes in electronics. In addition, using a series of compounds which contain stronger halogen bonds would cause larger changes in the covalent carbon-halogen bond, which would have more of an effect on the NMR parameters of the *ipso* carbon atom.

A second strategy which would be more difficult to implement but would also give more useful results would be to find a series of compounds analogous to the haloanilines but which do not contain hydrogen bonds. In so doing, the results of halogen bonding alone could be separated from those of hydrogen bonding, and changes in SSNMR parameters could more convincingly be applied to halogen bonding as opposed to being attributed to a series of different effects.

A third technique which would allow for a more definitive study of the impact of halogen bonding on SSNMR parameters would to take the route many crystal engineers have. A large majority of these studies use perfluorinated molecules and focus only on covalent iodine, which forms the strongest halogen bonds. Though this does limit the number of compounds and combinations which are possible to study bonding, it does give an assurance that halogens bonds which are formed are quite strong, as nearby covalent fluorines are electron-withdrawing and strengthen the covalent iodine bond. This in turn increases the size of the sigma hole, leading to the possibility of a stronger halogen bond. In terms of available compounds, this technique probably makes the most sense, since many iodoperfluorinated organic compounds exist already, and would be quite conducive to NMR studies provided the choice of Lewis base was restricted to a group or atom amenable to SSNMR studies, such as the quadrupolar halogens.

Appendix A

Crystallographic Information Files

CIF File for Compound 2

```
data_db006a

_audit_creation_method            SHELXL-97
_chemical_name_systematic
;
 ?
;
_chemical_name_common             ?
_chemical_melting_point           ?
_chemical_formula_moiety          ?
_chemical_formula_sum
 'C6 H7 Br Cl N'
_chemical_formula_weight          208.49

loop_
 _atom_type_symbol
 _atom_type_description
 _atom_type_scat_dispersion_real
 _atom_type_scat_dispersion_imag
 _atom_type_scat_source
 'C'  'C'   0.0033   0.0016
 'International Tables Vol C Tables 4.2.6.8 and 6.1.1.4'
 'H'  'H'   0.0000   0.0000
 'International Tables Vol C Tables 4.2.6.8 and 6.1.1.4'
 'N'  'N'   0.0061   0.0033
 'International Tables Vol C Tables 4.2.6.8 and 6.1.1.4'
 'Cl'  'Cl'   0.1484   0.1585
 'International Tables Vol C Tables 4.2.6.8 and 6.1.1.4'
 'Br'  'Br'  -0.2901   2.4595
 'International Tables Vol C Tables 4.2.6.8 and 6.1.1.4'

_symmetry_cell_setting            Orthorhombic
_symmetry_space_group_name_H-M    Pca2(1)

loop_
 _symmetry_equiv_pos_as_xyz
 'x, y, z'
 '-x, -y, z+1/2'
```

```
 'x+1/2, -y, z'
 '-x+1/2, y, z+1/2'

_cell_length_a                    15.606(2)
_cell_length_b                    5.4026(7)
_cell_length_c                    8.7865(11)
_cell_angle_alpha                 90.00
_cell_angle_beta                  90.00
_cell_angle_gamma                 90.00
_cell_volume                      740.80(17)
_cell_formula_units_Z             4
_cell_measurement_temperature     200(2)
_cell_measurement_reflns_used     3447
_cell_measurement_theta_min       2.61
_cell_measurement_theta_max       28.22

_exptl_crystal_description        block
_exptl_crystal_colour             white
_exptl_crystal_size_max           0.32
_exptl_crystal_size_mid           0.25
_exptl_crystal_size_min           0.21
_exptl_crystal_density_meas       ?
_exptl_crystal_density_diffrn     1.869
_exptl_crystal_density_method     'not measured'
_exptl_crystal_F_000              408
_exptl_absorpt_coefficient_mu     5.816
_exptl_absorpt_correction_type    multi-scan
_exptl_absorpt_correction_T_min   0.2576
_exptl_absorpt_correction_T_max   0.3747
_exptl_absorpt_process_details    'SADABS, Bruker (2003)'

_exptl_special_details
;
 Data collection is performed with three batch runs at phi =
0.00 deg
 (650 frames), at phi = 120.00 deg (650 frames), and at phi =
240.00 deg
 (650 frames).
 Frame width = 0.30 deg in omega.
 Data is merged, corrected for decay (if any), and treated with
multi-scan
 absorption corrections (if required).  All symmetry-equivalent
reflections
 are merged for centrosymmetric data.
 Friedel pairs are not merged for noncentrosymmetric data.
;
```

```
_diffrn_ambient_temperature       200(2)
_diffrn_radiation_wavelength      0.71073
_diffrn_radiation_type            MoK\a
_diffrn_radiation_source          'fine-focus sealed tube'
_diffrn_radiation_monochromator   graphite
_diffrn_measurement_device_type   'Bruker APEX-II CCD'
_diffrn_measurement_method        '\f and \w scans'
_diffrn_detector_area_resol_mean  ?
_diffrn_reflns_number             5679
_diffrn_reflns_av_R_equivalents   0.0246
_diffrn_reflns_av_sigmaI/netI     0.0251
_diffrn_reflns_limit_h_min        -20
_diffrn_reflns_limit_h_max        16
_diffrn_reflns_limit_k_min        -7
_diffrn_reflns_limit_k_max        7
_diffrn_reflns_limit_l_min        -11
_diffrn_reflns_limit_l_max        11
_diffrn_reflns_theta_min          2.61
_diffrn_reflns_theta_max          28.31
_reflns_number_total              1695
_reflns_number_gt                 1589
_reflns_threshold_expression      >2sigma(I)

_computing_data_collection        'APEX II, Bruker (2009)'
_computing_cell_refinement        'APEX II, Bruker (2009)'
_computing_data_reduction         'XPREP, Bruker (2009)'
_computing_structure_solution     'SHELXS-97 (Sheldrick, 2008)'
_computing_structure_refinement   'SHELXL-97 (Sheldrick, 2008)'
_computing_molecular_graphics     'SHELXTL, Bruker (2004)'
_computing_publication_material   'SHELXTL, Bruker (2004)'

_refine_special_details
;
 Refinement of F^2^ against ALL reflections.   The weighted R-
factor wR and
 goodness of fit S are based on F^2^, conventional R-factors R
are based
 on F, with F set to zero for negative F^2^.  The threshold
expression of
 F^2^ > 2sigma(F^2^) is used only for calculating R-factors(gt)
etc.  and is
 not relevant to the choice of reflections for refinement.   R-
factors based
 on F^2^ are statistically about twice as large as those based
on F, and R-
```

```
 factors based on ALL data will be even larger.
;

_refine_ls_structure_factor_coef  Fsqd
_refine_ls_matrix_type            full
_refine_ls_weighting_scheme       calc
_refine_ls_weighting_details
 'calc w=1/[\s^2^(Fo^2^)+(0.0397P)^2^]'
_atom_sites_solution_primary      direct
_atom_sites_solution_secondary    difmap
_atom_sites_solution_hydrogens    geom
_refine_ls_hydrogen_treatment     constr
_refine_ls_extinction_method      none
_refine_ls_extinction_coef        ?
_refine_ls_abs_structure_details
 'Flack H D (1983), Acta Cryst.  A39, 876-881'
_refine_ls_abs_structure_Flack    0.019(14)
_refine_ls_number_reflns          1695
_refine_ls_number_parameters      82
_refine_ls_number_restraints      1
_refine_ls_R_factor_all           0.0259
_refine_ls_R_factor_gt            0.0239
_refine_ls_wR_factor_ref          0.0623
_refine_ls_wR_factor_gt           0.0614
_refine_ls_goodness_of_fit_ref    1.084
_refine_ls_restrained_S_all       1.083
_refine_ls_shift/su_max           0.001
_refine_ls_shift/su_mean          0.000

loop_
 _atom_site_label
 _atom_site_type_symbol
 _atom_site_fract_x
 _atom_site_fract_y
 _atom_site_fract_z
 _atom_site_U_iso_or_equiv
 _atom_site_adp_type
 _atom_site_occupancy
 _atom_site_symmetry_multiplicity
 _atom_site_calc_flag
 _atom_site_refinement_flags
 _atom_site_disorder_assembly
 _atom_site_disorder_group
Br1 Br 0.393839(16) 0.25103(4) 0.01832(8) 0.02436(9) Uani 1 1 d
.  .  .
```

```
Cl1 Cl 0.53010(4) 0.80842(11) 0.92009(8) 0.02288(13) Uani 1 1 d
.  .  .
C6 C 0.28365(18) 0.8305(6) 0.2614(3) 0.0248(6) Uani 1 1 d .  .
.
H6A H 0.3031 0.9626 0.3238 0.030 Uiso 1 1 calc R .  .
C5 C 0.1972(2) 0.8008(6) 0.2321(4) 0.0315(7) Uani 1 1 d .  .  .
H5A H 0.1568 0.9120 0.2754 0.038 Uiso 1 1 calc R .  .
C1 C 0.34229(18) 0.6632(5) 0.1978(3) 0.0191(5) Uani 1 1 d .  .
.
C4 C 0.16938(19) 0.6081(6) 0.1394(3) 0.0309(7) Uani 1 1 d .  .
.
H4A H 0.1099 0.5896 0.1190 0.037 Uiso 1 1 calc R .  .
C3 C 0.22677(17) 0.4444(5) 0.0769(3) 0.0275(6) Uani 1 1 d .  .
.
H3A H 0.2073 0.3120 0.0148 0.033 Uiso 1 1 calc R .  .
C2 C 0.31408(15) 0.4750(4) 0.1060(3) 0.0211(5) Uani 1 1 d .  .
.
N1 N 0.43389(15) 0.6927(4) 0.2305(3) 0.0206(4) Uani 1 1 d .  .
.
H1C H 0.4641 0.5734 0.1808 0.031 Uiso 1 1 calc R .  .
H1A H 0.4428 0.6785 0.3325 0.031 Uiso 1 1 calc R .  .
H1B H 0.4516 0.8445 0.1986 0.031 Uiso 1 1 calc R .  .

loop_
 _atom_site_aniso_label
 _atom_site_aniso_U_11
 _atom_site_aniso_U_22
 _atom_site_aniso_U_33
 _atom_site_aniso_U_23
 _atom_site_aniso_U_13
 _atom_site_aniso_U_12
Br1 0.03175(15) 0.01654(13) 0.02478(15) -0.00520(8) 0.00359(14)
0.00036(9)
Cl1 0.0271(3) 0.0159(2) 0.0257(3) 0.0030(3) 0.0060(3) 0.0011(2)
C6 0.0304(14) 0.0181(12) 0.0259(14) -0.0055(11) 0.0057(11) -
0.0011(12)
C5 0.0277(15) 0.0271(13) 0.0396(18) -0.0056(14) 0.0045(13)
0.0056(12)
C1 0.0224(13) 0.0155(12) 0.0193(13) 0.0028(10) 0.0031(9) -
0.0001(10)
C4 0.0201(13) 0.0376(17) 0.0349(17) -0.0066(13) 0.0002(11) -
0.0027(13)
C3 0.0292(13) 0.0222(12) 0.0310(14) -0.0051(10) -0.0025(10) -
0.0056(11)
C2 0.0262(12) 0.0170(11) 0.0199(11) 0.0019(10) 0.0037(10)
0.0007(9)
```

```
N1 0.0244(11) 0.0156(9) 0.0218(11) 0.0000(9) -0.0001(9) -
0.0022(9)

_geom_special_details
;
 All esds (except the esd in the dihedral angle between two l.s.
planes)
 are estimated using the full covariance matrix.   The cell esds
are taken
 into account individually in the estimation of esds in
distances, angles
 and torsion angles; correlations between esds in cell
parameters are only
 used when they are defined by crystal symmetry.   An
approximate (isotropic)
 treatment of cell esds is used for estimating esds involving
l.s.  planes.
;

loop_
 _geom_bond_atom_site_label_1
 _geom_bond_atom_site_label_2
 _geom_bond_distance
 _geom_bond_site_symmetry_2
 _geom_bond_publ_flag
Br1 C2 1.899(2) .  ?
C6 C5 1.382(4) .  ?
C6 C1 1.402(4) .  ?
C5 C4 1.391(5) .  ?
C1 C2 1.371(4) .  ?
C1 N1 1.467(4) .  ?
C4 C3 1.373(4) .  ?
C3 C2 1.396(3) .  ?

loop_
 _geom_angle_atom_site_label_1
 _geom_angle_atom_site_label_2
 _geom_angle_atom_site_label_3
 _geom_angle
 _geom_angle_site_symmetry_1
 _geom_angle_site_symmetry_3
 _geom_angle_publ_flag
C5 C6 C1 119.2(3) .  .  ?
C6 C5 C4 120.0(3) .  .  ?
C2 C1 C6 120.2(3) .  .  ?
C2 C1 N1 120.6(2) .  .  ?
```

```
C6 C1 N1 119.2(2) .  .  ?
C3 C4 C5 120.8(3) .  .  ?
C4 C3 C2 119.1(2) .  .  ?
C1 C2 C3 120.6(2) .  .  ?
C1 C2 Br1 120.06(19) .  .  ?
C3 C2 Br1 119.34(19) .  .  ?

loop_
 _geom_torsion_atom_site_label_1
 _geom_torsion_atom_site_label_2
 _geom_torsion_atom_site_label_3
 _geom_torsion_atom_site_label_4
 _geom_torsion
 _geom_torsion_site_symmetry_1
 _geom_torsion_site_symmetry_2
 _geom_torsion_site_symmetry_3
 _geom_torsion_site_symmetry_4
 _geom_torsion_publ_flag
C1 C6 C5 C4 -0.6(5) .  .  .  .  ?
C5 C6 C1 C2 1.0(4) .  .  .  .  ?
C5 C6 C1 N1 -179.2(3) .  .  .  .  ?
C6 C5 C4 C3 0.5(5) .  .  .  .  ?
C5 C4 C3 C2 -0.8(5) .  .  .  .  ?
C6 C1 C2 C3 -1.2(4) .  .  .  .  ?
N1 C1 C2 C3 178.9(2) .  .  .  .  ?
C6 C1 C2 Br1 179.3(2) .  .  .  .  ?
N1 C1 C2 Br1 -0.6(3) .  .  .  .  ?
C4 C3 C2 C1 1.2(4) .  .  .  .  ?
C4 C3 C2 Br1 -179.4(2) .  .  .  .  ?

_diffrn_measured_fraction_theta_max    0.985
_diffrn_reflns_theta_full              28.31
_diffrn_measured_fraction_theta_full   0.985
_refine_diff_density_max    0.282
_refine_diff_density_min   -0.719
_refine_diff_density_rms    0.103
```

CIF File for Compound 13

```
data_db002a
_audit_creation_method 'SHELXL-97'
_audit_creation_date     2011-08-26
_audit_update_record     2011-08-26
_chemical_formula_sum    'C6 H7 Br Cl N'
_chemical_formula_weight 208.490
_refine_ls_R_factor_all  0.027
_cell_length_a 16.1551(5)
_cell_length_b  5.5958(2)
_cell_length_c  8.4538(2)
_cell_angle_alpha   90.000
_cell_angle_beta    90.000
_cell_angle_gamma   90.000
_cell_volume   764.2(0)
_cell_formula_units_Z    4
_symmetry_int_tables_number   29
_symmetry_space_group_name_H-M     'P c a 21'
_symmetry_space_group_name_Hall    'P_2c_-2ac'

loop_
_symmetry_equiv_pos_site_id
_symmetry_equiv_pos_as_xyz
1 x,y,z
2 -x,-y,0.500+z
3 0.500-x,y,0.500+z
4 0.500+x,-y,z

loop_
_atom_type_symbol
_atom_type_oxidation_number
_atom_type_radius_bond
Br   ?    1.200
Cl   ?    1.200
N    ?    1.200
H    ?    1.200
C    ?    1.200

loop_
_atom_site_label
_atom_site_type_symbol
_atom_site_fract_x
_atom_site_fract_y
_atom_site_fract_z
_atom_site_occupancy
```

```
_atom_site_symmetry_multiplicity
_atom_site_Wyckoff_symbol
_atom_site_attached_hydrogens
_atom_site_calc_flag
_atom_site_thermal_displace_type
_atom_site_u_iso_or_equiv
Br1 Br  0.5285(0)  0.6505(0)  0.3443(0)  1.000 4 a ? d Uani
0.03053(8)
Cl2 Cl  0.8671(0) -0.1602(1)  0.2690(1)  1.000 4 a ? d Uani
0.03625(15)
N1 N  0.5730(1)  0.1548(3)  0.1575(3)  1.000 4 a ? d Uani
0.0302(4)
H1A H  0.5621  0.0209  0.2149  1.000 4 a ? calc Uiso  0.04500
H1B H  0.5475  0.1444  0.0618  1.000 4 a ? calc Uiso  0.04500
H1C H  0.5540  0.2854  0.2103  1.000 4 a ? calc Uiso  0.04500
C1 C  0.6626(2)  0.1767(4)  0.1341(3)  1.000 4 a ? d Uani
0.0255(5)
C4 C  0.8311(2)  0.2349(5)  0.0984(3)  1.000 4 a ? d Uani
0.0316(5)
H4A H  0.8892  0.2551  0.0870  1.000 4 a ? calc Uiso  0.03800
C6 C  0.7146(2)  0.0111(4)  0.2020(3)  1.000 4 a ? d Uani
0.0273(5)
H6A H  0.6934 -0.1207  0.2601  1.000 4 a ? calc Uiso  0.03300
C5 C  0.7995(2)  0.0439(4)  0.1823(3)  1.000 4 a ? d Uani
0.0268(4)
C2 C  0.6920(2)  0.3703(4)  0.0490(3)  1.000 4 a ? d Uani
0.0319(5)
H2A H  0.6548  0.4827  0.0038  1.000 4 a ? calc Uiso  0.03800
C3 C  0.7763(2)  0.3967(5)  0.0311(3)  1.000 4 a ? d Uani
0.0354(6)
H3A H  0.7972  0.5277 -0.0282  1.000 4 a ? calc Uiso  0.04300


loop_
_atom_site_aniso_label
_atom_site_aniso_U_11
_atom_site_aniso_U_22
_atom_site_aniso_U_33
_atom_site_aniso_U_12
_atom_site_aniso_U_13
_atom_site_aniso_U_23
Br1  0.02778(13)  0.02499(13)  0.03881(12)  0.00289(7)
0.00265(10)  0.00152(15)
Cl2  0.0269(3)  0.0314(3)  0.0505(3)  0.0028(2) -0.0026(3)
0.0070(3)
```

```
N1  0.0257(11)  0.0252(11)  0.0397(11)  0.0015(7) -0.0001(8)
0.0027(7)
C1  0.0261(12)  0.0215(11)  0.0290(11) -0.0015(8) -0.0010(9) -
0.0026(8)
C4  0.0254(11)  0.0318(13)  0.0374(12) -0.0068(10)  0.0017(9)
0.0010(12)
C6  0.0275(12)  0.0207(11)  0.0336(11) -0.0026(9)  0.0008(8)
0.0019(8)
C5  0.0258(11)  0.0230(11)  0.0316(10) -0.0002(9) -0.0017(8) -
0.0012(9)
C2  0.0347(13)  0.0243(12)  0.0366(13) -0.0001(9) -0.0022(9)
0.0064(9)
C3  0.0392(14)  0.0278(12)  0.0393(13) -0.0065(10)  0.0017(11)
0.0091(10)

loop_
_geom_bond_atom_site_label_1
_geom_bond_atom_site_label_2
_geom_bond_site_symmetry_1
_geom_bond_site_symmetry_2
_geom_bond_distance
_geom_bond_publ_flag
Cl2 C5 .  .   1.742(2) no
N1 C1 .  .   1.465(3) no
C1 C6 .  .   1.376(3) no
C1 C2 .  .   1.385(3) no
C4 C5 .  .   1.380(4) no
C4 C3 .  .   1.389(4) no
C6 C5 .  .   1.394(3) no
C2 C3 .  .   1.378(4) no

loop_
_geom_angle_atom_site_label_1
_geom_angle_atom_site_label_2
_geom_angle_atom_site_label_3
_geom_angle_site_symmetry_1
_geom_angle_site_symmetry_2
_geom_angle_site_symmetry_3
_geom_angle
_geom_angle_publ_flag
C6 C1 C2 .  .  .  122.2(2) no
C6 C1 N1 .  .  .  119.4(2) no
C2 C1 N1 .  .  .  118.4(2) no
C5 C4 C3 .  .  .  118.6(2) no
C1 C6 C5 .  .  .  117.5(2) no
C4 C5 C6 .  .  .  121.9(2) no
```

```
C4 C5 Cl2 .  .  .  119.4(2) no
C6 C5 Cl2 .  .  .  118.73(18) no
C3 C2 C1 .  .  .  118.7(2) no
C2 C3 C4 .  .  .  121.0(2) no

loop_
_geom_torsion_atom_site_label_1
_geom_torsion_atom_site_label_2
_geom_torsion_atom_site_label_3
_geom_torsion_atom_site_label_4
_geom_torsion_site_symmetry_1
_geom_torsion_site_symmetry_2
_geom_torsion_site_symmetry_3
_geom_torsion_site_symmetry_4
_geom_torsion
_geom_torsion_publ_flag
C2 C1 C6 C5 .  .  .  .  -0.1(4) no
N1 C1 C6 C5 .  .  .  .  -177.4(2) no
C3 C4 C5 C6 .  .  .  .  -0.5(4) no
C3 C4 C5 Cl2 .  .  .  .  -179.5(2) no
C1 C6 C5 C4 .  .  .  .  0.1(4) no
C1 C6 C5 Cl2 .  .  .  .  179.14(18) no
C6 C1 C2 C3 .  .  .  .  0.4(4) no
N1 C1 C2 C3 .  .  .  .  177.8(2) no
C1 C2 C3 C4 .  .  .  .  -0.8(4) no
C5 C4 C3 C2 .  .  .  .  0.9(4) no
```

References

[1] In *NMR Spectroscopy: New Methods and Applications*; Comstock, M. J., Ed.; American Chemical Society: 1982; Vol. 191.

[2] Yves, G.; et al. *J. Phys. D: Appl. Phys.***2010**, 43, 213001.

[3] Bryce, D. L.; Wasylishen, R. E. *Acc. Chem. Res.* **2003**, 36, 327.

[4] J. Herzfeld, A. E. Berger, *J. Chem. Phys.* **1980**, *73*, 6021.

[5] Andrew, E. R.; Bradbury, A.; Eades, R. G. *Nature* **1958**, 182, 1659.

[6] (a) Chapman, R. P.; Bryce, D. L. *Phys. Chem. Chem. Phys.* **2007**, *9*, 6219; (b) Bryce, D. L.; Sward, G. D.; Adiga, S. *J. Am. Chem. Soc.* **2006**, *128*, 2121.

[7] Pickard, C. J.; Mauri, F. *Phys Rev B: Condens. Matter* **2001**, *63*, 245101.

[8] Gaussian 09, Revision **A.02**, Frisch, M. J.; Trucks, G. W.; Schlegel, H. B.; Scuseria, G. E.; Robb, M. A.; Cheeseman, J. R.; Scalmani, G.; Barone, V.; Mennucci, B.; Petersson, G. A.; Nakatsuji, H.; Caricato, M.; Li, X.; Hratchian, H. P.; Izmaylov, A. F.; Bloino, J.; Zheng, G.; Sonnenberg, J. L.; Hada, M.; Ehara, M.; Toyota, K.; Fukuda, R.; Hasegawa, J.; Ishida, M.; Nakajima, T.; Honda, Y.; Kitao, O.; Nakai, H.; Vreven, T.; Montgomery, Jr., J. A.; Peralta, J. E.; Ogliaro, F.; Bearpark, M.; Heyd, J. J.; Brothers, E.; Kudin, K. N.; Staroverov, V. N.; Kobayashi, R.; Normand, J.; Raghavachari, K.; Rendell, A.; Burant, J. C.; Iyengar, S. S.; Tomasi, J.; Cossi, M.; Rega, N.; Millam, N. J.; Klene, M.; Knox, J. E.; Cross, J. B.; Bakken, V.; Adamo, C.; Jaramillo, J.; Gomperts, R.; Stratmann, R. E.; Yazyev, O.; Austin, A. J.; Cammi, R.; Pomelli, C.; Ochterski, J. W.; Martin, R. L.; Morokuma, K.; Zakrzewski, V. G.; Voth, G. A.; Salvador, P.; Dannenberg, J. J.; Dapprich, S.; Daniels, A. D.; Farkas, Ö.;

Foresman, J. B.; Ortiz, J. V.; Cioslowski, J.; Fox, D. J. Gaussian, Inc., Wallingford CT, 2009.

[9] Bloch, F. *Phys. Rev.* **1946**, 70, 460-473.

[10] Massiot, D.; Farnan, I.; Gautier, N.; Trumeau, D.; Trokiner, A.; Coutures, J. P. *Solid State Nucl. Magn. Reson.* **1995**, *4*, 241.

[11] MacKenzie, K. J. D.; Smith, M. E. *Multinuclear solid-state NMR of inorganic materials*; Pergamon, 2002.

[12] (a) Bryce, D. L.; Sward, G. D. *Magn. Reson. Chem.*, **2006**, 44, 409.

[13] Widdifield, C. M.; Chapman, R. P.; Bryce, D. L. *Annu. Rep. Nucl. Magn. Reson. Spectrosc.*, **2009**, 66, 195.

[14] Gordon, P. G.; Brouwer, D. H.; Ripmeester, J. A. *Chem. Phys. Chem.* **2010**, *11*, 260.

[15] Rossini, A. J.; Mills, R. W.; Briscoe, G. A.; Norton, E. L.; Geier, S. J.; Hung, I.; Zheng, S.; Autschbach, J.; Schurko, R. W. *J. Am. Chem. Soc.* **2009**, *131*, 3317.

[16] Chapman, R. P.; Bryce, D. L. *Phys. Chem. Chem. Phys.* **2009**, *11*, 6987.

[17] Widdifield, C. M.; Bryce, D. L. *J. Phys. Chem. A* **2010**, *114*, 2102.

[18] Persons, J.; Harbison, G. S. *J. Mag. Reson.* **2007**, *186*, 347.

[19] Gordon, P. G.; Brouwer, D. H.; Ripmeester, J. A. *Chemphyschem* **2010**, *11*, 260.

[20] (a) D. L., Bryce; G. D., Sward, *J. Phys. Chem. B.*, **2006,** 110, 26461.

(b) D. L., Bryce; G. D., Sward; Adiga, S., *J. Am. Chem. Soc.*, **2006,** 128, 2121; (c) D. L. Bryce; Gee, M.; Wasylishen, R. E., *J. Phys. Chem. A,* **2001,** 105, 10413.

[21] Chapman, R. P.; Widdifield, C. M.; Bryce, D. L. *Prog. Nucl. Magn. Reson.*

Spectrosc. **2009**, *55*, 215.

[22] Medek, A.; Harwood, J. S.; Frydman, L. *J. Am. Chem. Soc.* **1995**, *117*, 12779.

[23] Gan, Z. *J. Am. Chem. Soc.* **2000**, *122*, 3242.

[24] Trill, H.; Eckert, H.; Srdanov, V. I. *J. Phys. Chem. B* **2003**, *107*, 8779.

[25] University of Ottawa NMR Facility Blog. QCPMG. http://u-of-o-nmr-facility.blogspot.com/2008/11/qcpmg.html (accessed Sept. 26, 2011)

[26] Larsen, F. H.; Jakobsen, H. J.; Ellis, P. D.; Nielsen, N. C. *J. Phys. Chem. A* **1997**, *101*, 8597.

[27] Kentgens, A. P. M.; Verhagen, R. *Chem. Phys. Lett.* **1999**, *300*, 435.

[28] Siegel, R.; Nakashima, T. T.; Wasylishen, R. E. *Chem. Phys. Lett.* **2004**, *388*, 441.

[29] Skibsted, J.; Jakobsen, H. J. *Inorg. Chem.* **1999**, *38*, 1806.

[30] O'Dell, L. A.; Schurko, R. W. *Chem. Phys. Lett.* **2008**, *464*, 97.

[31] Terraneo, G.; Bruce, D. W.; Cavallo, G.; Metrangolo, P.; Abate, A.; Pilati, T.; Resnati, G.; American Chemical Society: 2010, p SESW.

[32] Lommerse, J. P. M.; Stone, A. J.; Taylor, R.; Allen, F. H. *J. Am. Chem. Soc.* **1996**, *118*, 3108.

[33] Politzer, P.; Murray, J. S.; Clark, T. *Phys. Chem. Chem. Phys.* **2010**, *12*, 7748.

[34] Roper, L. C.; Prasang, C.; Whitwood, A. C.; Bruce, D. W. *CrystEngComm* **2010**, 12, 3382.

[35] Clark, T.; Hennemann, M.; Murray, J.; Politzer, P. *J. Mol. Model.* **2007**, *13*, 291.

[36] Cincic, D.; Friscic, T.; Jones, W. *CrystEngComm*, **2011**, 13, 3224.

[37] Amezaga, N. J. M.; Pamies, S. C.; Peruchena, N. l. M.; Sosa, G. L. *J. Phys. Chem. A* **2009**, 114, 552.

[38] Rissanen, K. *CrystEngComm* **2008**, *10*, 1107.

[39] Metrangolo, P.; Neukirch, H.; Pilati, T.; Resnati, G. *Acc. Chem. Res.* **2005**, *38*, 386.

[40] Emsley, J. *Chem. Soc. Rev.* **1980,** 9, 91–124.

[41] Awwadi, F. F.; Willet, R. D.; Peterson, K. A.; Twamley, B. *J. Phys. Chem.,* **2007**, 111, 2319–28.

[42] Chudzinski, M. G.; McClary, C. A.; Taylor, M. S. *J. Am. Chem. Soc.* **2011**, 133, 10559.

[43] Guthrie, F. *J. Chem. Soc*. **1863**, *16*, 239.

[44] Mulliken, R. S. *J. Am. Chem. Soc.* **1950**, 72, 600.

[45] Mulliken, R. S. *J. Phys. Chem.* **1952**, 56, 801.

[46] Hassel, O. *Dan. Tidsskr. Farm.* **1962**, *36*, 41.

[47] Cincic, D.; Friscic, T.; Jones, W. *Chem. Mater.* **2008**, 20, 6623–6626

[48] Wu, G.; Freure, C. J.; Verdurand, E. *J. Am. Chem. Soc.* **1998**, *120*, 13187.

[49] Weingarth, M.; Raouafi, N.; Jouvelet, B.; Duma, L.; Bodenhausen, G.; Boujlel, K.; Schollhorn, B.; Tekely, P. *Chem. Commun.* **2008**, 5981.

[50] Sheppard, D.; Li, D.-W.; Godoy-Ruiz, R.; Brüschweiler, R.; Tugarinov, V. *J. Am. Chem. Soc.* **2010**, 132, 7709.

[51] Plevin, M. J.; Bryce, D. L.; Boisbouvier, J. *Nat. Chem.* **2010**, 2, 466.

[52] Caballero, A.; White, N. G.; Beer, P. D. *Angew. Chem. Int. Ed.* **2011** 50, 1 – 5.

[53] Kilah, N.; Wise, M.; Serpell, C.; Thompson, A.; White, N.; Christensen, K.; Beer, P. *J. Am. Chem. Soc.* **2010**, *132*, 11893–11895.

[54] Parisini, E.; Metrangolo, P.; Pilati, T.; Resnati, G.; Terraneo, G. *Chem. Soc. Rev.* **2011**, 40, 2267–2278.

[55] Metrangolo, P.; Resnati, G. *Halogen bonding: fundamentals and applications*, Springer, Berlin, London, **2008**, 221 p

[56] Biella, S.; Cametti, M.; Caronn, T.; Cavallo, G.; Forni, A.; Metrangolo, P.; Pilati, T.; Resnati, G.; Terraneo, G. *J. Supramolecular Chemistry* **2011** 23, 3, 256 — 262.

[57] Gray, L.; Jones, P. G. *Z. Naturforsch.* **2002**, *57b*, 61

[58] APEX Software Suite v.2010; Bruker AXS: Madison, WI, **2005**.

[59] Blessing, R. *Acta Cryst.* **1995**, *A51*, 33.

[60] Sheldrick, G.M. *Acta Cryst.* **2008**, *A64*, 112.

[61] Lommerse, J. P. M.; Stone, A. J.; Taylor, R.; Allen, F. H. *J. Am. Chem. Soc.* **1996**, *118*, 3108.

[62] Bondi, A. *J. Phys. Chem.* **1964**, *68, 441.*

[63] Shannon, R. D. *Acta Cryst.* **1976**, *A32*, 751.

[64] Chapman, R.P.; Bryce, D.L. *Phys. Chem. Chem. Phys*. **2007**, 9, 6219.

[65] Barbieri, M. *Lab. 2000* **2001**, *15*, 28.

[66] Dapprich, S.; Komáromi, I.; Byun, K. S.; Morokuma, K.; Frisch, M. J. *J. Mol. Struct. (Theochem)*, **1999**, 462**,** 1.

[67] Vreven, T.; Morokuma, K.; Farkas, Ö.; Schlegel, H. B.; Frisch, M. J., *J. Comp. Chem.* **2003**, 24, 760.

[68] Vreven, T.; Morokuma, K. *Annual Reports in Comp. Chem*. **2006**, 2, 35-51.

[69] (a) Becke, A. *J. Chem. Phys.* **1993**, *98*, 1372. (b) Lee, C.; Yang, W.; Parr, R. G. *Phys. Rev. B* **1988**, *37*, 785.

[70] Dapprich, S.; Komáromi, I.; Byun, K. S.; Morokuma, K.; Frisch, M. J. *J. Mol. Struc.: (Theochem)* **1999**, *461-462*, 1.

[71] Harris, R. K.; Hodgkinson, P.; Pickard, C. J.; Yates, J. R.; Zorin, V. *Magn. Reson. Chem.* **2007**, 45, S174–S186

[72] Ploug-Sørensen, G.; Andersen, E. K. *Acta Cryst.* **1985**, *C41*, 613.

[73] Portalone, G. *Acta Cryst. E* **2005**, *E61*, o3083.

[74] Raatikainen, K.; Cametti, M.; Rissanen, K. *Beilstein J. Org. Chem.* **2010**, *6*.

[75] Liu, Z.; Yu, W.-T.; Tao, X.-T.; Jiang, M.-H.; Yang, J.-X.; Wang, L. *Z. Kristallogr. NCS* **2005**, *220*, 415.

[76] Chia, L. S.; Cullen, W. R.; Gerry, M. C. L.; Yiaw, P. S. *Can J Chemistry* **1974**, 52, 3484.

[77] Shlyapnikov, D.; Feshin, V. *Z. Naturforsch.* **2002**, 57 a, 974–976.